Characterization of Micro-Machining of Dental Screws and Abutments

by
Richard York

Supervised by:

Dr. Michel Nganbe
Dr. Marc Doumit

A thesis submitted
to the Faculty of Graduate and Postdoctoral Studies
in partial fulfillment of the requirements for the degree of

MASTER OF APPLIED SCIENCE

In Biomedical Engineering

Ottawa-Carleton Institute for Mechanical and Aerospace Engineering
University of Ottawa
Ottawa, Canada

April 2017

Abstract

In today's society, dental implants are a growing solution for dental care. However, most dental components are very expensive when imported, and are purchased at premium costs solely from a few international companies. It is estimated that the current market price of dental implants is as much as one thousand times the material cost. To be cost effective in a growing competitive market, a local company is looking into producing their own components, and requires knowledge of manufacturing and quality assurance or expertise in order to validate the effectiveness of their fabricated components. These fabricated components need to be tested against currently in use market components in order to assure that prototype components are not inferior to the current market supply.

The present study focuses on the analysis of the fabrication process of dental implants, specifically the abutments and screws. The objective is to compare material properties of prototype and market components to determine if the prototype components have adequate quality. Furthermore, simulated models are developed for predicting material property changes due to the manufacturing process. The material properties are determined through hardness testing and microstructure analysis. Visual inspection is then used to investigate and characterize the components. The simulations use different machining parameters, such as the feed rate and the cutting speed to determine residual stress patterns.

Dental implant abutments and screws were successfully tested and compared. The prototypes show a good hardness and microstructure properties similar to market components, indicating a high level of prototype quality. The simulated models were successfully created and provided an adequate level of customization to be usable in place of future mechanical testing and showed results that complimented experimental findings. The standard cutting speed of 2000 rpm (100%) in the prototypes produced the optimal hardness and surface roughness. Prototypes were found to have an acceptable level of both hardness and surface finish for the investigated 50%, 100% and 150% of the standard 2000 rpm feed rate.

Acknowledgments

I would first like to thank my thesis supervisor Dr. Michel Nganbe, and my thesis co-supervisor Dr. Marc Doumit, both of whom provided the opportunity and knowledge that not only helped me build the necessary skills and background I needed during the course of my degree, but also helped lead me to pursue this degree even before they became my supervisors. Without their guidance and direction, this thesis would not have been possible.

I would also like to thank the University of Ottawa mechanical and biomedical engineering faculty members who helped me overcome difficulties during the course of my research. Additionally, I would like to extend my gratitude to my fellow Master's students and the Ph.D students who helped me overcome any difficulties during the course of my degree.

Finally, I would like to express my thanks to my friends and family members, both immediate and extended, who gave me their support throughout my years of study. Without them, I would not be the person I am today.

Table of Contents

Table of Figures

1 Introduction

1.1 Background

There are a myriad of ways in which someone may experience an injury related to the jaw or mouth, ranging anywhere from a simple accident to a job related injury. When injuries cause the loss of one or more teeth, it may become necessary to have a replacement for the damaged or extracted teeth. A dental implant becomes a replacement for both the root and the body of a tooth, consisting of: an anchor set into the jaw bone, an abutment to affix the crown to, an attachment screw to connect the abutment anchor, and a replacement tooth or crown. An example of how these components function together can be seen in Figure 1.

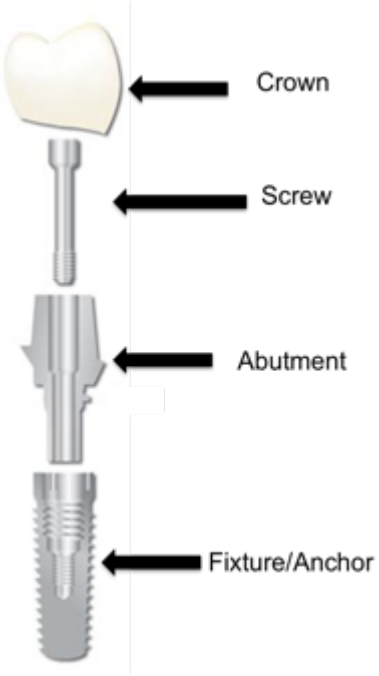

Figure 1: Dental implant system modified from [1]

Generally, most people who have lost teeth and are in good health are candidates for dental implants [2]. More than 15 million people in the U.S. currently live with crown or bridge replacements for missing teeth [3]. There are at least 3 million people living in the U.S. alone with dental implants, and that number is expected to grow by approximately 500 000 people a year [3]. As such, dental implants are a growing market, with a large projected market value of 6.4 billion dollars by the end of 2018 [3].

With the growing demand of implants comes a fierce market competition in the dental laboratory industry that is putting enormous pressure to offer higher quality implants at lower competitive prices. However, there are currently a very limited number of suppliers on the world stage for high-precision key dental components, such as abutments, and they have to be imported to Canada at premium prices. This challenge has been pushing dental laboratories to expand their capabilities to micromachining of dental abutments, screws and implants. In-house production is estimated to yield substantial cost reductions when compared to imported components [4]. With the emergence of implant manufacturing, companies that are just starting up require some form of manufacturing and quality assurance expertise. Dental laboratories may reverse engineer currently existing dental implants and insure that their products have an adequate level of dimensional and functional accuracy. However, it is still important to determine whether these parts are of an equivalent quality compared to current market components with respect to microstructure, mechanical properties and service life.

A local dental laboratory, that has been a leading provider of high-quality dental products and services to dental professionals for over 20 years, is consistently faced with local and international competition that has forced them to offer competitive pricing. Over the years, this has become a challenge, particularly the high costs of imported implant components. Thus, to be a successful company, this Canadian dental laboratory has been exploring the manufacture of in-house dental components. The components are principally being reverse engineered. However, manual and optical assessments of the prototypes dimensional accuracy had been the only quality control methods used so far. The dental laboratory needed more systematic and exhaustive manufacturing and quality control guidelines to ensure that there are no machining-based defects in fabricated components. The fabricated prototype components are of the types illustrated in Figure 2 and 3.

Figure 2: Conical connection screw (left) [5] and Nobel M1.4 connection screw (right) [5]

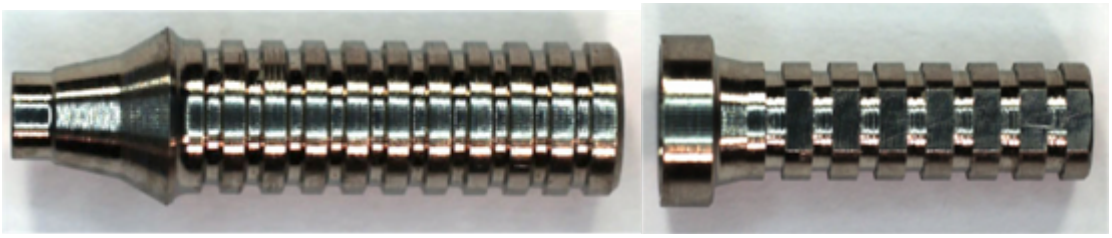

Figure 3: Conical connection abutment (left) [5] and Nobel connection abutment (right) [5]

To ensure that there are no machining-based defects in fabricated dental components, the dental laboratory and the University of Ottawa have formed a collaboration aiming to analyze and optimize the micromachining process. Examples of the implant types produced by the local company are presented in Figures 2 and 3. However, it is also imperative to test and validate the quality of the fabricated components for their intended usage over the life cycle of the components. In addition to their complex shape, dental implant components are less than 10 mm in length and about 1 mm in diameter. As such, mechanical and quality validation by tensile, fatigue or impact testing is impossible under standard testing setups due to the small size of the components. Therefore, a comprehensive mechanical modeling of the dental components is crucial in order to validate the original dental component design or any design optimization before the fabrication process.

1.2 Objectives

The present thesis focuses on the fabrication of dental implant abutments and screws and the micromachining processes associated with them. The objective is to first experimentally investigate the manufacturing processes and resulting material properties changes caused by the component fabrication. Secondly, this thesis aims to develop numerical models to describe the micromachining and to elucidate potential weaknesses in the implants through the use of simulated finite element models.

The specific objectives of this research are:

- To comparatively investigate Ti6Al4V alloy rods and blanks from suppliers, as well as prototypes manufactured by the partner company.
- To study potential microstructure changes and pre-damages during the micromachining fabrication of dental implant prototypes.

- To study work hardening and potential thermal degradation during macro machining of dental implant abutments and screws.
- To develop numerical models to describe the micromachining and potential weak points during use.

1.3 Methodology

Material property changes are examined through comparative micro-hardness testing against tensile samples using Vickers hardness testing, visual inspection and microstructure analysis via optical microscopy, and scanning electron microscopy. Property changes are compared against patterns obtained by other researchers and literary sources, and areas of potential failure in both prototype and market components are discussed. Additionally, numerical models are proposed for individual manufacturing processes, and residual stress patterns are compared against other reference experiments that document residual stress distributions during machining. Furthermore, experimental and numerical results are compared and contrasted in order to determine if the numerical models can be used to assist in reducing induced residual stress levels during the fabrication of dental implant components. The obtained results are expected to both give insight into the locations and causes of dental implant failures, as well as offer an avenue in order to improve implant quality and lifespan.

1.4 Thesis Contribution

This thesis first presents a comprehensive literature survey covering types of dental implants, different modes of failure, factors affecting fatigue life, material properties, and various numerical models pertaining to the manufacturing processes involved in the fabrication of dental implants. This literature review provides reasons for dental implant failure, as well as common failure modes and locations of failure. Additionally, the effects of machining on material properties, particularly those of metallic materials, are explored in relation to machining work and induced residual stresses relating to strain hardening. Finally, numerical models are created and examined for the purpose of providing an initial basis for the creation of a numerical model more tailored towards the prediction for the machining of dental implants.

Secondly, this thesis describes comprehensive experimental testing including visual inspection of components and image analysis using Scanning Electron Microscopy (SEM), Electron Diffraction Spectroscopy (EDS), and 3D microscopy. Additionally, hardness testing of prototypes, market components and failed tensile samples was performed using Vickers hardness testing. Finally, microstructure analysis was performed on etched samples using optical microscopy. Some major findings include: areas of design consideration in prototypes due to geometry affecting stress concentrations, areas of rougher quality on machined surfaces, locations of increased hardness due to machining effects, and a noticeable lack of microstructure changes induced during the manufacturing process.

Third, this thesis has provided numerical models in the form of finite element models simulated using ABAQUS/Explicit software. These provided models present residual stress distributions for the individual machining processes involved in the fabrication of the dental implant components. The models were created with the intention of easily altered machining variables, such as machining speed and cut depth, in order to optimize the machining processes in terms of strain hardening occurring in the implant components, as well as manufacturing speed. Models provided in this thesis also validate related studies pertaining to variables such as the impact of multiple cuts on the depth of residual stresses produced.

This thesis provides a reference point to create quality standards for components that could soon go out into the market, as well as validates the quality of the fabricated prototype components against current market components. These standards and validations may then be used as a baseline for other companies and manufacturers wishing to begin implant production. Additionally, the simulated models may be used to predict critical areas of interest in fabricated components, as well as to implement manufacturing changes in order to assess final component quality, without the need to manually produce and test components.

Development of a numerical simulation model will help dental laboratories to produce future components without the need to manually investigate sample components. This will result in saving both time and cost in the development process, while at the same time ensuring their standard quality. Thus, developing a numerical model of the dental components is critical to mitigate technical and commercial risks.

1.5 Thesis Outline

This thesis is organized into six chapters. Chapter 1 introduces the goal and rationale for the investigation of dental implants, including current market status as well as company goals. Additionally, this chapter contains thesis contributions and the adopted methodology used in order to achieve the thesis goals.

Chapter 2 presents a literature review regarding implant manufacturing and materials, as well as failure modes during use. Additionally, previous computational models are presented and discussed. The structure of this review is separated into two main categories related to the experimental testing and numerical modeling, respectively.

Chapter 3 presents the methodology behind the experimental and numerical testing, as well as providing the set-up and procedures used.

Chapter 4 presents the results obtained from the testing process and discusses the results obtained, while correlating the results from both numerical and experimental testing, as well as relating results to previously published studies. This chapter is segmented according to experimental and numerical results, respectively.

Chapter 5 presents the conclusions for the thesis and Chapter 6 provides future recommendations for research into both numerical modeling and material testing and parameters of possible interest.

2 Literature Review

2.1 Implant Background

Over the last few decades, a significant increase in life expectancy, as well as major scientific-technological progress in Material Science, Computer Aided Design and Manufacturing have led to an increase in the use of surgical implants to replace teeth and enhance the clarity of speech in patients who are either without teeth or lacking fully functioning teeth [6]. Because modern dental implants are inserted into the sockets of missing teeth, the implants must mimic the initial properties of the tooth in order to bear and transfer loads between the tooth (prosthesis) and the alveolar bone surrounding the socket [7]. Due to these considerations, dental implants must meet a certain quality in order to be effective for use. In this segment, implant types, parameters, failure modes, and materials will be discussed.

2.1.1 Types of Implants

There are three main types of dental implants that are commonly used in modern dentistry: subperiosteal, endosteal, and root-form endosteal, which can be seen in Figure 4. Subperiosteal implants are large metal frameworks with protruding metal abutments. These types of implants are set on the jawbone, underneath the gum layer, and protrude through the gums. Subperiosteal implants are used when the jawbone is unable to withstand an internal type of implant due to factors including inadequate implant area or poor bone osseointegration complications. Subperiosteal implants are more expensive than endosteal, primarily due to the fact that they must be custom fitted to a patient's jaw; either from taking impressions after a small surgical operation or from Computed Tomography (CT) scans. Endosteal type implants are directly inserted into the jawbone, and are the more common form of implant compared to the other mentioned types. These implants are inserted after drilling a core area out to be used as the insert site of the dental anchor.

Endosteal implants come in two main types: plate and root-form. The plate and root-form designations are used to describe the characteristic insertion end of the dental anchor. Plate type endosteal implants have long, thin protrusions that sit into the jawbone in a horizontal manner, whereas root-form types sit vertically in the jawbone, as can be seen from Figure 4, with the

plate form on the left of a) and the root form on the right of a). These implants will then be fitted with a ceramic cap, known as a crown, that takes the form of the missing tooth.

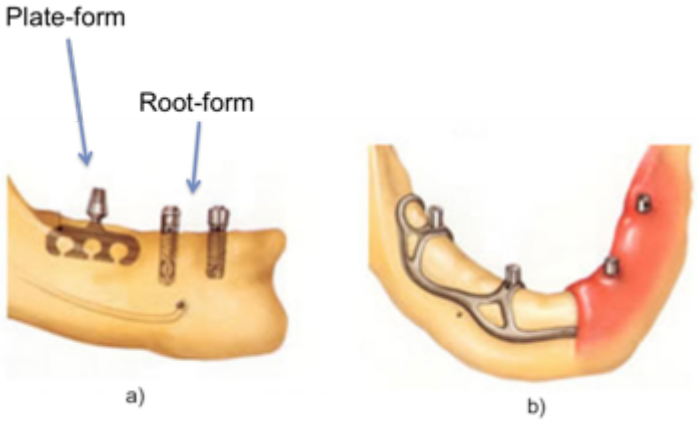

Figure 4: a) Endosteal (plate and root-form), and b) subperiosteal dental implant types, modified from [8]

Both endosteal and subperiosteal implants may be fabricated as either two individual pieces with a connecting screw, or as one single body, depending on whether the implant surgery is a single stage or two-stage procedure. For single stage operations, the anchor and abutment are fabricated as a single unit and inserted as a whole in a single process. In a two-stage procedure, the implant body (anchor) is first placed into the tooth socket, and the wound is then sutured closed for a few months, in order to prevent loads on the anchor and allow the surrounding bone and soft tissue to heal and integrate with the implant [7]. For the second stage of the surgery, a permanent abutment is fixed to the main implant body by the means of a screw. There are advantages and disadvantages in both processes, and in order to determine whether a dental replacement procedure will be a single stage or two-stage operation it is important to plan accordingly with the surgeon who will be performing the operation. Single stage operations may be faster and less invasive than the two-stage operations, but it is important to be aware of dental and oral habits, as there is no setting time for the single stage implant, which would otherwise allow the implant to integrate with the bone structure. This leaves the single-stage implant more vulnerable to early loosening and overall failure of the implant if not handled properly.

2.1.2 Implant Failure Modes

The major types of failure for dental implants can be attributed to either biological or mechanical factors. Biological failure of dental implants can happen even after sufficient rigid fixation has been achieved, as the implant (especially root-form types) may become loose due to bone resorbtion [7]. Mechanical failure can be attributed to either injury or fatigue due to excessive oral activity, but can also occur commonly due to lateral loading on the prosthesis, imparting both static and dynamic torque to the abutment and screw, leading to loosening of the dental implant or fatigue failure of the anchor-abutment connection.

Even with the vast growth in research on dental implant processes and operations, there are still a large number of cases where implant fracture has been reported [9]. While accidents may occur due to an impact to the prosthesis itself, the implants can also experience cyclic fatigue failure due to daily actions such as chewing.

Implant failure can be subdivided into two different categories of failure modes: early failure and late failure. Early failure of implants normally takes place during the first year after implantation, and is most often linked to poor integration ability. Poor integration ability may be associated with multiple sources, including improper selection of implants, surgical technique and poor oral hygiene [7]. It is precisely due to this reason that most dental surgeons will screen their patients in advance to ensure that their oral hygiene is adequate and they have no prior dental diseases that could contribute to the failure of the dental implant.

After the implant anchor has been inserted and the insertion site has healed, the abutment and screw will then be fixed in place, either as two individual units for a two-stage operation, or as single combined unit for a single-stage operation. The success or failure of the implant now becomes dependent on whether or not the mechanical properties of the implant can withstand the loading conditions in the mouth. When mechanical failure occurs, there are three main divisions they can be associated with in order of frequency: loosening of the abutment or screw, fracture of the crown, or other technical complication such as abutment and screw fracture [10].

2.1.3 Forms of Mechanical Failure

The first type of failure, loosening between the abutment and the screw, is one of the most common occurring issues for single tooth implants. Loosening of the screw has been found

to occur in 5.6% of dental implant failures within a period of 4.8 years for single implant restoration, and will occur due to reasons such as inadequate preloading during initial screw tightening, excessive occlusal forces, or variations in either screw or abutment geometry design [10]. While pre-tension can help prevent loosening, there is also the risk of the screw being over-tightened. Ultimately, surgeon ability plays a large part in this type of failure.

The fracture of the crown is the second most common method of failure. From collected data, the amount of failures over a five year period were 3.4% from crown fracture for single implant restoration [10]. With crown fractures, the most common fracture location was found to be in the posterior region of the mouth [10].

The final and least often occurring method of failure is actual component failure of either the screw or the abutment, attributing to only 0.5% of the failure cause for the abutments and 0.3% for the screws each case individually [10]. While this type of failure may be the least common, whether a component will undergo this type of failure or not is heavily reliant upon both implant design and habitually produced loading cycles.

For a partially fixed implant-supported prosthesis, these values were found to be 8% failure for chipping or fracture of the veneer crown, 6.1% for screw loosening, and 3.6% rate of screw fracture [10]. It is important to note that these studies had total failure rates of 10.8% for single implant restoration and 16.1% for the partially fixed implant-supported prosthesis. These studies also had a mean of less than five years generally, and implant fracture was a more common concern for long-term implants [10]. Rates of failure are also highly dependent on implant type, design, and material, as there have been implants that have failed due to fracture within two to three months after surgery [6].

One of the most frequent failure locations is the neck region of the screw, as shown in Figure 5, between the head and the threading, where the highest stress concentrations are likely to occur.

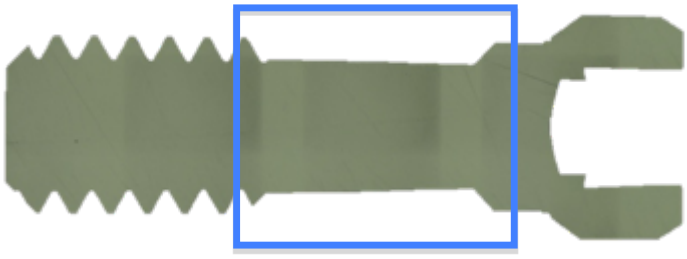

Figure 5: Neck area of a connecting screw

Failure of a dental implant can be seen in Figure 6. Main stress peaks were found to occur around the neck of the implant in the cases of both abutments and screws [11]. Additional testing of implants with simulated in vivo aspects was performed by Freitas-Júnior et al. [12] using water as a medium to simulate conditions in the mouth. Testing was performed with a loading cycle of 50 000 cycles at a load of 200 N in order to simulate real-life usage conditions. Normal masticatory loads generally range anywhere from 40 to 250 N, although actual forces will differ from person to person and tooth to tooth. The results of the study show that the primary failure zone for the abutments was at the conical joint region, and the screw fracture occurred at the neck region. It is important to note that implants are designed to fail at this component (i.e. screw) as it represents the safest scenario and the minimum cost of repair. However, whether the actual implants are failing at the desired cycle or magnitude is yet to be validated, as there are no such literature sources on the subject.

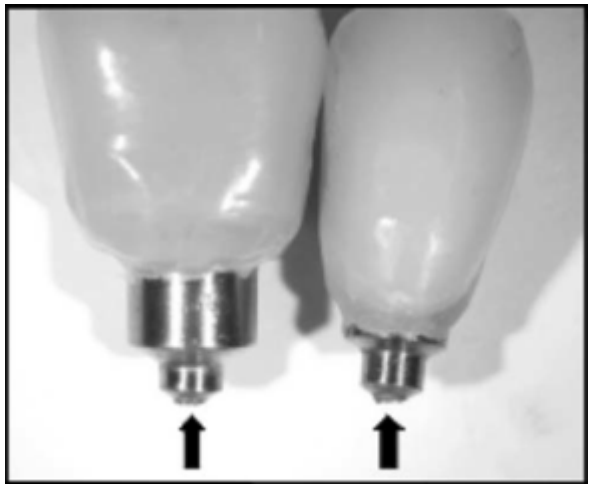

Figure 6: Example of implant fracture area [6]

2.1.4 Method of Failure and Fatigue Life Factors

Since failure of a dental implant is determined to occur primarily in set areas of both the abutments and screws [11], it is necessary to determine whether the component will fail under an instantaneous load or a continuously applied load.

Despite being a highly desired field of study, research into implants that have failed in use, as opposed to mechanical simulation, has been subjected to many setbacks. Detailed fracture analysis of retrieved dental implants is a rare commodity for both the dental and biomechanical

literature fields. The largest contributing factor to this lack of data is that the rate of fractures of dental implants and implant parts is quite low [13]. Compounding the low fracture rate, the implants that do undergo fracture tend to be left in the alveolar bone due to the difficulty of retrieving them. The risks of further damaging the implant or harming the patient are too high in procedures to adequately remove the failed components. Additionally, the fracture surface of the implants, which is necessary for fracture analysis, is generally destroyed or damaged to the point that fractographic analysis becomes impossible [13].

In terms of titanium-based dental implants, there have been some investigations into the type of failure that occurs. Yokoyama et al. [14] managed to compare retrieved fractured dental abutment screws made out of CP-Ti to an as-received abutment screw through the use of microstructural examination and SEM testing. Mixed ductile fracture and fatigue striations were discovered on the fracture surface of the retrieved implants, which led Yokoyama et al. to theorize that the failure was due to trans-granular stress corrosion cracking [14].

An analysis was carried out by Choe et al. [15] using SEM fracture surface analysis on six fractured CP-Ti dental implants. Each of these implants had fractured intra-orally after 30 months. This analysis claimed to have identified fatigue striations in all of the specimens, yet suffered in credibility due to the low resolution of the SEM fractographic images [13]. Choe et al. concluded that fracture had been reached primarily due to the development of corrosion, despite the fact that there were no clear indications of such in the SEM images [13].

Similar to the two previously mentioned studies, additional studies were carried out by Manda et al. [16] and by Sbordone et al. [17] regarding the main methods of failure in titanium based implants. Both of these studies also indicated markers of fatigue-based failure, but also attributed failure to either calcium and phosphorous oxide deposits or cleavage type fracture, respectively.

The study by Shemtov-Yona [13] recognized this inconsistency and sought to perform a detailed systematic failure analysis on retrieved dental implants made from both CP-Ti and Ti-6Al-4V. Shemtov-Yona collected a total of twenty-four in vivo fractured dental implants, or implant parts, in order to examine the failure methods. No background data about either the implants (such as oral position, service years, and eventual bone loss) or the patients (age, gender, oral habits) was provided, thus granting a situation where the retrieved parts were examined purely from a technical standpoint, without addressing related medical concerns [13].

Fractographic images taken during the study show that both the CP-Ti and Ti-6Al-4V implant parts displayed a generally uniform and flat fracture surface, indicating that there was a single failure operation mechanism until the implant finally failed [13]. Fracture surface topographies revealed that more than 90% of the fracture surfaces on both the CP-Ti and Ti-6Al-4V implant samples contained typical fatigue markings. In the end, all of the samples exhibit striations indicative of fatigue failure. The study also determined, through the use of house-made implants, that implants and implant parts may also break at relatively low cyclic loading values, similar to those produced during a standard chewing action [13].

2.1.5 Mechanical Behaviour of Dental Implants

Most studies have concluded that dental implants are predominantly failing due to a fatigue root-cause, when failure occurs under mechanical conditions. Due to this fatigue root-cause, related mechanical fatigue behavior of implant materials such as titanium alloys and how they impact the life expectancy of the implant were examined.

The fatigue behavior of metals such as titanium alloys may vary greatly depending on the properties imbued in them. Most notably, the variables that have the greatest impact on similar types of metals include: Hardness (or strength level), ductility, cleanliness of the material, residual stresses, surface conditions, and aggressive environments [18].

Hardness, or strength level, has a varying impact on metals. For instance, most steels with a hardness below 400 HB have a fatigue limit that is approximately half of the ultimate tensile strength [18]. This means that any sort of heat treatment or alloying addition that increases the hardness would be expected to thereby increase the fatigue life of the implant components as well. This only applies to lower alloy materials however, as medium level alloys may not have the higher fatigue levels associated with a higher hardness value [18]. The higher hardness, lower fatigue values associated with medium level alloys pertain to cycles that are less than 10^3, as at that point, ductility becomes a more important factor.

Ductility is primarily important to fatigue life under low-cycle conditions, with exceptions during spectrum loading, which consists of an occasional overloading period with millions of smaller cycles, or for extremely brittle materials, as crack propagation would begin to dominate [18].

Surface conditions also play a role in fatigue life, especially with components that are interacting with other components/materials. Poor surface finishing can result in fretting, which is a wear phenomenon that occurs between two mating surfaces [18]. Fretting will cause vibrations between parts, usually leading to oxidation, which can be hazardous if the implant material does not have some form of protective layer. This is of special concern in most biological implants, as fretting can cause wear of the material and potentially lead to serious adverse effects for the patient. Fretting normally occurs between two tight-fitting components that experience a cyclic, relative motion of extremely small amplitude [18].

While a component is experiencing fretting, cracks can be initiated at very low stresses that are well below the fatigue limit of similar components not experiencing fretting [18]. This is important to note when looking at the method of attachment for the abutments and abutment screws. There is a small gap produced during the securing of the abutment via the screw.
Since chewing, or grinding your teeth, can be a relatively small cyclic force, this gap may help prevent fretting from occurring between the abutment, screw, and anchor.

An illustration of how the implant forms as a whole can be seen in Figure 7. The fatigue properties of a material are also greatly impacted by residual stresses in a material. Generally, compressive residual stresses at the surface of a component can help improve the fatigue life, whereas tensile residual stresses have the tendency to reduce fatigue life.

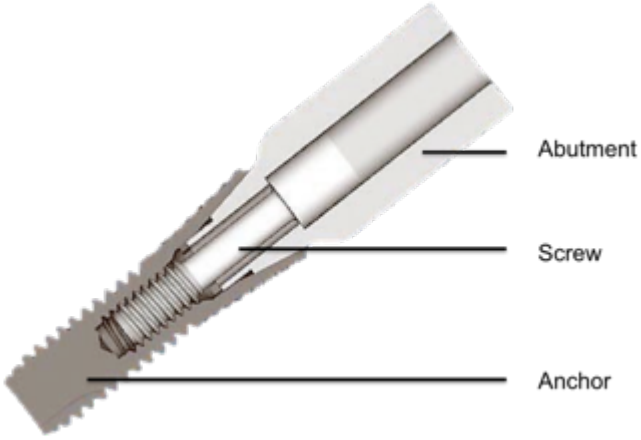

Figure 7: Astra Tech internal conical connection type implant [19]

These beneficial compressive stresses may be introduced through surface alloying, surface hardening, cold working, or a combination of the aforementioned procedures [18]. Surface

alloying consists of introducing carbon or nitrogen, or both, into the surface layer of the part. While this normally represents a particular advantage since the alloyed surface follows the original contour closely, problems may arise if used with titanium-based implants for two primary reasons. Firstly, titanium naturally produces a thin oxide layer, which helps greatly in preventing corrosion, granting a higher level of biocompatibility. Additionally, an oxide layer can also help by removing potentially toxic elements, such as Ni, from the surface of the material. If this oxide layer can no longer form on its own due to the alloying, the biocompatibility of the part will drop. Secondly, dental implants are meant to be small in order to properly fit the mouth. Since the alloying layer would be required to be at least thick enough to prevent operating stresses, this could become a great setback due to size limitations. Cold working of the surface of the material will effectively increase the fatigue resistance of the part [18]. Cold working the surface of a component can produce helpful compressive stresses. Apart from cold working, standard machining operations can have an impact on most of the aforementioned properties, making the machining process a possible venue to improve effective implant lifespans.

2.1.5 Design Effects on Dental Implant Failure Criteria

One predominant aspect of determining the lifespan of dental implant components is their inherent geometrical properties. While excluding material property effects, the life of a component can be greatly impacted by factors such as: implant height, diameter, implant shape, and connection type [22-29]. Implant height is predominantly determined by the length of the anchor, but may also refer to the height of the anchor-abutment interface. A careful balance must be obtained in order to achieve an ideal height for the abutment-anchor or anchor-bone interface. This concern is important in the abutment-anchor interface as shorter implants may not provide the necessary stability, whereas longer implants may be more prone to fracture due to increased bending moments due to lateral forces and subsequently stresses. In regards to implant length as determined by the abutment-anchor interface, there are few literature resources that examine failure for this specific aspect. Of what is available, it was determined by Dittmer et al. [20] that the implant-abutment connection design has a significant impact on the load bearing aspects of the implants, however fatigue life was not explored. Dittmer et al. concluded that long opposing lateral surfaces for implant-abutment interface presented advantages in terms of load bearing

capacity, as opposed to short surfaces. Another study by Gil [21] analyzed fatigue life for different components, and discovered that the external hex type of 0.6 mm height did not provide enough stability to be able to adequately test using standard procedures, and so a 1.8 mm height connection type was used instead. For small connection sizes such as these the screw normally ends up taking the bulk of the load from the lateral forces acting upon the prosthetic. The study by Gil also proposed that the reason for acceptable results for shorter implant-abutment connections are most likely attributed to improved screw designed and increased connection height [21]. There has been a great deal more research done into the effects of anchor length on successful implant procedures, as opposed to abutment-anchor connection. While many studies have been performed on investigating the impact of anchor length on dental implant success rates, most studies imply that shorter anchor lengths have lower success rates [22]. This is reasonable considering that the anchor is the portion of the implant that is set into the bone, and shorter anchor will thereby have less area for osseointegration. Amongst the shortest implant types that are commonly produced, the 7 mm anchor was associated with greater failure than all other anchor lengths [23]. Despite this discovered correlation, other studies have demonstrated that there may not actually be a direct relationship between implant anchor length and rate of failure. Due to this consideration, it is theorized that the correlation between anchor length and implant failure is not due to geometry, but rather due to experience of the surgeon and the area where the implant will be inserted [22]. Shorter implants are used more often in the maxillary posterior region, which are the teeth found in the upper jaw at the back of the mouth, as may be seen in Figure 8.

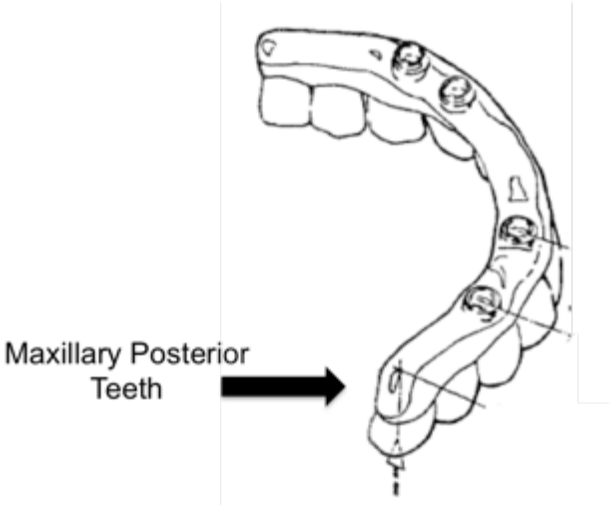

Figure 8: Maxillary posterior teeth [24]

This area of the jaw tends to have much poorer bone quality than the other areas of the jaw. Additionally, studies that show correlations between short implants and failure were predominantly taken from surgeries performed either by dental students or younger practitioners, thus the failure could reasonably be attributed to the experience of the practitioner, as the difficulty level of surgery for both the region and procedure of implant would be greater [22].

Another aspect of implant design is the diameter of the anchor. The diameter of an implant is measured from the peak of the widest thread to the same point on the opposite side of the implant [22]. It is especially important to be aware of the fact that implant diameter refers to the anchor, and not the abutment or screw. Wider anchors will, however, have more available room for both wider screws and abutments. Currently available implants may have diameters that range from 3 to 7 mm, and are chosen based on specific surgical and prosthetic requirements [22]. Implant diameters are chosen in order to provide the best stability from the alveolar bone, and have both advantages and demerits of being either wide or narrow type implants. Advantages of using wide-diameter implants include: more bone-implant contact, bicortical engagement, immediate placement in failure sites, and a reduction in abutment stresses and strain [25]. Studies on produced strains have shown that increasing the diameter of an implant will reduce the strains produced in the abutment portion of the prosthesis [25]. Wide-diameter implants are also useful for immediate placement, especially in the molar region, where tooth removal produces larger cavities due to the inherent nature of how the roots flare, creating the largest defect in the area that requires the most stability [22]. While larger diameter implants may produce many benefits, one of the largest problems with the larger implants is directly related to the increased diameter. If wider implants are used, it means that more bone must be removed in order to insert the implant. While this provides more contact surface area than narrow diameter implants, depending on region and bone geometry, wider implants may cause serious integrity issues in the bone structure. In the event that narrow diameter implants fail, wider diameter implants may be used to replace the failed implant, although it is reported that the success rates of said operations decrease drastically when compared with non-replacement implants. Narrow-diameter implants have the greatest advantage because they are less than 5 mm in diameter, which allows for insertion into small areas without removing a sizable amount of bone, while still allowing for enough space to display adequate stress distribution. This allows surgeons to replace teeth in close proximity to each other, as well as insert implants in areas where bone

width would otherwise be unable to support the wider implant types. In addition to narrow type implants, there are also mini implants, with diameters of 2.7 mm or less, however they have not been validated for definitive fixed prostheses [22]. Possibly the most concerning disadvantage for most narrow implants is the reduction in resistance to occlusal loading [26]. However, since there has been a correlation between retention and length of the implant, not the diameter, provided that the occlusal forces acting upon the tooth or teeth to be replaced would not be considered significant, narrow-diameter implants would still be a viable option [22].

Implant shape and connection type refer to the insertion shape and the abutment-anchor interface, respectively. Implant shapes can be generally classified as plate, root-form, or subperiosteal designs. Subperiosteal designs are custom made to wrap and form around the jawbone, and thus failure of these types of implants is dependent more on whether the forces acting upon the implant are greater than expected. Both plate and root type implants are set directly into the bone, and therefore failure is more dependent on the shape they take. Plate type implants are less favourable as a general practice, even though after osseointegration has occurred the implant may actually end up more stable than a root type counterpart. However, their implantation requires difficult surgery procedures and a large amount of bone needs to be removed during surgery [22]. Root type implants are the general standard that most procedures will use, barring any specific circumstances that would make their use less favourable, such as bone density and geometry. Root type implants are generally fabricated as either screw type or stepped cylinder bases. The stepped cylindrical implants tend to show stress distributions that are more even when compared to unaltered cylindrical or tapered implants, and show improved loading of the crestal bone supporting the alveolar bone [27]. The screw shaped implants provide the greatest retention immediately after implant placement, and have an increased surface contact area due to the development of serrated threads [22]. The pitch of the threading is an important factor in determining implant stability, as increased pitch and increased depth will produce a greater surface area. It was determined through a stress analysis that stress distribution in the supporting bone around the implant is more heavily influenced by the implant root shape as opposed to the implant size [22].

Connection types may be classified as either internal or external connections, and may come in a number of different styles, such as: conical, hexagonal, Morse taper, etc. Dental professionals still debate about the suitability for different types of connections, and there has

been no real consolidation as to whether one type of connection, whether defined by either shape or internal/external, can be considered more appropriate or universally applicable: some of the more common types used are both interior and exterior hexagonal and internal conical insertion connections. A comprehensive evaluation of published papers performed by Sadid-Zadeh et al. [10] determined that internal connections fared better for both loosening of the abutment or screw, with an incidence rate 18.3% at a mean of 5.3 years for external type connections and a rate of 2.7% incidence rate for internal connections for a mean of 4.5 years. Similarly for fracturing of the veneering ceramic or crown, an incidence rate of 5.4% after 5.4 years and 2.9% after 4.7 years for external and internal type connections, respectively [10]. As for the comparison between different shaped connections, such as hexagonal or conical, a study performed by Freitas-Júnior [12] determined that the internal conical insertion connection presented lower stress concentration in the abutment screw as compared to both the internal and external hexagonal counterparts. The impact of the interior connection height on the load bearing capacity of the hexagonal connection can be seen in Figure 9. The conical and nobel connection types were displayed in Figures 2 and 3.

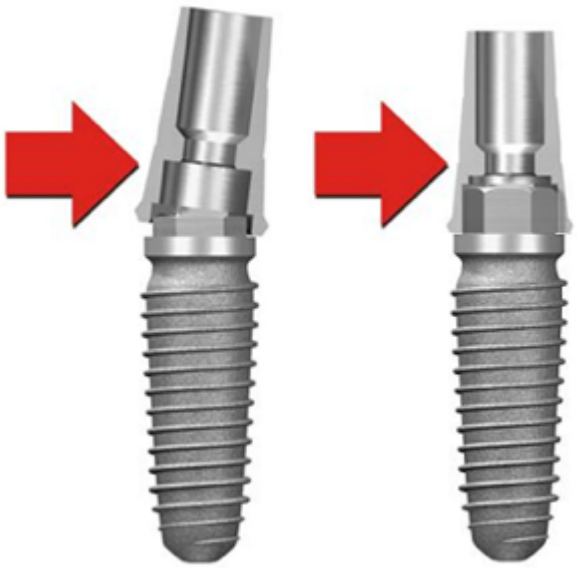

Figure 9: Impact of connection height on hexagonal connections [21]

A further review by Schmitt et al. [28] looked at the general comparison between conical connections and as many other connection types as they were able to obtain relevant source material for. Schmitt et al. determined that in vitro testing of implants indicated that the conical connection was of a superior type, being more resistant to abutment movement, torque loss,

fatigue loading and bending; as well as indicating lower abutment screw stresses as opposed to hexagonal connections. For the *In vivo* results, however, both conical and nonconical connection systems tended to be comparable in terms of success and survival rate.

2.1.6 Implications of Dental Implant Failure

Dental implant failure may happen in a number of ways including both biological and mechanical causes. From a biological perspective, implants may fail due to: poor osseointegration, premature loosening of the implant, negative reactions to implant materials, or oral disease. Mechanical failure may occur as: loosening of the dental screw or abutment, or fracture of a component. One further concern related to biological failure is peri-implantitis. Peri-implantitus is an inflammatory process caused by bacteria that get into the gaps between the abutment and the anchor. The bacteria will later return to adjacent tissue to cause peri-implantitis.

Implant complications may be categorized as either early stage or late stage complications. Early stage complications will occur before the implant has had time to fully integrate with the jawbone. Late stage complications occur after the implant has already integrated into the jaw, and usually consists of mechanical failures such as abutment screw or crown fracturing, but may also include other complications involving the surrounding tissues. If an incident involving the fracture of the abutment, abutment screw, or crown occurs, the issue is quite easy to remedy. The broken abutment, abutment screw, or crown is removed and replaced. While the recourse is different depending on facility, it is entirely possible to have the abutment and abutment screw replaced free of charge, although some offices will charge to have crowns replaced. While incredibly rarely, occasionally the anchor itself may fracture. When this occurs, the broken anchor must be removed and the site must be cleaned and prepared for an additional implant. Depending on the severity and geometry of the patient's alveolar bone, additional bone may need to be grafted onto the implant site. After waiting five or more months for the bone to heal, the site can be prepared and a new implant can be inserted. Depending on the reason for the fracture, new implants may have wider diameters than the fractured implants, in order to increase the resistance to occlusal forces, provided the state of the alveolar bone will allow such.

As with any surgery, there are also possible complications that could occur due to either human error, or improperly maintained or cleaned equipment and surgery site. As mentioned

previously, peri-implantitis is one of these possible complications, as it can occur not only due to oral bacteria, but it can also be induced by other factors, such as improperly grafted or overheated bone. Peri-implantitis not only causes inflammation, but also bone loss, and can result in serious complications if not treated. Treatment options differ depending on institution and insurance coverage, as well as the initial cause of the complication. Some cases may be resolved with simple cleaning, or reattachment of the crown, whereas more sever cases may require the complete removal of the implant and placement of a new one to take its place. As with any surgery, it is important to discuss in detail with the surgeon before deciding on any course of action.

2.2 Dental Implant Alloys and Physical Properties

Dental implants are manufactured from different types of base materials and alloys, including ceramics as well as metals and alloys. This subsection will discuss various types of dental implant materials, their prevalence, their typical use, and physical properties that make them both advantageous and disadvantageous for use.

2.2.1 Dental Implant Materials

In this work, the Titanium alloy Ti-6Al-4V was used as the basis of experimentation and modeling. There are, however, many other types of implant materials, such as commercially pure Titanium, Zirconia compounds, or even different types of coating layers for the implants.

Although there are many different options for implants, the most common materials used are commercially pure (CP) Titanium and Titanium alloys. Titanium, the most commonly used material, can be subdivided into four different grades of CP Titanium and two different Titanium alloys, all of which exhibit significantly different mechanical and physical properties [29]. Titanium is used as a dental implant base material for multiple reasons, as it is known for its strength, abundance of mining opportunity, and for the special trait that Titanium exhibits. Titanium possess both good biocompatibility and a self-repairing oxide layer that contributes to its passivity [29]. The ASTM Committee F-4 on Materials for Surgical Implants recognizes four grades of commercially pure Titanium, grades I through IV, and two alloys, Ti-6Hl-4V and Ti-6Hl-4V extra low interstitial [30]. Apart from Titanium, other implant materials include stainless

steel and Cobalt-based alloys [29]. The predominant reason neither of these materials is more commonly used is due to their less desirable corrosion resistance as compared to Titanium based materials, although the Cobalt-based materials fare better due to an oxide layer similar to Titanium. The choice of implant material is dependent upon implant size, as well as the area of implant and how large the occlusal forces are in the specific patient's mouth.

Table 1: Mechanical properties of selected materials, appropriated from [30]

Material	ElasticModulus (GPa)	Ultimate Tensile Strength (MPa)	Yield Strength (MPa)	Elongation (%)	Density (g/cc)
cp grade I Ti	102	240	170	24	4.5
cp grade II Ti	102	345	275	20	4.5
cp grade III Ti	102	450	380	18	4.5
cp grade IV Ti	104	550	483	15	4.5
Ti-6Al-4V ELI	113	860	795	10	4.4
Ti-6Al-4V	113	930	860	10	4.4
Co-Cr-Mo	240	700	450	8	8.5
316 L steel	200	965	690	20	7.9
Cortical Bone	18	140	n/a	1	0.7
Dentin	18.3	52	n/a	0	2.2
Enamel	84	10	n/a	0	3

As can be seen from Table 1, the material properties of the metals used in implants vary greatly. If a patient has a history of aggressive biting habits or implant fracture, it is suggested to choose a Titanium alloy rather than a grade of CP Titanium [29]. Additionally, smaller diameter implants may use Titanium alloys for higher strength, or surgeons may choose to consistently use higher grade Titanium or Titanium alloys so they can feel comfortable with the implant procedure.

Although Titanium is a very useful base material for dental implants, there are potential side effects of a Titanium base, including allergic reactions as well as nonspecific immunomodulation and autoimmunity [31]. Amongst the most prevalent concerns are aesthetic

because some patients would prefer either custom made implants or do not like the appearance of the currently available Titanium based implants. Because of both of these disadvantages, novel implant designs made from ceramics such as Zirconia have become attractive because they are considered to be inert in the body as well as exhibiting minimal ion release compared to metallic implants [31]. Zirconia based implants are theorized to produce similar levels of osseointegration and stress distribution compared to Titanium implants. Additionally, Zirconia particles may have the potential to improve initial bone healing and torque removal resistance [31]. While there are reports indicating that Zirconia based implants provide satisfactory results, there are very few, and currently not many explore the long-term performance of these Zirconia implants. Further studies have concluded that most of the current results from Zirconia based dental implants are short term and have very few participants, and the results are considered to be suspect [32]. Further study is suggested to get a more complete understanding of the behavior of Zirconia implants.

There are many different coating options for dental implants, including: calcium phosphates, Titanium nitrides, carbon, glass, and Titanium dioxide. One of the primary reasons these coatings may be used is to promote healing for osseointegration [33]. Since the surface of a dental implant is the only part that is in contact with the bio-environment, it stands to reason that the surface of an implant will have an effect on the level of the implant-tissue interface. Surface coatings can be either added material, like Titanium nitrides, or can be produced through machining effects, such as producing rougher surfaces. Surface treatments have been found to control bone cell growth and metabolic action, and promote bone apposition [33]. Additionally, rough surfaces promote cytokine and growth factor production by bone cells, which directly increases bone cell propagation.

2.2.2 Hardness-Yield Relation

One of the goals of this study is to provide a computational model that can act as an estimate of the stresses produced during the machining process for the various dental components provided by the dental laboratory. As such, a relation between the experimentally determined hardness values and the residual stresses produced through the machining processes needs to be determined. An investigation by Takakuwa et al. [34] was performed on finding a method to use Vickers hardness results in order to estimate the yield stress of a metallic material

while also taking residual stresses into account. Takakuwa et al chose to use Vickers hardness testing because of the dependency on both the yield and the residual stress, and experimentally examined both residual stress and Vickers hardness values. A simple method of estimating yield stress for a material, without residual stresses, based on the Vickers hardness results, was proposed and validated by Tabor [35]. This method showed that the Vickers hardness and yield stress held a linear relationship. Also, the method proposed by Takakuwa et al. [34] discovered a linear relationship between the Vickers hardness and the stress produced in the experimental workpiece.

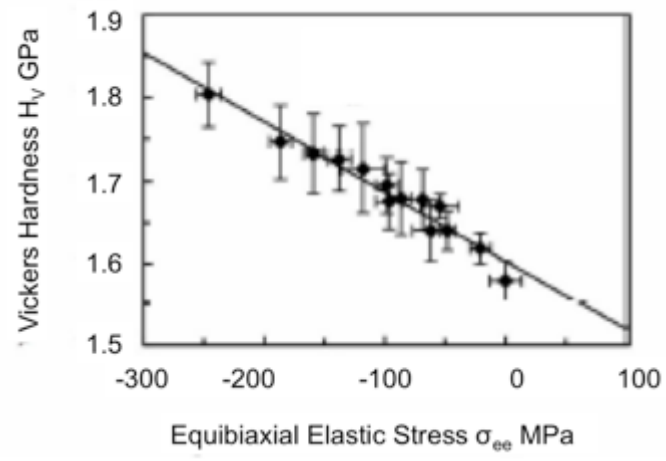

Figure 10: Vickers hardness-residual equibiaxial stress relation [34]

As can be noted from Figure 10, the relationship is linear. Although the article by Takakuwa et al. [34] only experimented with stainless steel and various forms of peening, it is asserted that similar trends will hold for other metallic materials that exhibit similar mechanical behavior. Additionally, a study by Kumar [36] tested the relationship between surface roughness and micro-hardness of the machined surface and established a correlation.

2.2.3 Strain Hardening

Strain hardening can be simply summarized as an apparent increase in yield strength. As a material is deformed past the elastic recovery stage, and into the plastic deformation stage, a higher level of stress is necessary in order to produce additional plastic deformation. Strain hardening reduces the ductility of a material, but ends up producing a higher yield point, thereby strengthening the material. As a general rule, a high strain hardening ability has been widely

accepted to imply good formability, promoting investigation into enhancing the strain hardening rate [37]. From a microstructure viewpoint, strain hardening occurs due to the inhibition of non-coplanar slip by dislocation pile-up and storage at matrix boundaries [37]. Because of the dislocation changes exhibited through strain hardening, most materials will exhibit less ductility, as there becomes fewer locations for dislocations to move to. This nature of metals gives rise to an increase in toughness, yield strength, and ultimate strength, however decreases the ductility of the material [38]. Research by Nan et al. displays a relationship between strain/stress rates and hardening effects in Titanium alloy [39]. Strain hardening through cold work will produce residual stresses in the worked material [38], and these residual stresses will alter material properties. For example, compressive residual stresses produced through strain hardening will inhibit tensile crack propagation, which thereby improves fatigue life by eliminating factors that could cause stress concentrations. The effects of strain hardening do not usually extend through the entirety of the workpiece, generally being limited to a surface depth of between 150-250 μm [36].

2.3 Manufacturing of Dental Implants

In this subsection, forms and methods of dental implant fabrication are introduced. Manufacturing of dental components can be performed in multiple fashions, such as: machining, casting, and sintering. While machining has been found to produce smoother and more accurate surfaces [40], there are many considerations to take into account, such as the impact the machining process may have on the physical and mechanical properties of the implants.

2.3.1 Micromachining of Dental Implants

During the manufacturing of dental implants, the components may go through many different types of processes. These processes include: boring, milling, turning, drilling, and broaching. Specific to the abutments and screws, a common progress of processes follows the steps of: turning, drilling, boring and milling (for the abutments) or broaching (for the screws).

All of these processes may be performed on a machine operated by computer numerical control (CNC). The first process, turning, is the removal of metal from cylindrical parts [41]. Turning removes material from the outer layer of a rotating workpiece as the tool bit moves

linearly across the surface of the workpiece. During the implant fabrication process, turning is used to achieve the surfaces for both the abutments and screws, as well as the threading for the screws. The cutting speed of a turning process is given in surface feet per minute (sfpm) and relates to the speed of the workpiece in regards to the stationary tool bit at the cutting surface [41]. Other important parameters include the feed rate, measured as unit distance per revolution, cutting depth, rake angle, and edge radius. The rake angle and edge radius are geometrical factors of the tool bit itself, however they also have impacts on the fabrication of the workpiece.

The drilling process consists of creating a hole of circular cross-section in the center of the abutments. These holes are smaller in diameter than the final product, and serve as pilot holes for the boring process that comes afterwards. Drilling may be performed either as a single continuous motion, or may be done in small segments, in order to remove material filings from the drill bit and to help reduce heat build-up.

Boring is performed after the drilling process, and is the enlargement of a previously fabricated hole. The boring process is used to remove the material on the inside of the abutments so as to produce a more accurate interior surface, perform the inner threading cycles, and to produce the interior taper. Similar to turning, boring is simply the same process but on the inside of a workpiece, instead of the exterior. Specific to the boring and turning processes are the threading procedures. Problems arising during the threading cycles can be attributed to multiple factors, the vast majority of problems that occur during threading may be solved by changing basic operating parameters. For example, torn threads on the workpiece may be resolved by: using a neutral rake angle, altering the infeed angle, decreasing the chip load, increasing coolant concentration, or increasing sfpm [41].

Milling is a cutting process involving the removal of material similar to drilling, however milling bits move horizontally across a workpiece instead of vertically. In regards to the abutments, this produces the flat face on either side of the main body of the abutment. One of the characteristic features of milling is that each tooth of the cutting tool takes a portion of the stock off in the form of small individual chips [41]. An important factor of the milling process is the number of teeth on the cutting tool. As example, the suggested feed per tooth for Titanium and Titanium alloys for the end mill used in the manufacturing process is 0.007 inches per tooth [41].

Broaching is a precision machining operation where a broach tool is either pulled or pushed through a hole in the workpiece or over a surface in order to produce a very accurate

shape such as a hexagon, spline, keyway, etc [41]. A broaching tool has multiple cutting teeth, which increase in depth along the axis. These progressive teeth take less material off per progressive tooth, starting with a rough cut and forming to a more accurate cut as the teeth progress. The broaching process is used during screw fabrication in order to produce the hex head insert.

In a metal turning process the rake angle has a great effect on the cutting forces [42]. Increasing or decreasing the rake angle will change both the cutting force and power of the process. The cutting angle may be either positive or negative, with a negative rake angle producing a more blunt tool edge, but increasing the strength of the cutting edge as well as friction, which results in higher temperatures [42]. Positive rake angles make for a more sharper and pointed cutting edge, reducing the cutting forces and power requirements and helps in continuous chip formation [42]. Increases in feed rate will also tend towards increases in cutting forces on the tool bit. Additionally, higher cutting speeds will increase the temperature at the tool tip [42]. Higher cutting speeds and honed tool cutting edges will result in a significantly lower tangential cutting force [43]. All mechanical machining processes are associated with heat generation, and except for dry machining, fluids are used for both cooling and lubrication in order to reduce the friction produced between the cutting edge of the tool tip and the workpiece [44]. For fluids, either water-based or oil emulsions may be used, which are either flushed or applied as a mist.

2.3.2 Heat Effects, Residual Stress, and Microstructure Changes

When performing machining routines, heat is generated not only by the contact friction between the tool bit and the workpiece, but also by the machine itself. The heat that flows into the cutting tool and workpiece during machining is an important factor that affects product dimensional accuracy and surface integrity [45]. Since heat generation will cause thermal expansion in a material, it is important to be aware of potential concerns overexpansion could cause, such as inaccurate product dimensions, increases in stresses, and rough surface finishes. Heat removal from a workpiece happens from chip formation and coolant application, as well as heat flow through the tool bit. Heat flows from the workpiece into the chip and coolant (if used), and is dispersed along with the ejected chip and coolant. When higher levels of heat are stored in the workpiece instead of being removed, it produces higher levels of Von Mises stress, especially

around the area of tool-chip interface and workpiece surface [45]. As the level of stress rises, the stress contours are extended into the machined surface of the workpiece [45].

Thermal effects from the cutting process may also produce a significant impact on the residual stresses produced in the workpiece [46]. Residual stresses result from removing an initial cause of stress in an object, yet still having stresses left over even after the initial cause has been removed. These stresses can be either compressive or tensile in nature, and have an impact on the fatigue life, corrosion cracking resistance, and shape of a component [47]. Factors that impact the results of residual stresses in machined components include cutting parameters and tool geometry [46]. Residual stress in machined components is important to consider because of the effect it has on the surface layer of the component. Residual stresses are most prevalent towards the surface of a machined component and, since fatigue characteristics of most materials are more sensitive to surface conditions than internal conditions due to environmental invasion and maximum loading on the surface [48], play a role in the fatigue life of components. Residual stresses are not necessarily bad, however, as compressive stresses at the surface of a component inhibit crack growth, they thereby increasing the fatigue life [46]. While these compressive residual stresses can assist in increasing fatigue life, the residual stresses also run the risk of negatively impacting dimensional tolerances, surface finish, and part quality. Thermal and tool geometry play a major role in determining residual stress distributions in machined components [45]. For thermal effects, researchers have shown that increased cutting temperatures produce higher tensile residual stresses on the surface of a machined component [49]. In regards to the tool bit geometry, one of the key influencing factors is the tool tip radius, referred to as the hone radius. Smaller hone radii will produce less maximum residual stress, both axial and hoop, as well as having a more shallow depth for the residual hoop stress [45]. Larger radii will produce higher maximum residual stress values, however axial stresses will have a more shallow depth profile. Smaller hone radii correspond to “sharper” tool tips, whereas larger hone radii correspond to more “blunt” tool tips.

Microstructure changes are greatly impacted by the heat generation, especially when considering Titanium alloys, as Titanium alloys have low thermal conductivity and high strength at elevated temperatures [50]. A study by Ginta and Amin [51] tested milling conditions of Ti-6Al-4V Titanium alloy in both high temperature and room temperature scenarios. The study discovered that at high temperatures, strain hardening and grain growth occur, which was

confirmed via micro-hardness distribution beneath the surface. Additionally, for the high temperature machining, there was found to be a greater amount of build-up of chip fragments, thereby depreciating surface quality. In the case of room temperature machining, there was no grain growth or microstructural changes observed [51].

2.3.3 Potential Defects During Micromachining of Dental Implants

The machining process is not perfect, so during any of the previously mentioned machining operations, defects may be produced. The machining process can produce: chipping, microcracks, poor surface roughness, holes, inclusions, metallurgical changes, and inaccurate tolerances. While these defects can occur during the machining process, it is also possible for defects to be carried over from earlier processes, such as the initial formation or alloying of the bulk material [52]. Defects that may be introduced during the bulk material processing stage will enter the fabrication stage, and run the risk of either causing a failure during the fabrication stage or during the service stage of the component [52]. The defects that may occur before the machining stage include holes and inclusions. Inclusions create films along grain boundaries, which can cause low ductility at hot working temperatures [52]. Additionally, during further working stages, inclusions may become elongated and aligned in the direction of working, resulting in poor transverse properties and areas susceptible to fatigue failure due to local notch effects [52]. During the actual component fabrication process, the more commonly seen defects are: microcracks, edge chipping, and burs. Microcracks and edge cracks perpendicular to the workpiece are especially important when the direction of cutting is performed axially along the workpiece, as it has been discovered that bending strength is negatively impacted by edge cracks caused by axial cutting procedures [53]. Additionally, the amount of material removed per pass is also a factor in producing defects, as larger removal rates contribute to surface defects and therefore poor mechanical strength [53]. For these reasons, it is important to select appropriate machining parameters in order to reduce the possibility of defects occurring during the machining processes.

2.4 Modelling and Machining Process

In this subsection, numerical modelling and analysis procedures and basis are reviewed.

2.4.1 Modeling and Machining Overview

Finite element models capable of accurately analyzing a machining process can be used to enhance productivity, increase tool life, and help prevent possible defects in the finished components. Titanium alloys, especially Ti6Al4V, are useful in a wide variety of applications, from aerospace to medical implants. However, Ti6Al4V is difficult to machine, primarily due to its low thermal conductivity [54]. The low thermal conductivity produces a considerable increase in the temperature of the component, especially around the tool edge [54]. Additionally, the chip morphology has a great impact on the thermo-mechanical interface between the workpiece component and the cutting tool [54]. It is important to ensure that the machining processes are modeled accurately, in order to best represent results that would occur during the real-life process.

The processes involved in the creation of the components received from the dental laboratory include: turning, boring, drilling, and broaching. Each individual process may have different effects on the state of the workpiece, and thus must be analyzed individually before being analyzed as a whole [55]. There are two main focuses for current machining simulations: orthogonal and oblique.

The orthogonal model is a 2-D model dealing with two forces from the tool bit, whereas the oblique model is 3-D and uses three forces in the analysis [55]. There has been a great deal of work that has been focused on determining machining performance using both orthogonal and oblique methods. Many have concluded that it is necessary to understand the orthogonal approach in order to model various machining procedures, as it is generally the basis on which subsequent models are created [56]. During orthogonal cutting, the cutting edge of the tool piece is considered as being perpendicular to the direction of motion of the workpiece. For the oblique models, the tool edge is not only inclined in regards to the workpiece, but also inclined to the direction of motion. While it may be true that the ideal orthogonal process can be used to approximate an actual machining process quite closely, the orthogonal process may not be able to accurately predict or analyze chip formation [56]. The oblique method of modeling a process, while significantly more complex, allows better chip formation analysis in a three-dimensional setting.

2.4.2 Meshing Models

In order to get an accurate result when running a simulation, it is important to consider the properties of the material, construct and compound being simulated. In finite element analysis, points of interest, called nodes, are generated at the vertices of a grid known as a mesh. There are three main styles of meshing: Eulerian, Lagrangian, and Arbitrary Lagrangian Eulerian, and each have their own positive and negative aspects.

2.4.2.1 Eulerian Meshing

A simple way of thinking of the Eulerian style mesh is to think of the mesh like a riverbed. The body of interest is the river flowing through it. The Eulerian mesh is more of a background mesh, where the body of interest moves relative to a fixed mesh. The coordinates for the nodes on a Eulerian mesh are fixed, whereas the material points will vary with time. The Eulerian style of mesh has the benefit of being able to handle large distortions easily, however, the accuracy tends to be the tradeoff [57]. Unfortunately, boundary conditions and interface conditions become difficult to apply, as the boundary nodes on the mesh may not line up with the material boundaries.

2.4.2.2 Lagrangian Meshing

The Lagrangian mesh solution is similar to a tattoo; the mesh is applied to a material, and will move along with the material. Lagrangian algorithms are usually used in structural mechanics, as it allows for easier tracking of free surfaces and interfaces between materials [58]. The weakness of the Lagrangian method is that it is unable to follow large distortions without the need to rebuild the mesh [58]. This can lead to extreme mesh distortions, if not properly accounted for.

2.4.2.3 Arbitrary Lagrangian Eulerian

Due to the limitations on both the Eulerian and Lagrangian approaches, a combined form, the arbitrary Lagrangian-Eulerian (ALE) description, was created. For the ALE description, the nodes of the mesh may be moved with the continuum in Lagrangian fashion, or they can be held fixed as in the Eulerian method [58]. The nodes can also be specified to move in a completely

arbitrary way, so as to allow for continuous rezoning of the mesh [58]. This allows for greater distortions than a purely Lagrangian method, but gives better resolution than a purely Eulerian method [58].

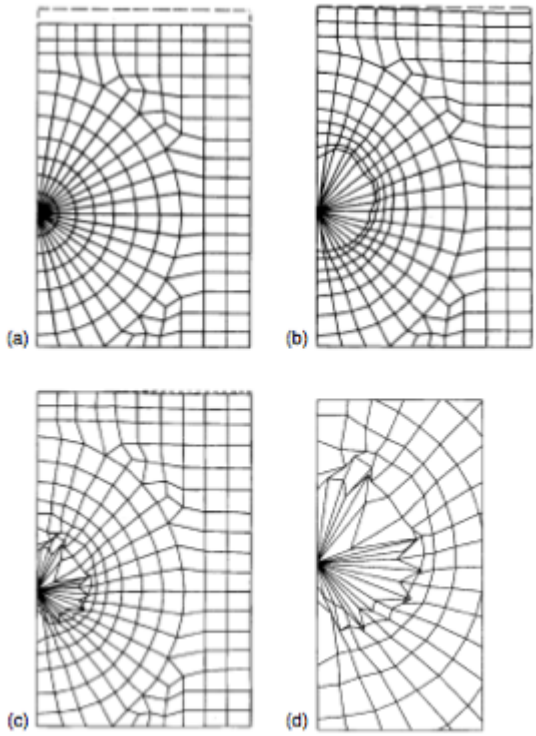

Figure 11: Example of ALE vs. Lagrangian mesh: a) initial mesh; b) ALE mesh after 1 ms; c) Lagrangian mesh at 1 ms; d) interface in Lagrangian description [58]

2.4.3 Turning Models

Turning models can be broadly categorized by four different aspects of the modelling process. These aspects are: style of meshing, two or three dimensional modelling, element type, and tool cutting edge.

The first model aspect, meshing style, is determined by the rules attributed to the meshes of the simulation. These rules can be attributed to the Eularian or Lagrangian style, or a combination of the two. Most software programs will offer the choice of Eularian or Lagrangian meshes, although some programs, such as Deform 2D, have an implicit Lagrangian meshing style [59]. Most models rely on the Lagrangian approach with a remeshing aspect. The models of Umbrello, Muhammad et al., Styger, and Nieslony [59–62] all use a Lagrangian style of meshing, whereas Strenkowski [63] uses an Eularian approach instead. Due to the nature of the

simulation being dynamic, and the focus being on the workpiece, the more apt style of meshing is Lagrangian in. The reason for Strenkowski not specifying a Lagrangian mesh style is due primarily to the fact that the model was not analyzed as a computer based simulation, but rather as a purely numerical model. Thus, the style of mesh was chosen based on a steady state cutting process instead [63]. Since the simulation presented in this paper has a focus on the changing workpiece, and since complications within the usable software with the ALE meshing option caused either failures or a drastic increase in computation time for similar results, a Lagrangian approach was decided upon.

The second aspect is whether to choose a two-dimensional or three-dimensional model. Out of the models presented in this paper, two models are presented as two-dimensional considerations, one is explicitly three-dimensional, one is three-dimensional using a two-dimensional base, and the final model proposes both a two-dimensional and three-dimensional model. Both two-dimensional models proposed by Umbrello and Styger respectively, are primarily concerned with only one single aspect of the analysis. The model proposed by Umbrello is a model to specifically predict the orthogonal cutting forces, and to compare different literature values for Johnson-Cook constants to see how they compare against the retrieved experimental data for both high speed and nominal speed turning processes [59]. The two-dimensional model proposed by Styger has as its core focus a comparison of different temperatures/strain rates used for measuring the Johnson-Cook parameters of three different models [61]. In the Styger model, a two-dimensional simulation is proposed precisely because the main focus is not the process as a whole, but the specific effects of select parameters. The paper from Styger also concludes that orthogonal models provide a reasonable degree of accuracy provided that there is a specific criterion of assessment [61]. The model proposed by Muhammad [60] is an explicitly three-dimensional model that focuses on the results in terms of cutting forces on the tool bit and thermal conductivity. The model proposed by Strenkowski [63] uses an orthogonal basis finite element model and couples it with a numerical three-dimensional cutting model. The entire cutting process for three-dimensions was treated as a series of successive cuts [63]. The cutting data for each slice was taken from orthogonal cutting tests [63]. Overall, the model showed good correlation to experimental test data [63]. Both an orthogonal and oblique model is proposed by Nieslony [62], and the models were created with the intent to determine the distribution of residual stresses in the sublayer of machined parts. After

comparison between both the two-dimensional and three-dimensional models, Nieslony concluded that the results for residual stresses from the two view differ significantly, with orthogonal results being lower than experimental values and 3D results being greater than experimental values, and that three-dimensional model is more accurate [62]. Additionally, both models gave adequately similar results to experimental test data, although the difference between the two was greater due to one being an overestimation and one being an underestimation [62]. Based on the points mentioned above, an oblique modelling system was developed, as there are numerous criteria of assessment, and a higher degree of accuracy was preferred.

In terms of element type, choice is primarily restricted to what the software will allow within the realm of the meshing constituents. For example, Patran-3D offers octahedral elements, however those elements will not work when used in an automatic remeshing environment [60]. The two main types of elements offered by most software that allow for remeshing are tetrahedral and quadrilateral elements. The difference between quadrilateral or tetrahedral elements boils down to three primary concerns: the need to use a remeshing procedure, whether the program restricts certain element types for remeshing, and what type of mesh coverage is necessary for the model. If both element types can be used for remeshing, then the greatest concern becomes model geometry. Tetrahedral elements are capable of meshing for any type of geometry, whereas quadrilateral elements may not be able to accurately cover the model. It is important to note that tetrahedral elements require a much larger number of elements to cover the same area as quadrilateral elements, therefore resulting in overall smaller elements and producing a longer computational run time. For this reason, all other aspects being applicable to both element types, quadrilateral elements are the preferred element type. This consideration is also displayed in the aforementioned models, as the only models to use tetrahedral elements for the non-rigid workpiece were the ones proposed by Nieslony, using the AdvantEdge software, which was not used by any other modeler.

The final aspect that requires attention is the cutting edge radius of the tool bit. The cutting edge of the tool bit cannot always be considered as perfectly sharp, especially after numerous uses on a high strength material. All of the discussed models either incorporate an edged tool bit, or comment on the realism of assuming a “sharp” tool bit against an “edged” tool bit. The model proposed by Strenkowski uses an orthogonal basis that was originally meant only for “sharp” tool bits. Experimental testing provided indications that at significantly higher

cutting speeds the edge radius would still produce adequate results [63]. In the analysis performed by Nieslony [62], on the other hand, it is concluded that, from a practical view, simulations of residual stresses in titanium machining using "sharp" tools cannot be recommended, and cutting tool models should be defined with an edge radius, especially if used in a two-dimensional model. An example of oblique cutting is displayed in Figure 12.

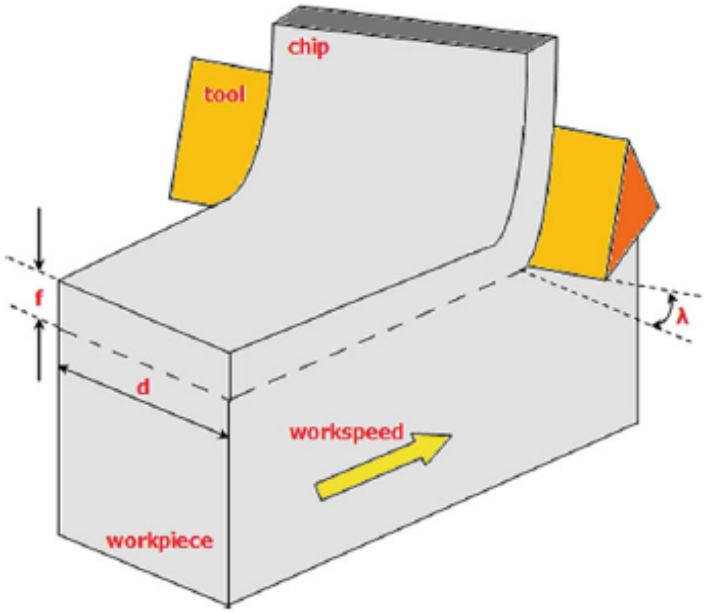

Figure 12: Oblique cutting operation [64]

2.4.4 Broaching Models

Broaching is a machining process becoming increasingly more useful in modern machining, primarily due to the advantages of high quantity of material removal and speed of cutting [65]. During broaching, the cutting tool is comprised of multiple cutting edges, each of which has progressively more depth than the previous edge [66]. Since each of these teeth have a built in feed, the only control the cutting machine has is the speed at which material is removed [67]. When performing internal broaching, as in the case of the interior of the screw head, a pilot hole is drilled, where the broach is pushed or pulled through [65]. The pilot hole is created just large enough for the front pilot section of the broach to enter freely [65]. As the broach progresses through the hole, each successive tooth takes gradually more material away [65].

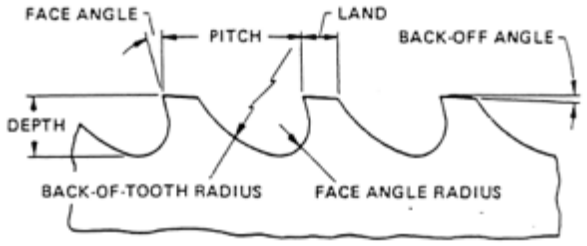

Figure 13: Example of broach teeth [65]

During rotary cut broaching, the teeth are arranged to take deep and narrow cuts [65]. The starting teeth have narrow cutting points and a heavy rise per tooth, which helps for deeper cuts [65]. The semi-finishing teeth are arranged in a staggered pattern of the same height, in order to remove any leftover material from the first group of teeth [65]. The final set of teeth are the finishing teeth, and are used for tolerance accuracy and for producing a smooth surface finish [65].

In regards to various studies on the broaching procedure, not many FEM analyses have been performed, as broaching tools are created primarily by experienced and seasoned workers, using the "cut and try" method [67]. Also, broaching is a highly competitive business market and results in a lot of the tool data or accurate research data being withheld by companies, in order to protect their products. Most of the studies performed on the actual machining process focus on linear broaching instead of rotary broaching. The two processes are similar in nature. Therefore considerations for the finite element models should be similar.

While there have not been many comprehensive models created for computer-based simulations, most of the models that do exist are two-dimensional models. The available models provide evidence that individual cuts of the successive broach teeth do not have a significant impact on following cuts, thereby allowing the process to be simulated as a single cut feature [67]. While it is possible to simulate using only a single cutting tooth, concerns have been raised about whether developed temperatures resulting from a single cut would adequately reflect experimental values [66]. The suggestion for this concern is to set a predefined starting temperature in order to more accurately depict residual stresses [66]. Broaching processes produce predominantly compressive stresses, which cause material bulging and the excess removal of material as a result of the material being forced into the free space of the broach, causing the hole to be oversized [67]. One of the larger concerns, however, is variable cutting

thickness, which Zanger [68] has shown to have an influence on both the residual stresses and the shear angle. From these studies, it can be shown that the work hardening zone usually only extends to approximately 500 μm below the surface of the workpiece [67].

2.4.5 Drilling Models

Drilling models primarily consist of three-dimensional simulations, as opposed to the two-dimensional simulations discussed in previous segments. Three-dimensional models are important for drilling simulations, as there is discrepancy in stresses produced depending on the depth of the drill and the shape of the drill head.

A simple finite element model was produced by Wern [69] using ABAQUS, where a two-dimensional model was created, as shown in Figure 14, and then extended into a cylindrical three-dimensional model by extending more nodes perpendicular to the two-dimensional surface.

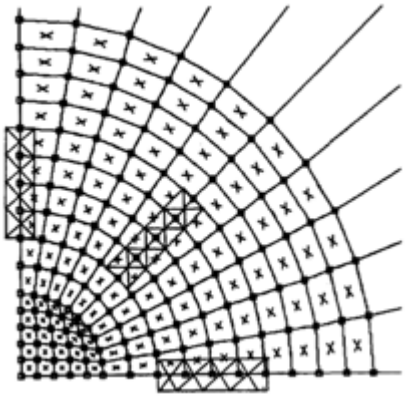

Figure 14: Wern's two-dimensional snapshot [69]

The model proposed by Wern [69] is a symmetric specimen, approximated by three-dimensional 8-node isoparametric hexahedrons. The model was simplified to a quarter section because of symmetry [69]. In this model, the drilling is simulated by gradually removing the effects of influence to the stiffness matrix that the 25 nodes in the bottom left of Figure 14 produce on the model [69]. These 25 nodes represent the hole produced from the drilling procedure. This model is coupled with data produced from strain gauges, denoted by the rectangular segments at 0, 45, and 90 degrees in Figure 14. The conclusion was that by using an integral method basis for analysis, the finite element model can be shown to produce acceptable results, using only material based parameters [69].

For a more extensive model, we can look to the model created by Isbilir and Ghassemieh [70]. The model they created is a three-dimensional model using the ABAQUS program. The model proposed simulates the drilling process by taking damage initiation and evolution of the workpiece into consideration [70]. This model does not include chip analysis or friction between chip and drill, in order to save on computational power. The model uses the Coulomb friction model, with a coefficient of 0.5, and interaction between workpiece and drill bit is modeled by surface-surface kinematic contact. Isbilir and Ghassemieh [70] used the flow stress model by Johnson-Cook, and the related damage model for titanium, in order to properly simulate material behavior under large deformations due to cutting.

Based on the results shown in Figure 15, Isbilir and Ghassemieh concluded that the model produced good estimation of thrust force whereas torque was overestimated by 20% and burr height was underestimated by between 50-75% [70]. The changes in cutting force, torque and stresses were estimated adequately.

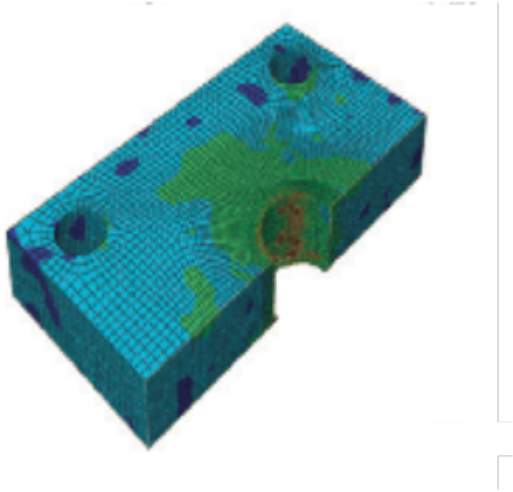

Figure 15: Results of Isbilir-Ghassemieh model appropriated from [70]

2.4.6 Boring Models

Boring is the process of removing material from the inside of a hole, or as a turning operation inside a hole [55]. As such, there are different ways one could treat the process from a modelling perspective. It could be treated as a turning problem, but inside a workpiece, or, depending on tool used, it could be treated as drilling with a preexisting hole.

A finite element analysis that was performed by Kakade and Chow [71] simulated a cylinder that underwent distortions, as can be seen in Figure 16. The analysis used cutting forces as a boundary condition, and primarily focused on the comparison between dry boring distortions caused by thermal and mechanical conditions.

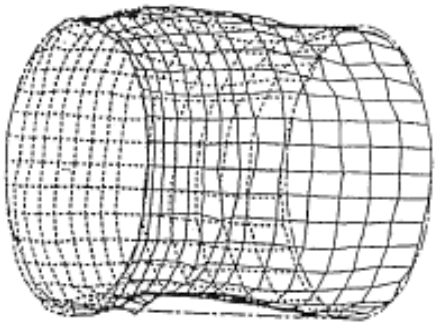

Figure 16: Distorted cylinder after boring [71]

Kakade and Chow came to four major conclusions based on their results. These conclusions were: as cutting speed is increased, there is a notable decrease in distortion; the effects of thermal and mechanical distortion can be studied separately, as mechanical conditions only accounted for roughly 10% of the total distortions; multiple inserts both increase the speed of the machining process and reduce distortions; and the simulation produced results similar to experimental values [71].

3 Methodology

3.1 Experimental Methodology

The Experimental Methodology section covers the physical testing portion of the thesis, which includes: the materials provided for testing, the different methods used for testing and analysis, as well as the procedure used when testing the materials.

3.1.1 Materials and Testing Methods

The dental laboratory provided three batches of four component sets, consisting of one dental abutment and one dental screw. For each batch of four abutments and four screws, three were manufactured at the dental laboratory and one was acquired as a standard market component template. The three components manufactured were produced using differing feed rates: one at the standard feed rate as specified by the equipment supplier, one at 50% of the standard feed rate, and one component at a 150% of the standard feed rate. Manufacturing processes and feed rates were unspecified for the market template components. All prototype components were fabricated using Ti6Al4V Titanium alloy, and it was stated that the template market components were supposed to be made of the same material. In addition to the provided components, leftover blanks were also provided in order to investigate initial material properties.

The components were investigated with respect to their microstructure, hardness, and surface roughness. Optical and Scanning Electron Microscopy were used for an overall inspection; in addition, electron diffraction spectroscopy was used to determine the elemental composition of selected samples. Hardness testing using both a Vickers and a Rockwell hardness tester were proposed, however sample sizes proved to be too small for accurate Rockwell hardness results. Therefore, only Vickers hardness testing was performed. Lastly, grain boundaries and grain deformation was explored by etching the surfaces of the samples with Kroll's Reagent, which is a recommended etchant for Titanium and Titanium alloys.

3.1.2 Testing Set-Up and Procedure

Samples were initially cleaned in an ultrasonic ethanol bath for thirty seconds and then left to air dry before microscopy commenced. Optical 3D microscopy was used to determine if there were any visible surface defects. The abutments were analyzed from four viewpoints, as seen in Figure 17. The four sides of the abutment dictated these four viewpoints, with two views associated with the flat surfaces and two views associated to the curved surfaces.

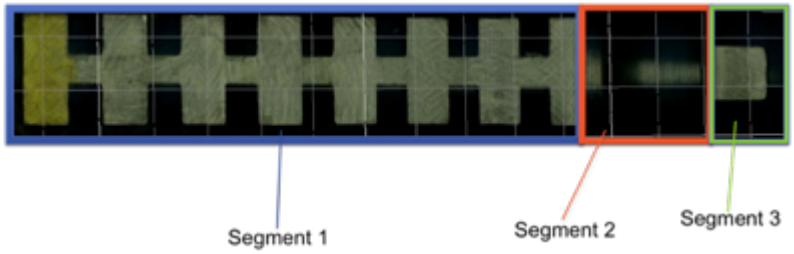

Figure 17: Abutment segmentation

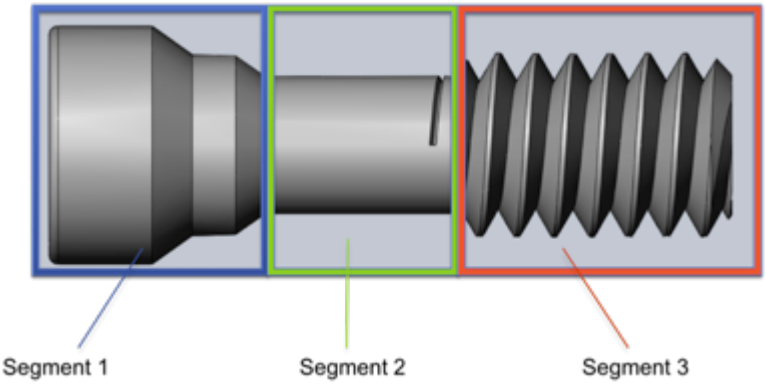

Figure 18: Screw segmentation

The screws, similarly, were divided into viewpoints based on the initial threading rotation at the base of the screw, as seen in Figure 18. Both the abutments and screws were also visually divided into segments related to areas of interest for analysis. After 3D Microscopy had been performed, potentially critical areas were further investigated using Scanning Electron Microscopy (SEM). Electron Diffraction Spectroscopy was then used on selected samples for chemical composition analysis.

After microscopy inspection, samples were prepared for micro-hardness testing. The preparation process of the specimens consisted of mounting the samples in epoxy resin, grinding them down until approximately the middle of the component, and then polishing them to an ultra-fine surface finish using a silica colloidal solution. Ground and polished samples were

cleaned and further images were taken of the mounted samples using the 3D Microscope. The Vickers hardness testing was performed using a Buehler MicroMet 6030 hardness tester, using a 500g indentation load and a ten second dwelling time. Indents were taken across the exterior surface edges of the samples, with a focus on areas where failure would be most likely to occur, such as the interior threads and underside of the head in the screws. Rockwell hardness testing proved to be ineffectual, as the indent eclipsed the specimen area and encroached on the mounting resin, thereby giving inaccurate values.

After the hardness tests had been completed, the samples were once again cleaned, polished, and then etched, for investigation of potential microstructure changes. The etching was performed using a Kroll's Reagent acquired from ES Laboratory, LLC. Etching was performed by brushing each sample with cotton swab that had been dipped in the reagent. The reagent was left on the samples for between eight to ten seconds. The sample was then rinsed, cleaned, and air-dried before further images were taken using 3D Microscopy.

Two of the blanks provided were machined into cylindrical tensile test samples, as shown in Figure 19, according to ASTM standard E8M, with a gauge diameter D of 6mm and a gauge length L of 30mm.

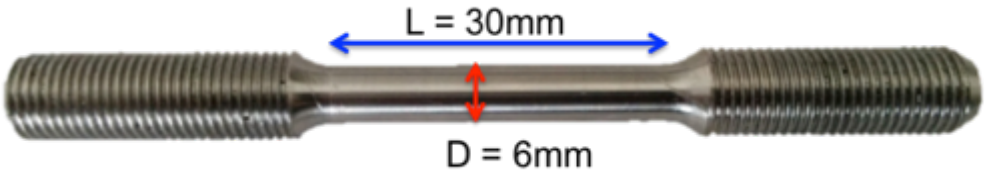

Figure 19: Rod type tensile sample

This standard corresponds to the 5-to-1 ratio for rod type specimens from the ASTM guidelines. The tensile samples were tested using a universal Instron 4482 testing machine at a strain rate of 0.15 mm/s. The necking and fracture regions, as well as the undeformed regions, were mounted in epoxy, ground, and polished in the same manner as the screws and abutments. They were then investigated visually and using a 3D microscope, as well as tested for hardness and strain hardening using Vickers hardness testing. The undeformed blanks were used as a baseline for strain hardening comparison.

3.2 Computational Modeling

The computational modeling section provides an overview of the program used for the modeling procedure, as well as outlines various set-ups and values used during the simulation process. Numerical modeling was chosen as a method to examine dental implants that were otherwise too small for a large range of standard testing. Since numerical modeling does not require physical components to be made, apart from verification, this provides companies a powerful tool to examine and test both prototype components and manufacturing processes without destructive testing or using potentially expensive materials.

3.2.1 Software and General Overview

The software used for the modeling process was ABAQUS. The ABAQUS finite element analysis program is especially useful in defining and analyzing non-linear problems, such as contact. Its design for use in production environments makes it a reliable choice to use for modeling the manufacturing processes associated with this work. ABAQUS/Explicit was used in the formulation of the models. Basic model parameters, such as material data, were applied across all the models. Workpieces were modeled with Ti6Al4V material properties, using Johnson-Cook constants to determine plastic deformation and material and damage evolution. Tool bits were modeled using average values for tungsten carbide bits. As the specific material composition and tool bit properties were not specified by the dental laboratory, average values and material properties associated with the machining of titanium alloys were used for cutting tools with Tungsten-Carbide coating. Meshes were defined using explicit elements with available element deletion. General contact was defined, with a friction penalty induced upon contact. Frictional coefficients used were determined to be within the range of 0.1 to 0.2, based on the suggested lubricants for cold forming and threading processes. An average value of 0.15 was used for the models. All models were created within ABAQUS with as much accuracy as was allowed.

3.2.2 Layout of Models

Models were produced in accordance with the models discussed in section 2 by adopting the most appropriate aspects from different models that functioned within the ABAQUS

program, with adjustments made in order to reflect specific machining conditions and parameters. The drilling model was created by having a rotating tungsten-carbide drill bit intersecting with a half-plate of titanium alloy. The half plate was used due to symmetrical effects, as well as to reduce computational time. The drilling process consists of three steps; initial penetration, the "back-off" step, and then the final penetration to the intended depth. Drilling of the screw head used a 1.27mm drill turning at 3000 rpm. The hole was drilled to a depth of 1.3mm in a step of one millimeter, followed by the drawback, and then another step to the full 1.3mm depth. The drilling set-up, seen in Figure 20, represents the general half-panel drilling format used for the analysis. The drilling set-up shown was determined by testing various shapes for the initial workpiece. A cylindrical workpiece required different element types in order to process the analysis, and residual stresses did not progress up to the edges of the material. Additionally, the symmetrical nature of the process would mean that the residual stresses would be mirrored across the workpiece. Due to these reasons, a half-plate set-up was chosen in order to reduce computation time while still providing acceptable results. The drill bit model is a result of limitations due to the ABAQUS interface, as sharper fluting was not able to be produced without creating a run-time error, and there was no available license to import external models into the ABAQUS simulation.

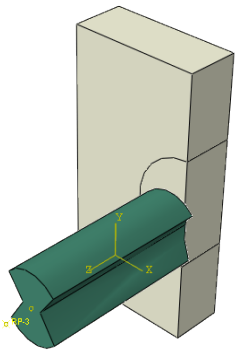

Figure 20: Drilling set-up

The portion in the center is partitioned to provide a greater number of elements, and therefore greater accuracy, in the vicinity where the most material changes are likely to occur. Drill and material thickness can be changed for different drill sizes or drill depths.

The type of broaching performed in the dental laboratory's manufacturing process was rotary broaching. This broaching process was modeled in a similar fashion to the drilling model, with the exception of the rotation. The broaching tool is inserted into a prefabricated hole, to represent the drilling process that would have occurred prior to the broaching. The broaching is only performed for the head of the screw, and uses a "custom broaching tool" dictated directly by the prototype provider. The broaching tool reaches a depth of 1.15mm. Since both the tool bit and workpiece are spinning at the same speeds during the process, the analysis does not include rotation for either piece. The broaching set-up, as seen in Figure 21, consists of the circular grey workpiece and the green broaching tool.

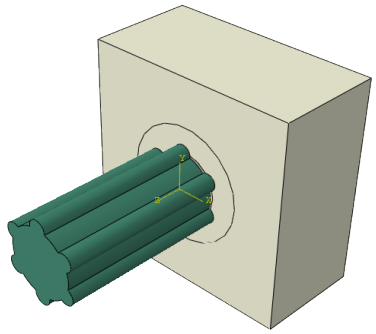

Figure 21: Broaching set-up

Since the broaching tool for the prototypes had neither set dimensions nor a product number, as it was a custom broaching tool, a tool in the general shape of the screw head insert was developed based roughly on the available Torx rotary broaches available from PolygonSolutions. The model created for the broaching procedure was produced following directives of the company liaison.

The turning models were created using a PH Horn RS 274 bit. The tool bit was replicated in ABAQUS using dimensions provided on the Horn website for the indicated tool bit. All of the turning operations were performed using the PH Horn, therefore the alterations to the set-up to reflect different conditions should primarily be speed or displacement conditions of the tool. Based on the available literature results, the turning set-up, as may be seen in Figure 22, was set up as tool bits passing over a brick of material. The example shown in Figure 22 was created to verify that multiple passes over a block of material would have little to negligible impacts on

successive cuts, as indicated by the literature. Tool speed was determined by translating the rpm of the workpiece into a linear velocity by using the final diameter of the workpiece. In addition to the multiple cut analysis, a heat analysis was also performed to determine how large of an impact heat effects would have on the production of a single piece.

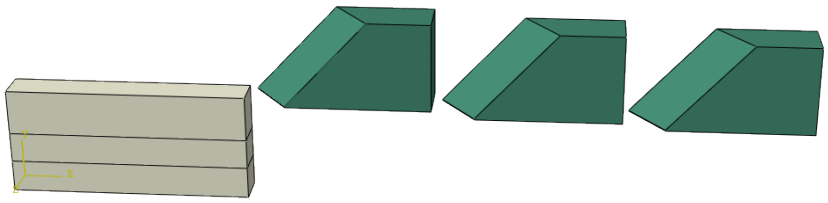

Figure 22: Turning set-up

As can be seen from Figure 23, the simulation process for determining heat effects is largely similar to the previously mentioned turning model. The primary differences being: a single tool bit passes across the work surface, and element types are changed to accommodate a combined thermal-displacement system.

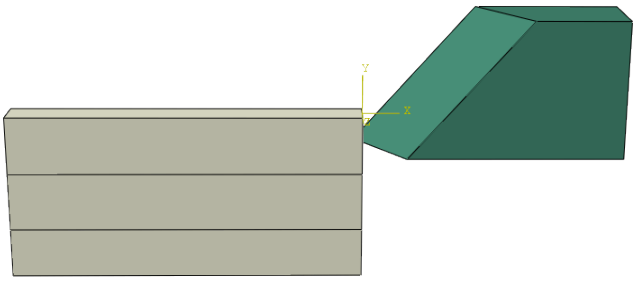

Figure 23: Heat and mechanical combined testing

The turning models presented are based on the set-ups provided in the literature review section [59-64]. The examined literature indicated that the presented models would provide an acceptable level of accuracy when compared to experimental results.

The boring models were created in a similar method as the turning models, as the boring process consists of a process similar to the turning process, except on the interior of a component. The boring process, used exclusively for the abutment fabrication, uses a PH Horn R105 tool. As can be seen from Figure 24, the set-up is similar to the turning operations. The tool dimensions were obtained from the Horn website. Under the same principle, the velocity of the boring tool was determined using the rpm of the workpiece and the final diameter of the machined component.

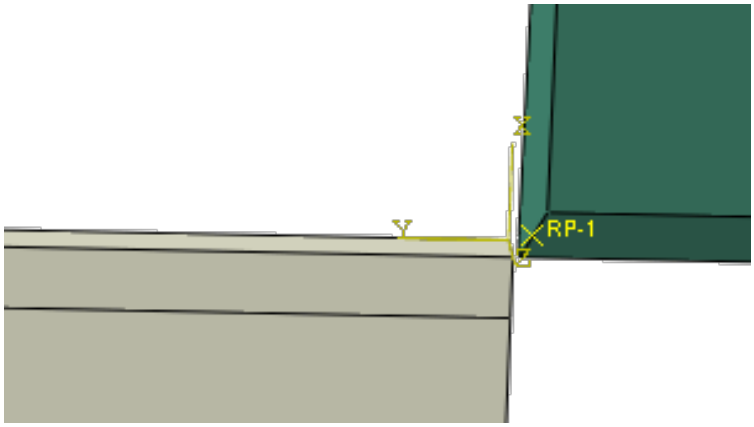

Figure 24: Boring set-up

Similar to the turning operations, the boring set-up is based on the cutting models provided in the literature review [55], [71].

4 Results and Discussion

This chapter presents the experimental and numerical results, and discusses the relationship between observed findings and prior literature findings. This chapter will first present the experimental findings, followed by the numerical findings. Both experimental and numerical sections will present observations and correlations, respectively.

4.1 Experimental Results

This section presents the experimental results obtained by conducting visual and image analysis through the 3D microscopy, SEM and EDS as well as results obtained from the hardness testing, and microstructure analysis results from etched samples. Visual inspection was initially performed in order to both verify and compare design decisions of the prototype and market components received. After visual inspection, hardness testing was performed as a method of comparatively determining the impacts of the machining processes on the property changes exhibited by the Titanium alloy used for the manufacturing of the implant components. Hardness values were compared against results obtained from tensile samples that were loaded to fracture, and then hardness tested along their length. These hardness results were examined as indicators of strain hardening produced through residual stresses produced during machining. Lastly, etching and microstructure analysis of the samples was performed in order to determine grain deformation as a method of both substantiating the results from hardness testing and indicating potential locations of higher stresses and microstructure alterations.

4.1.1 Visual and Image Analysis Results

The initial method of inspection was performed using optical microscopy, and images were taken in order to analyze design aspects of both prototype and market components. Figure 25 shows images of the prototype abutment body in comparison to the market component body. Rounded corners of the ribbed valleys in the retention area of the prototype abutments are found compared to the sharper corners of the market component. In contrast Figure 26, which shows the prototype abutment head regions compared to the market component head, illustrates the sharper corners towards the abutment head in the prototypes as compared to the rounded market

components. Sharper corners can be expected to cause higher levels of stress concentrations, rendering the respective locations more critical with respect to strength and service life. It is well known that stress concentration will increase as the radius of curvature of a crack, or corner, decreases [72]. The sharp corners towards the head of the prototype components will produce areas of stress concentration where the abutments are more likely to develop micro cracks and fracture.

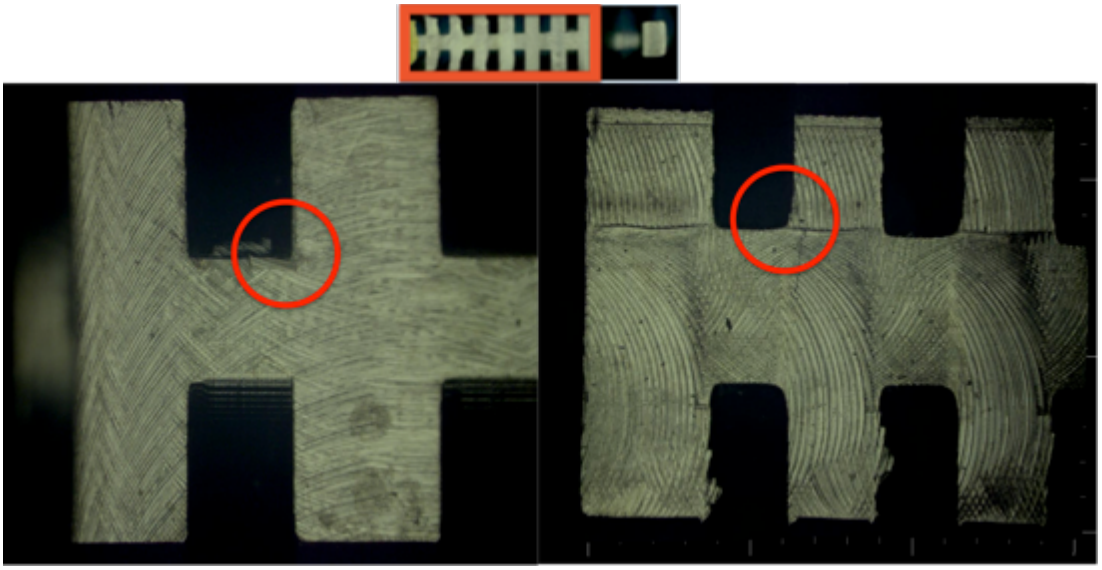

Figure 25: 3D optical micrographs of market (left) and prototype (right) abutments: a more rounded transition radius is observed in the retention valleys of the prototypes compared to market abutments

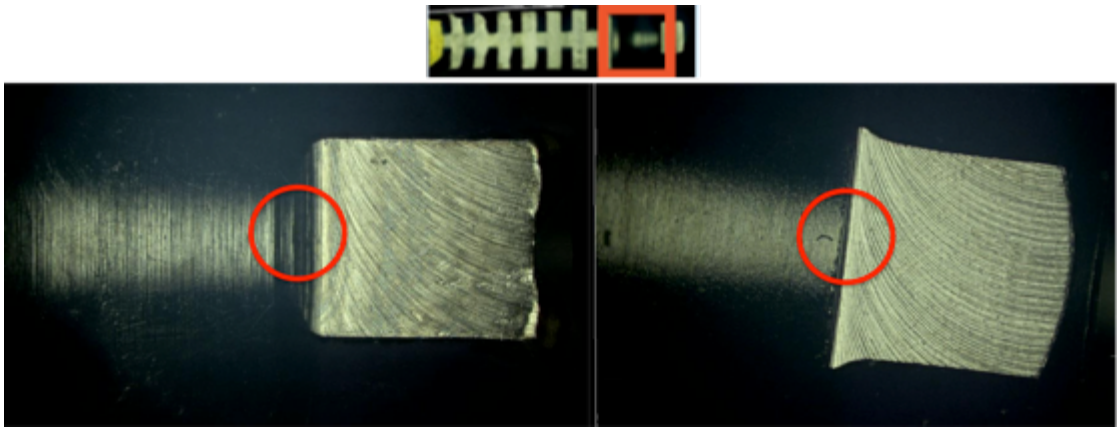

Figure 26: 3D optical micrographs of market (left) and prototype (right) abutments: a sharper corner is observed towards the head of prototypes compared to market abutments

Figure 27 presents the images of the head region of the prototype screws compared to the market component screw. As can be seen from Figure 27, the screws also exhibited visible defects, including divots, indents, and scratches on the screw heads at approximately the same location in all three prototypes of the first set of screws. It was theorized that the indents and scratches were caused by tool holder contact during the machining process and thereafter confirmed with the company liaison that this was the case. This theory was emphasized by the discrepancy in chip sizes between feed rates. Since the higher feed rates remove more material per pass, this means that the tool bit will protrude further into the workpiece during the pass, whereas at the lesser feed rates, the tool bit will be drawn across the surface of the workpiece.

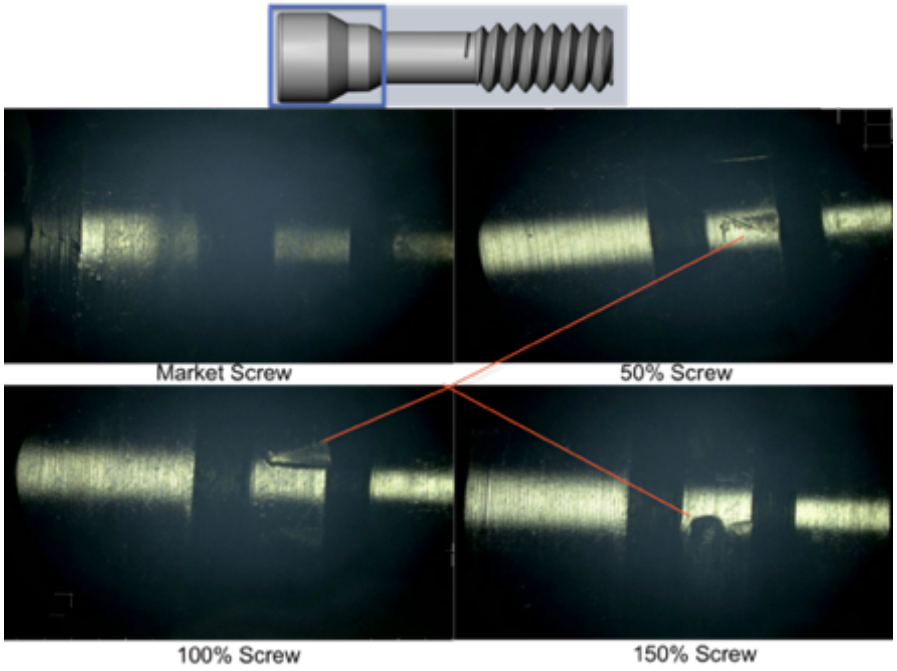

Figure 27: Divots/indents on screw heads of set 1 as seen using 3D microscopy

Additional analysis was performed through the use of SEM imaging, in order to examine potential micro-defects that may not have been visible through traditional visual inspection alone. SEM investigations showed micro-size defects and cracks across most surfaces of both the prototype and market components. Sample images of the defects in the prototypes for both screws and abutments in the second set of samples can be seen in Figures 28 and 29. Similar images were obtained for the market and prototype components of set 1.

In regards to the screws, the stress concentration areas are more likely to be at the sharp corners between the screw head and the body for the 1.4mm screws. The screws from sets one and three had stepped head segments, and are less likely to develop cracks in the head region. The observed stress concentration areas are primarily design choices, and may be solved by having softer radii at the edges and corners of components. Conversely, one may design areas of the implants with sharper radii in order to have the implant fail around a specifically designed area. This is called the fail-safe concept.

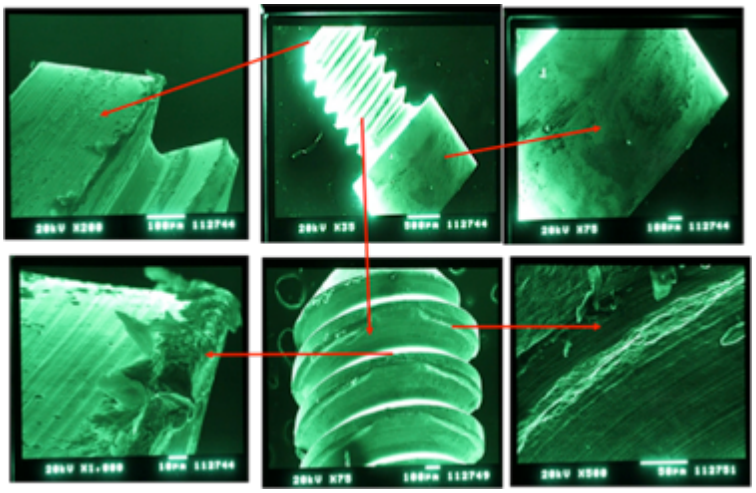

Figure 28: Surface defects and scratches on market screws as seen using SEM

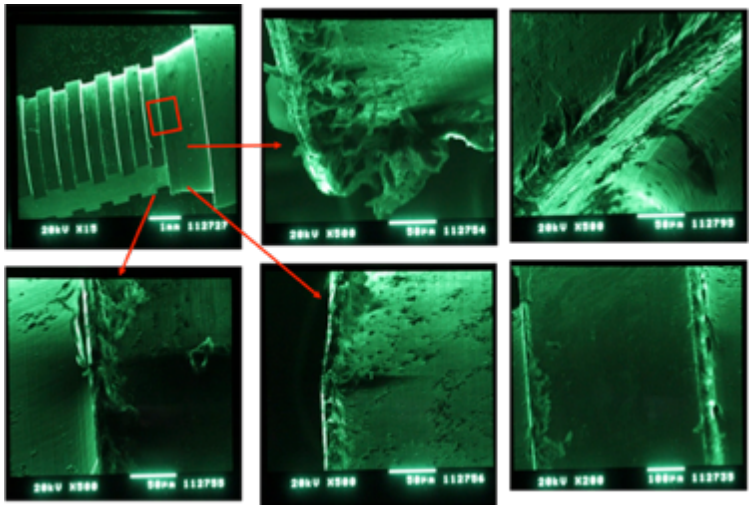

Figure 29: Surface defects and scratches on prototype abutments, as seen using SEM

For the abutments, having the area around the head fail first could cause abutment fragmentation, introducing harmful material shards to both the surrounding tissue and the rest of the mouth and throat. If the abutments were designed to fail just under the head region, the implant would more likely fail as two larger, distinct components. This would also be more beneficial in removing the screw to replace the abutment, as the screw head would thereby be exposed and easily accessible. For the screws, it is more desirable for them to fail around the head region, as opposed to in the threaded region. If the screws were to fail in the threaded region, it would require more work to remove the threaded portion left still attached to the main body of the implant, and would also risk damaging the threading on the inside of the implant body. These failure areas can be seen in Figure 30.

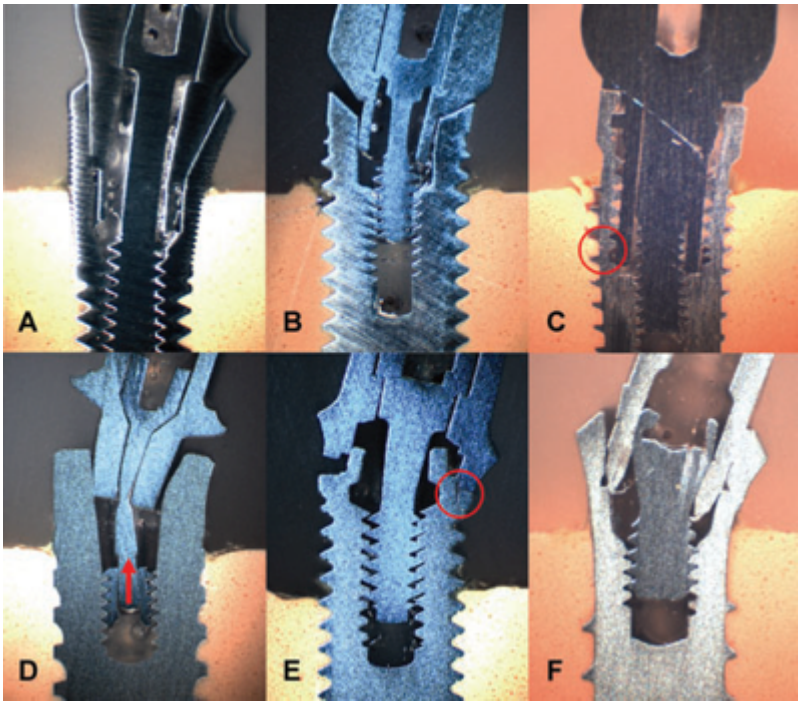

Figure 30: Polished cross-sections of embedded failed specimens of different implant-abutment connection types [20]

4.1.2 Hardness Results

After optical inspection, the samples were examined for property changes as a result of induced residual stresses via hardness testing. The Vickers hardness profiles at characteristic locations along the length of all abutments of sets 1, 2, and 3 are comparatively illustrated in

Figures 31, 32, and 33, respectively. These graphs are representative of the hardness values using a 500 gram weight and ten second dwell time. Positions along the abutment begin at the end of the body and ending at the peak of the head. For the first set of sample abutments, only prototypes manufactured at 100% feed rate were received from the dental laboratory. By examining Figures 31, 32, and 33, it can be seen that the trends in the market abutments (upper left) are similar to the trends seen in the prototype abutments. This indicates that the level of strain hardening is similar in both the market and prototype abutments. The observed differences are small and oscillate within a statistical scatter round a similar mean value.

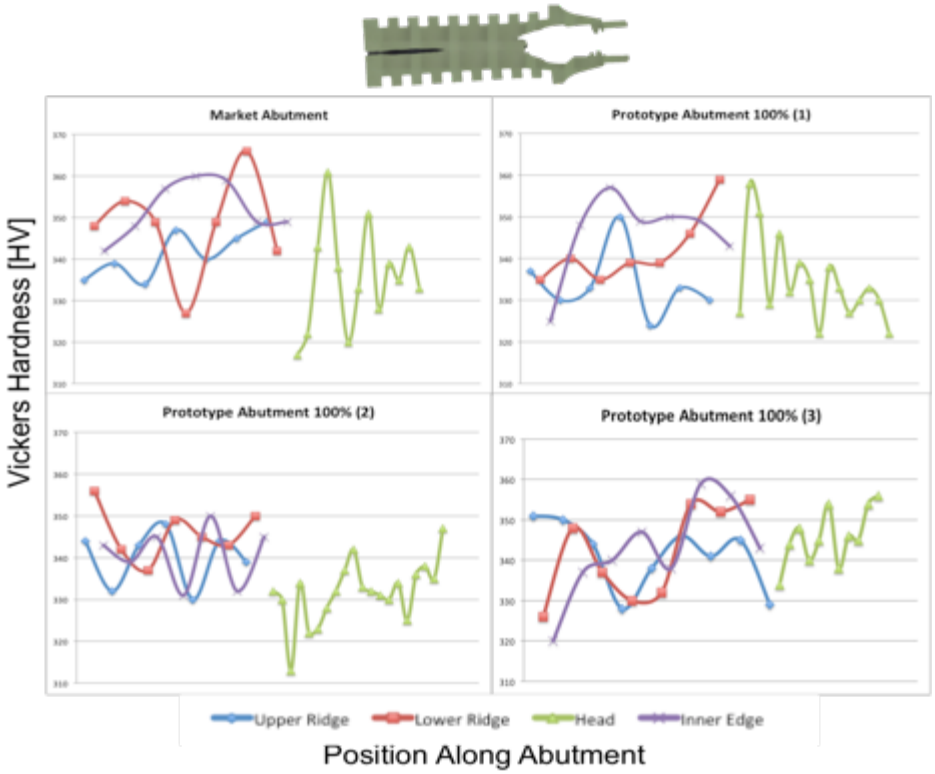

Figure 31: Abutment hardness comparison in set 1

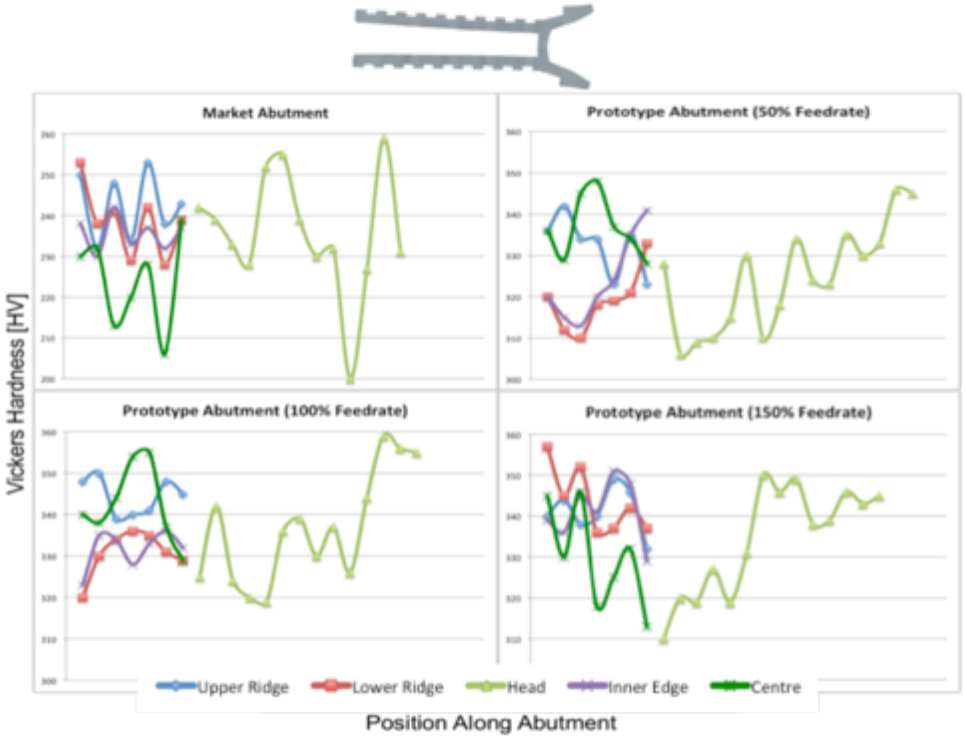

Figure 32: Abutment hardness comparison in set 2

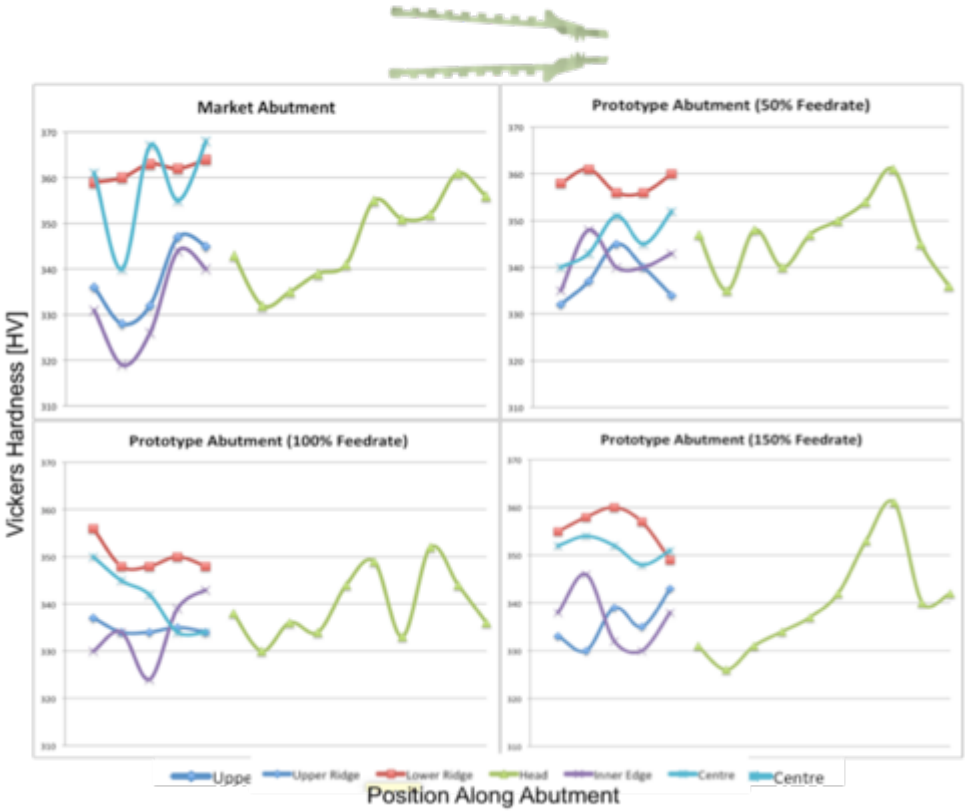

Figure 33: Abutment hardness comparison of set 3

Figures 34, 35, and 36 illustrate a comparison between the most strain hardened prototype abutment components in sets 1, 2, and 3, respectively, with the hardness profile of the fractured tensile samples. These figures are for the most critical abutments discovered during the hardness testing process for each respective batch. A critical component is defined as the component, both screw and abutment, that had the highest hardness values closest to the peak of the failed tensile samples. Therefore, they display the greatest risk of fracture upon additional mechanical loading during use, potentially leading to early fatigue failure. The tensile sample profile is depicted by the two curves approaching the height of the graphs. During the hardness testing process, much lower hardness was noted on the market abutment in set 2. A subsequent SEM-EDS analysis indicated that this market component was made of pure titanium and not the Ti6Al4V like the rest of the investigated samples. Possible reasons for this change in material could be either to reduce the cost of either procuring or manufacturing the Ti6Al4V alloy, or there could be a specific use for the implants in mind during fabrication, such as a transitional implant piece. While it has been shown that, experimentally, commercially pure titanium and Ti6Al4V exhibit similar machined surface morphology, topography, phase composition, and chemistry, it is not certain whether long term effects, or actual *in vivo* testing, will reveal any distinct differences between the two base materials [73]. While *in vitro* testing failed to disclose many differences between the two materials from a dentistry perspective, at the time there are no comparative clinical studies which could provide insight as to whether one material is superior to the other. It should be noted, however, that Ti6Al4V is significantly stronger than pure titanium, yet still has the same stiffness and, apart from thermal conductivity, very similar thermal properties. An additional benefit is that the titanium alloy is fully heat treatable, allowing the material to undergo precipitation hardening. The hardness values for the prototype abutments tend to average approximately halfway between the failure hardness levels and the undeformed blank hardness levels of the tensile sample. This implies a safety factor of about two for both the prototype and market components with respect to failure under tensile loading. As such, the components are considered sufficiently safe for use. Additionally, the prototype abutments tended to have slightly lower hardness values in the body sections than the market components, and the head area of the prototype abutments was the primary critical location.

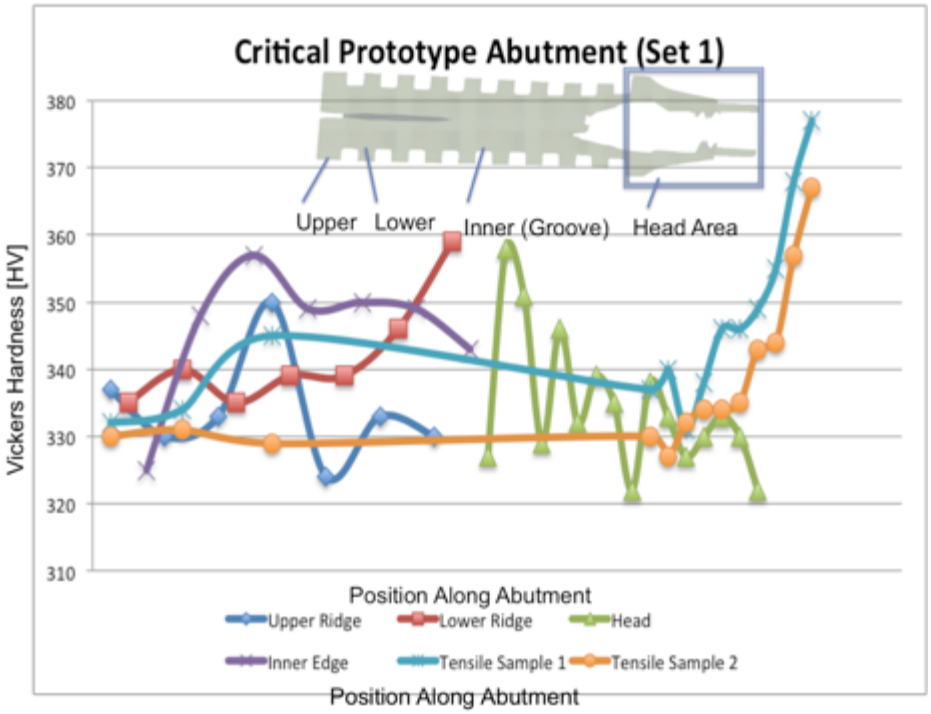

Figure 34: Comparative plot of the hardness in fractured tensile samples and the prototype abutment with highest hardness values in set 1

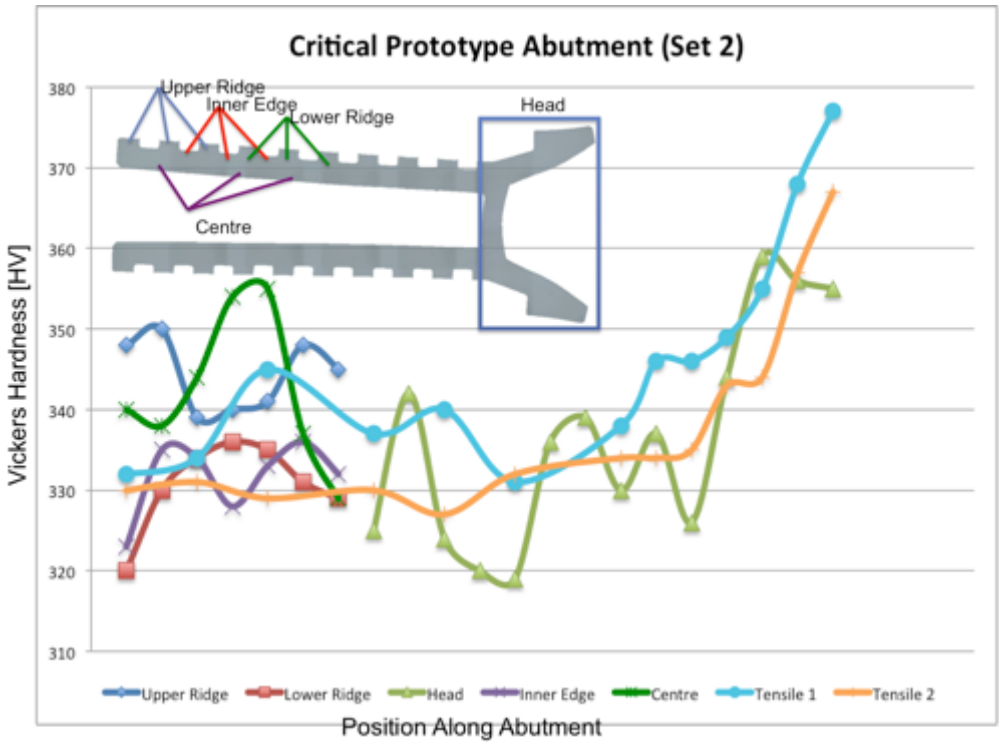

Figure 35: Comparative plot of the hardness in fractured tensile samples and he prototype abutment with the highest hardness values in set 2 (100%)

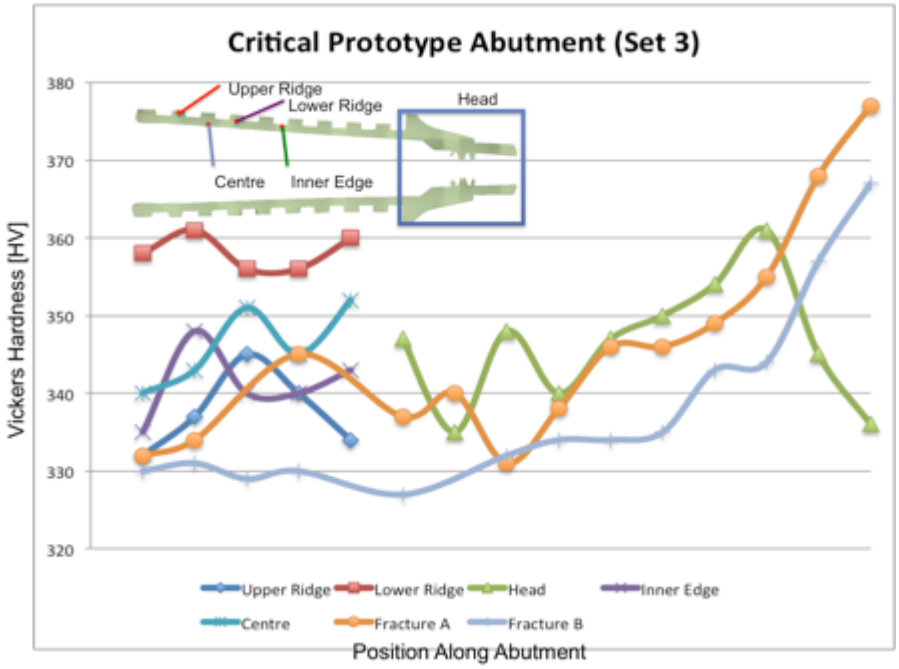

Figure 36: Comparative plot of the hardness in fractured tensile samples and the prototype with the highest hardness values in set 3 (50% feederate)

Similarly to the abutments, Figures 37, 38, and 39 show relative hardness comparisons for all the sample screws within each set, and Figures 40, 41, and 42 show comparisons of the highest prototype hardness compared against the fractured tensile samples for sets 1, 2, and 3, respectively. The screws tended to yield results with less variation than the abutments. Similar to the comparison between the prototype and market abutments, the prototype and market screws also display similar trends and values in their associated areas. This indicates that the prototype screws undergo a similar level of strain hardening and are of a similar quality as the market screws.

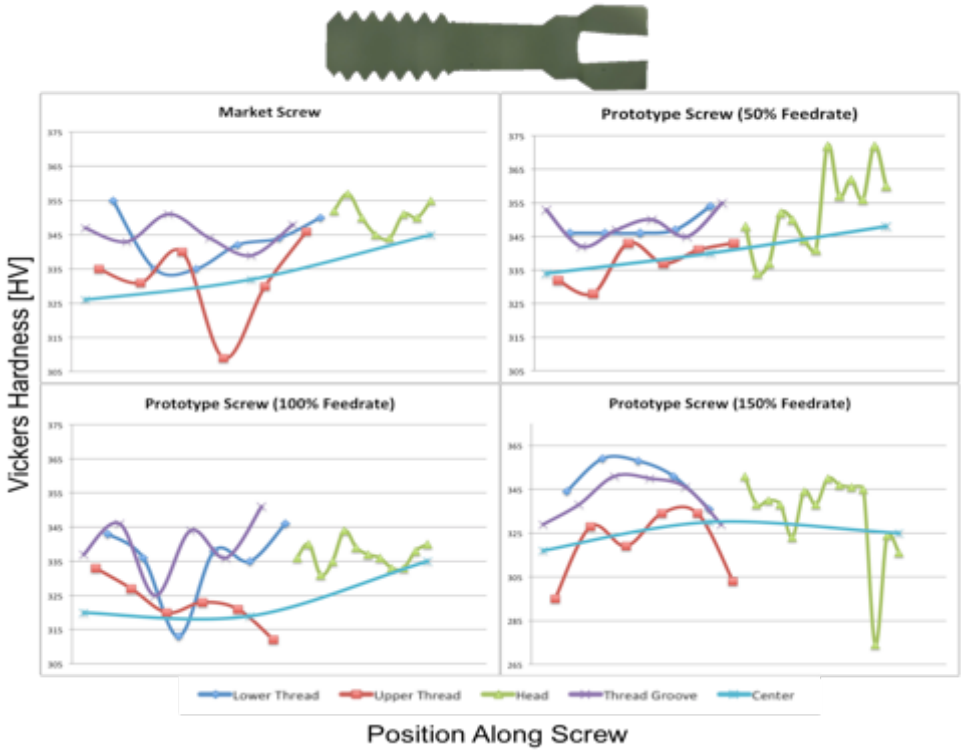

Figure 37: Screw hardness comparison in set 1

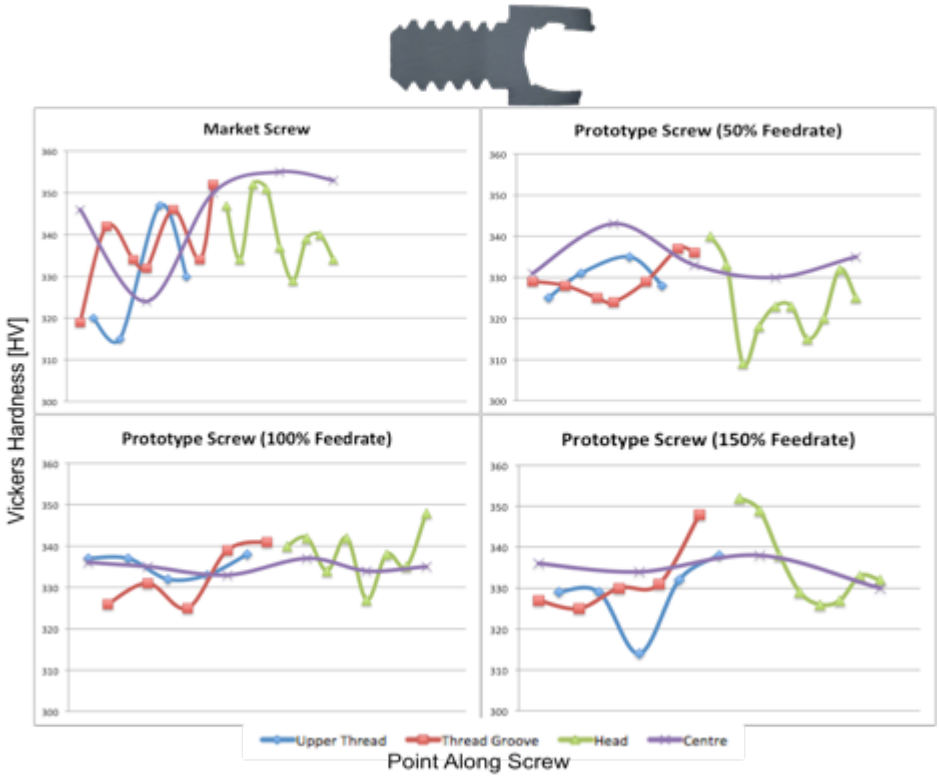

Figure 38: Screw hardness comparison in set 2

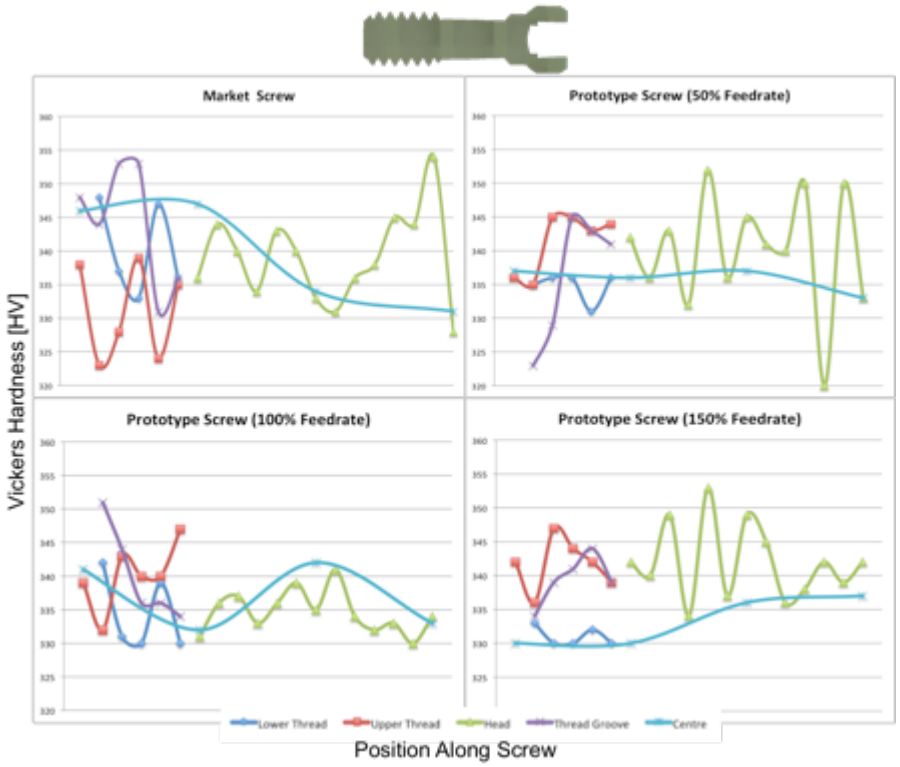

Figure 39: Screw hardness comparison in set 3

From the depicted graphs and from knowing which machining processes were performed at different parts of the screws, it can be determined that the strain hardening caused by the broaching of the screw head was lower and less critical for the 100% and 150% feed rates. It was also noted that the abutments tended to have higher hardness values the closer the test points progressed towards the interior of the abutments. Based on literature examples [74], the level of cold working was not expected to progress significantly deep into the material. In terms of the screws, it was expected that the highest hardness values would be found around the broached area at the head, as the broaching and boring processes consist of a process that closer resembles scraping material off with a blunt face, as opposed to the drilling or turning operations, which constitute a process closer to shearing material away. While most hardness values did sit closer to the baseline value of the undeformed samples, the hardness values around the head of the screws did tend to have a higher peak and average values than most other locations along the screw. In regards to the abutments, the key area of concern would be along the inside of the cylinder beneath the retention rings. This is because of the boring procedure that is used to widen the initial pilot hole in order to arrive at the desired interior diameter.

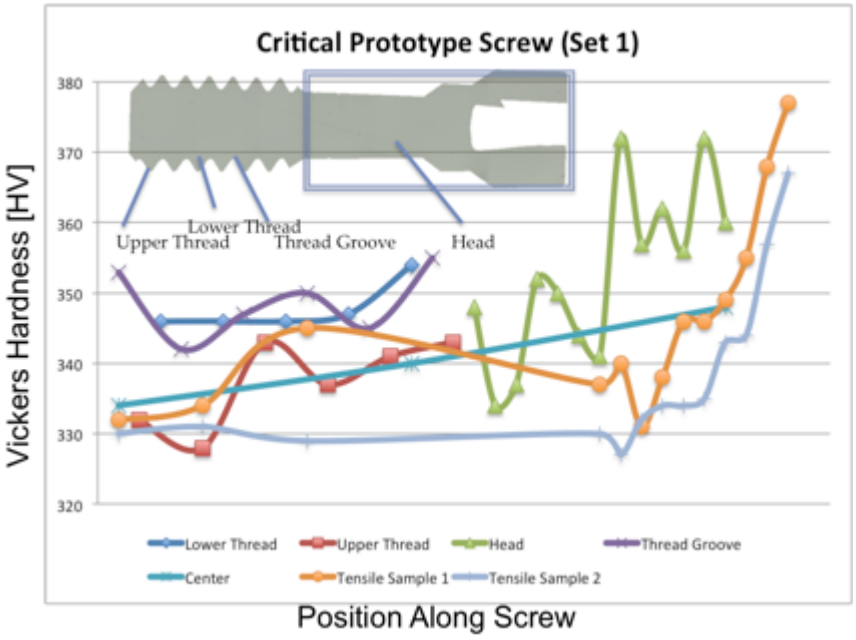

Figure 40: Comparative plot of the hardness in fractured tensile samples and the prototype screw with highest hardness values in set 1 (50% feederate)

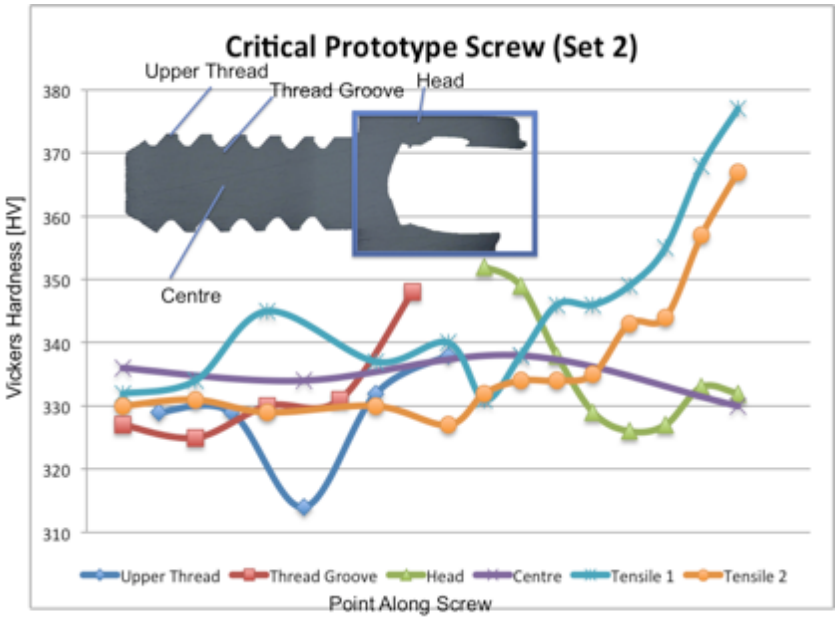

Figure 41: Comparative plot of the hardness in fractured tensile samples and the prototype screw with highest hardness values in set 2 (150% feederate)

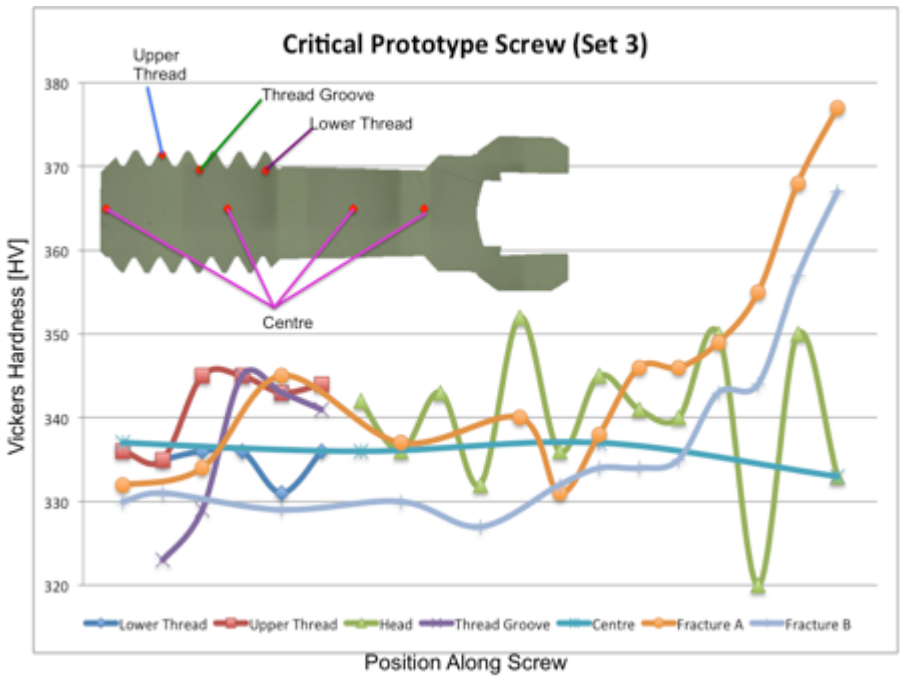

Figure 42: Comparative plot of the hardness in fractured tensile samples and the prototype screw with highest hardness values in set 3 (50% feederate)

As can be noted from the results of the abutment hardness tests, the area around the inner portions of the abutments did tend towards higher hardness values, indicating more cold work and larger residual stress values in that area. In addition to the centre portion of the abutments having higher hardness values, sets 2 and 3 exhibited higher hardness values in the ridge and inner regions, respectively. A hardness comparison of all components with fractured tensile test samples for the abutments and screws showed that the strain hardening caused by the macro-machining process is low. Both prototypes and market components exhibit similar hardness levels in the range of the hardness of the blanks and the undeformed regions of the tensile samples. Therefore, machining cold work can be considered relatively low, and falls outside of critical levels expected to cause component cracking or failure during fabrication. Additionally, no signs of considerable softening annealing or recrystallization were found. However, the strong deformation during the broaching process at 50% feed rate leads to strong cold work of the screw heads comparable to the neck region of the fractured tensile samples. This can potentially cause cracking of the screw head during fabrication. Overall, average trends and values for hardness testing indicate that the prototype abutments and screws are very similar to market products.

Figures 43 and 44 display a relationship between the amount of cold work and residual stresses vs. subsurface depth of cut into the workpiece material. As illustrated from Figure 44, the impact of cold working does not extend past a few hundred micrometers from the surface of the material. Similarly, the residual stress does not go past a few hundred micrometers deep into the material either. Since the titanium alloy used in this work is expected to behave in a manner similar the Titanium alloy examined in Figures 43 and 44, the residual stresses, and thereby hardness levels, should not extend very deep into the material. The material used in the study by Nalla et al. was in a solution treated and over-aged state, and residual stress testing was performed after deep rolling. However, general trends are expected to be similar after machining with somewhat more localized deformation at the component surface [75]. From this information, we can infer where the residual stresses lie in the material based on the changing hardness values. In addition, multiple cuts during the turning process were theoretically found to have an impact on the degree of strain hardening near the machined surface. A study by Liu and Guo [76] discovered that the first cut of a turning operation would have a higher level of strain hardening near the surface of the cut and affect the chip formation, whereas a subsequent cut would have a lower level of strain hardening, as illustrated in Figure 45.

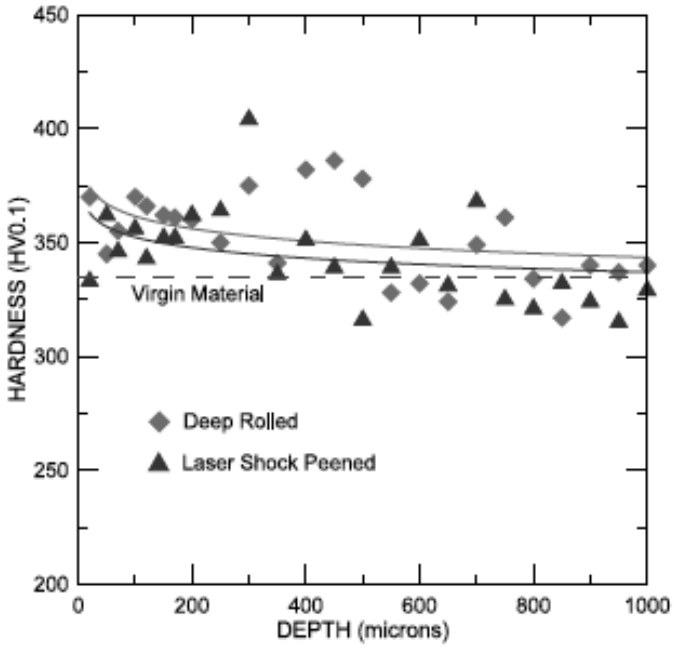

Figure 43: Sample hardness vs subsurface depth in Ti6Al4V

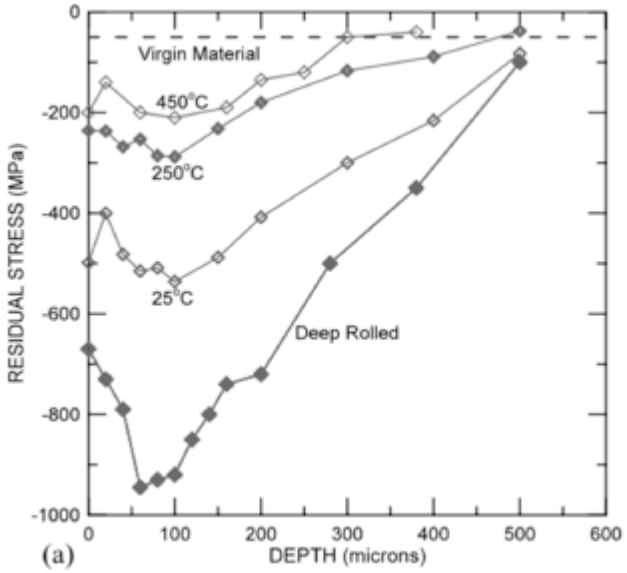

Figure 44: Level of residual stress vs subsurface depth in Ti6Al4V [75]

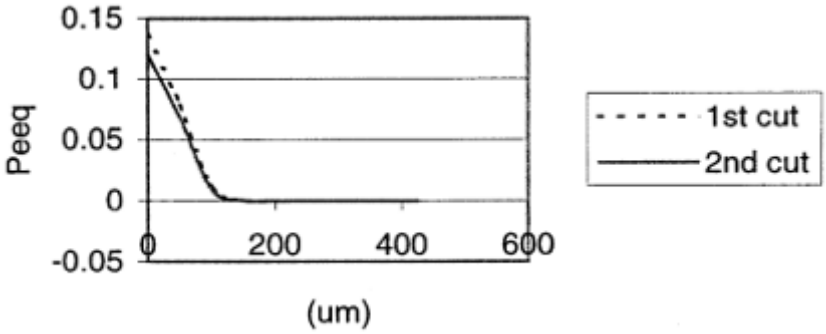

Figure 45: Equivalent plastic strain (Peeq) distribution in subsurface depth direction of 304 stainless steel [76]

To demonstrate this, the abutments of set 2 had higher hardness values in the ridge than the top of the groove, which should have been machined under similar conditions. The reason that the ridge hardness values are higher than the groove could be due to either the effects of multiple sequential cuts, or the effects of compressive to tensile residual stresses depending on surface depth from the machined surface. If the boring process were to produce tensile residual stresses that overlap with the compressive stresses produced during the turning process, this could reduce the local hardness near the groove portion of the abutment, especially when considering that the abutment walls are comparatively thin. Set 3 abutments displayed higher

hardness along the centre of the hollowed abutment and the area between the ridge and the hollowed centre. The abutments in set 3 had relatively thinner walls than set 2, so the depth distribution of the residual stresses would overlay in different areas. While the centre hardness increase was to be expected, it was also expected for the groove segments to have higher hardness values due to the residual stress depths of the machining processes. It is theorized that the groove hardness values were taken too close to the edge of the material, and thus there would be unwanted material shift that would reduce the hardness values. This theory is complimented by the initial test trials of the Vickers hardness tester, as hardness indents taken too close to the mounting resin and away from the centre of the tested material would cause the indent to slide on the material. Since hardness values are dependent upon the size of the indent, this slide would produce a larger indent hole, and therefore a lower hardness value. It could also be possible that the points near the centerline were taken either too far or too close to the edge of the material. Since the abutments specifically were both round and hollow, this makes it difficult to acquire values with assurance that the point being measured is not on an overhanging rim from the grinding process. Another possible reason for the higher than expected hardness values could be due to the aforementioned trends of the residual stresses and their variations through depth. The boring process may have created an area of higher tensile stress rather than compressive by the depth of the groove with respect to the interior of the abutment. This could in turn reduce the magnitude of the residual stress in the area near the groove, but does not fully extend to the area around the ridge.

4.1.3 Microstructure Analysis Results

Microscopy analysis was performed on etched samples in order to determine grain deformation or distortion. It allowed validating prior hardness trends and identifying potential critical design areas to complement hardness testing. Figures 46 and 47 illustrate the abutment and screw areas that were found potentially most critical due to the highest cold work, and were therefore used for the microstructure investigations.

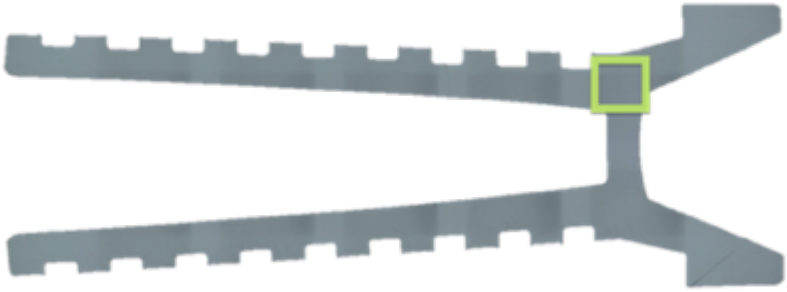

Figure 46: Illustration of the abutment section (in square) used for microstructure investigation

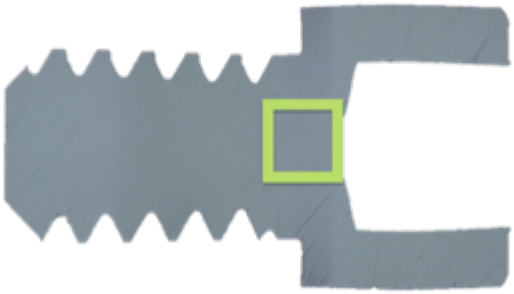

Figure 47: Illustration of the screw section (in square) used for microstructure investigation

As can be seen in Figure 48 compared to Figures 49 and 50, no considerable grain distortions or microstructure alterations were observed. No signs were found for either grain elongation or recrystallization and the grain structure and size were comparable to those of the undeformed Ti6Al4V blanks. When compared against the undeformed samples, as seen in Figure 48, the grain structure remains similar both before and after the machining process in the central areas of the components.

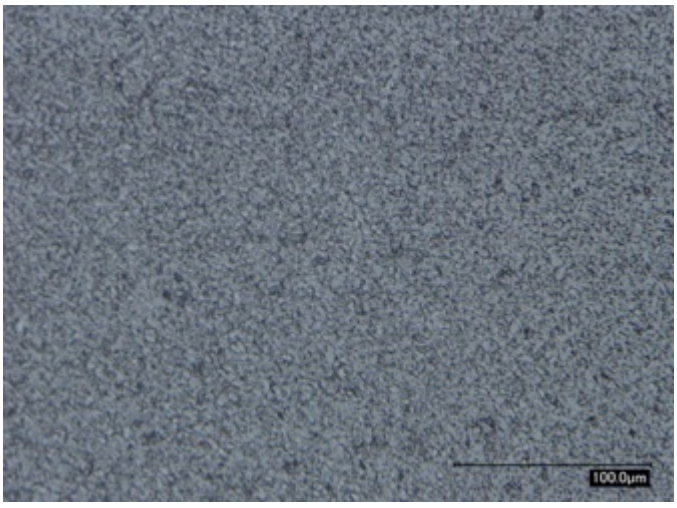

Figure 48: Undeformed blank after etching

This suggests that the deformations caused by micromachining and broaching as well as the associated heat effects do not remarkably affect the components' microstructure in the central areas of the components.

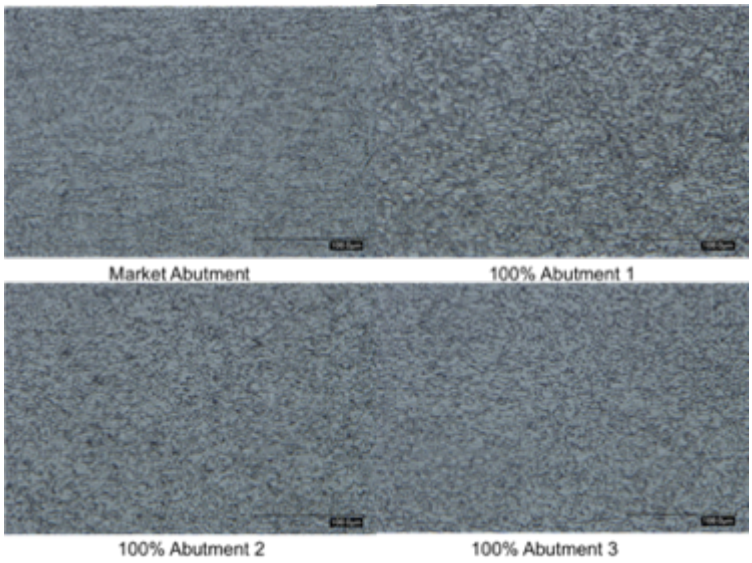

Figure 49: Optical micrograph of the sample microstructure of the etched abutment samples from set 1

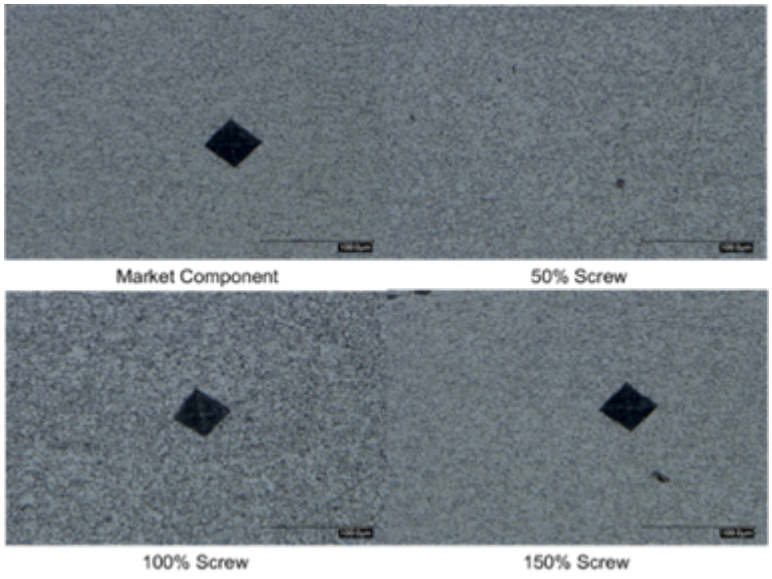

Figure 50: Optical micrograph of the sample microstructure of the etched screw samples from set 2

This was largely to be expected, as the relative level of cold work was quite low, and the effects of the cold working would only be primarily visible on the surface. Figure 51 provides a

view of the edge of the machined screw prototype. By observing the edge closely, it is possible to notice that there is some grain alteration, but only at the edges of the machined material. Only grains in the surface layer show some elongation or distortion extending approximately 30 micrometers below the component surface. This correlates with literature grain distributions as can be seen in Figure 52.

Figure 51: Optical micrograph of the etched screw sample illustrating deformed grains at surface layer

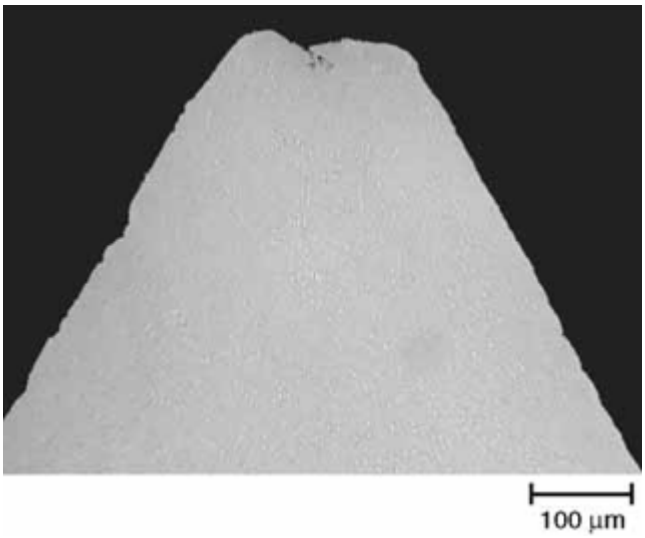

Figure 52: Literature example of Ti6Al4V grain formations [77]

4.2 Numerical Results

The numerical results section covers the output results obtained through numerical modeling using ABAQUS. Presented here are the drilling, broaching, turning, boring, and heat

effect results. All the results presented in this section are for the purpose of pattern recognition and correlation with the mechanical test results presented in section 4.1. Note that all models used portions of the models discussed in chapter 2, and aspects were used based on: feasibility, processing time, availability within ABAQUS, and trial and error to find the best fitting model while reducing computing time. All displayed stresses are in Pascals and are representative of the Von Mises stresses obtained through calculation.

4.2.1 Drilling

The drilling process was modeled as a drill bit contacting a half-sheet of material. This was done due to symmetry, as well as reducing computing and processing time. Figure 53 illustrates example results from the 1.3mm depth drilling process. Figure 54 illustrates the final point in the process, where the drill is fully inserted close to the 1.3mm depth. The colours on the meshes indicate the level of stress in the vicinity, with darker red colours indicating higher stress levels, and colours closer to blue indicating less stress in the area. The white of the drill bit is indicative of a rigid body that does not experience stress. The first simulation, drilling, exhibited the highest levels of stress at the tip of the drill bit. The stresses around the circumference of the drilled hole tended to be relatively low in comparison to the tip of the drill bit. The stresses throughout the timesteps did fluctuate, but remained within a set range throughout the simulation. The high level of stresses around the ultimate strength value of 1200 MPa produced at the tip of the drill bit were expected, as the tip of the drill bit is pushing material into the hole, whereas the circumferential stress is more of a shaving action. The residual stresses produced were found to be in the range of 800 MPa and progressed about 300 micrometers into the work material.

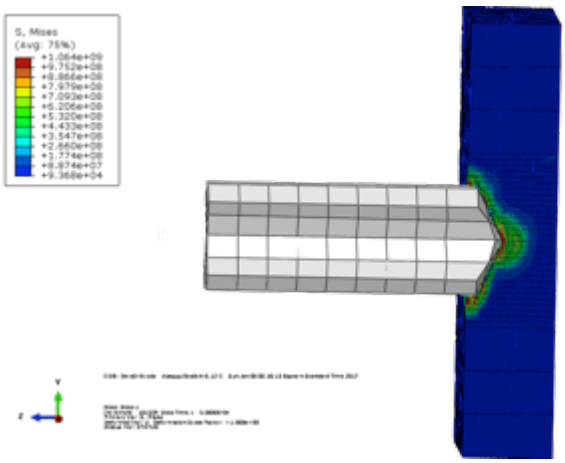

Figure 53: Drilling model during the process

Actual stresses during the machining process around the drilling site may differ from the modeled values, as the drill shape was restricted due to both company and software limitations. The drill bit shape was limited by ABAQUS due to run-time errors being produced with fluting that was sharper than displayed in the model. Additionally, the dental laboratory only revealed the information of the drill bit size and manufacturer, but did not give a product number. It is expected that most of the residual stress would be constituted by the boring and broaching processes, as they remove the drilled surfaces and are expected to produce higher stress values.

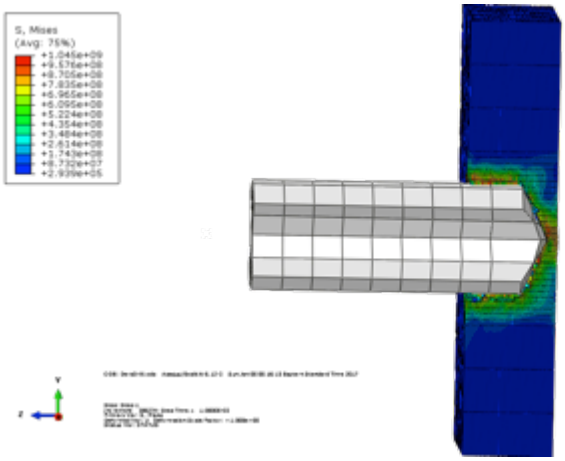

Figure 54: Drilling results at the end of the process

4.2.2 Broaching

The broaching procedure consisted of a single striking motion to remove material. At the end of the striking procedure, the broach was removed in order to present more realistic after

effects. Figure 55 illustrates the striking process step. Figure 56 shows a top view of the broaching set-up after the broach removal step has been completed.

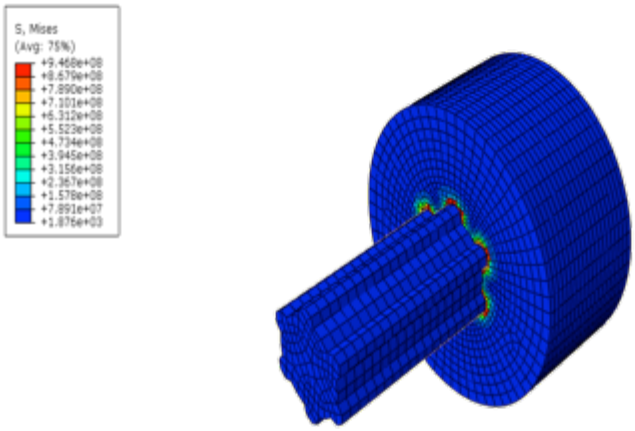

Figure 55: Broaching during insertion process

The broaching process produced very little stress normal to the component surface, and instead produced stress in the circumferential direction. Coupled with the results from the drilling, this will produce an area of high cold work around the head of the screw, as this is the only place where the broaching process occurs. Once again, we can see that the stress distribution does not extend significantly deep into the material, indicating that most of the cold work will appear on the surface of the component. The broaching procedure produced residual stresses within the range of 850 to 870 MPa that were found to progress up to approximately 600 micrometers into the work material.

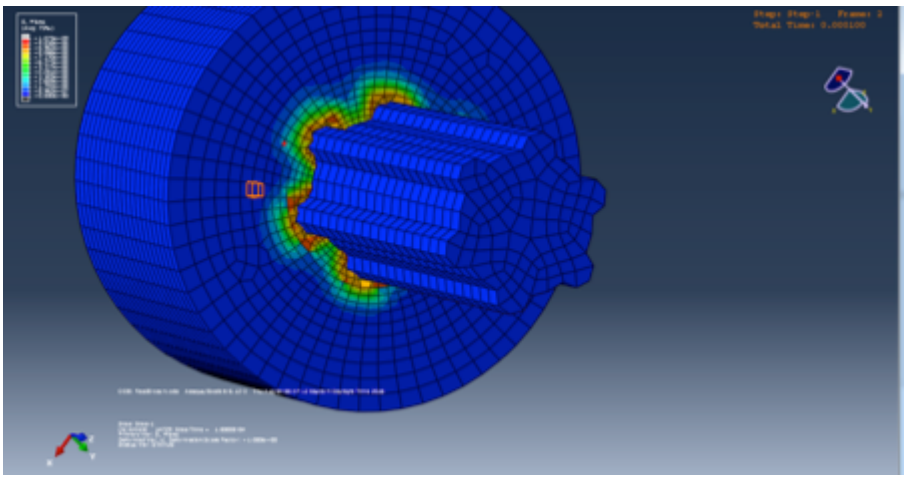

Figure 56: Broaching top view of broached material

4.2.3 Turning

The turning process constitutes the majority of the surface formation, as it is used for crafting both the general shape of the component and the threading on the screws and rings on the abutments. In order to verify the models discussed in literature, a three stage turning process was initially set-up. The results of the turning process can be seen in Figures 57 to 59. Figure 57 indicates the first cutting process performed during turning. Figure 58 represents the second stage of turning, and Figure 59 represents the final stage of cutting.

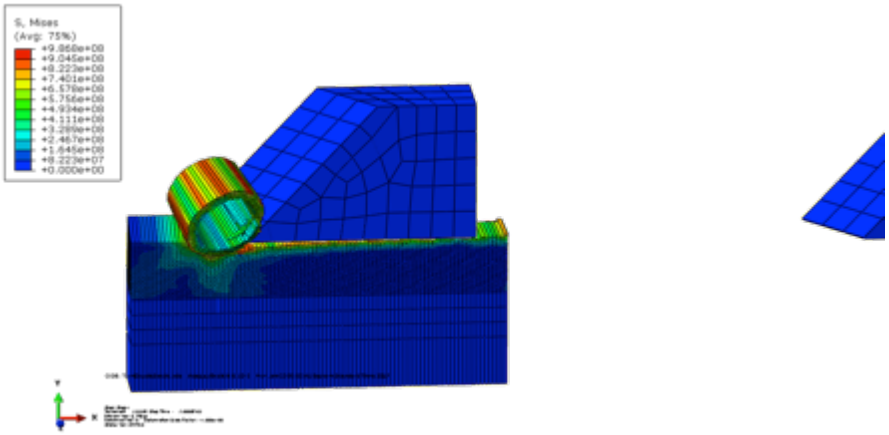

Figure 57: Simulation halfway through first turning cut

The first segment of the turning operation is comprised of multiple cutting procedures. This is in part to validate the paper outlined earlier [76] in regards to multiple cuts having lower residual stress levels after subsequent cuts. This allows us to investigate whether the turning

process could be feasibly simulated using only a single pass if one is more concerned with general patterns of residual stress distributions, and not highly accurate results. For the validation of the multiple cuts producing lower residual stresses, it can be seen by comparing the final images in each of the three timesteps, that the magnitude and depth of the residual stresses is lower as subsequent cuts are performed.

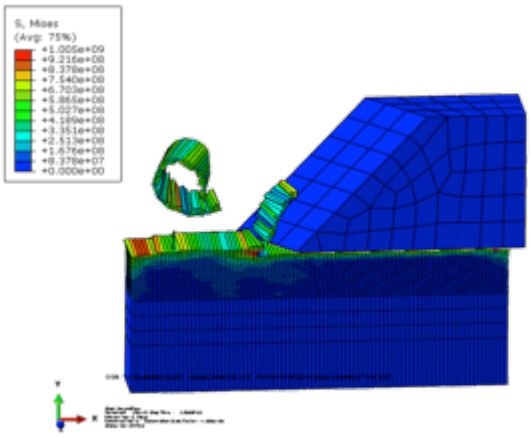

Figure 58: Simulation halfway through second turning cut

The first two sets of cuts depict most of the residual stress being removed along with the chip, whereas the third step indicates the chip formation is closer to a shattering of pieces than a smooth chip formation. The first step has the chip come off the material in a wave, the second step has the chip removed as a curl, and the third step has the chip break off in pieces. There are multiple possibilities for why the chip formation varies between steps, including whether the tool bit intersects between elements or in the middle of elements. The chip formation also depends on the boundary conditions set to secure the workpiece and on changes in residual stress produced during the previous cuts. Liu and Guo [76] determined that subsequent cuts did have an impact on chip formation. After testing various boundary conditions including tool bit placement and cutting parameters, it was concluded that chip formation primarily depends on the state of residual stresses.

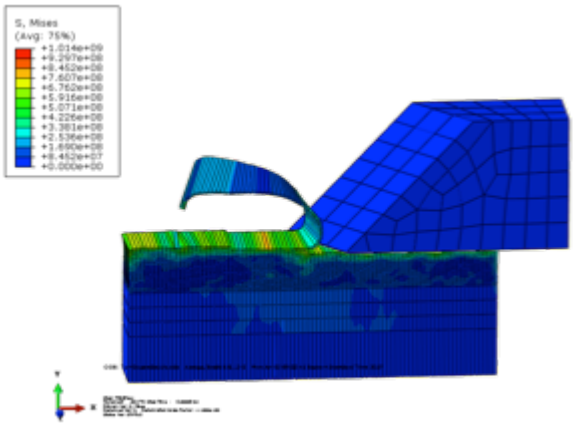

Figure 59: Halfway through third turning cut

In regards to the chip formation itself, it can be seen that there are variations along the top layer of the chip when it is separating from the workpiece. These variations travel across the chip in tandem with the tool bit moving across the workpiece. The highest levels of residual stress tended to be at the initial contact point between the tool bit and the workpiece, and at the end of the cut. As with the previous models, the depth of the residual stress, even when comparing the third cut, does not extend past a few hundredths of a millimeter at maximum. This is to be expected based on previous studies done involving residual stress values in machined or cold worked components. Since the general pattern of general stress distribution was similar between all three cuts, it can be considered probable that a single cut model could provide enough information to give a general understanding of how the stress and cold work of a machined component could propagate through a workpiece. Residual stresses from the turning operation were found to be up to 750 MPa after the first cut, and progressed no further than 200 micrometers into the material.

In addition to the three-stage turning, a one-stage heat analysis was performed for the turning operation. Similar to the three-stage process, Figure 60 is the local stress distributions, and Figure 61 is the thermal results throughout the timestep.

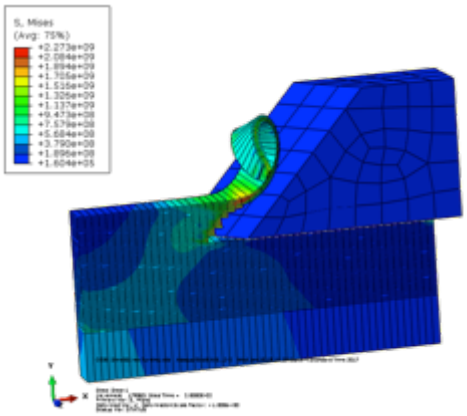

Figure 60: Heat and mechanical combined stress halfway through timestep

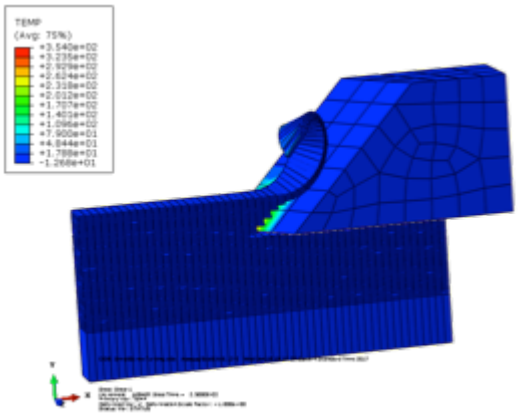

Figure 61: Thermal temperature results halfway through turning cut

Both Figures 60 and 61 represent the stress distributions associated with a turning procedure that include both mechanical and thermal effects. As can be seen from the results, the total stress from the heat included turning did not result in a significantly higher residual stress, instead it resulted in generally lower stress values, but with more depth than the case without heat effects. As seen above, the heat is mostly in the tool bit or torn away with the chip formation process.

4.2.4 Boring

The boring process occurred in a similar fashion to the turning process. Figures 62 and 63 show the stress results from the initial boring testing during the initial material contact stage.

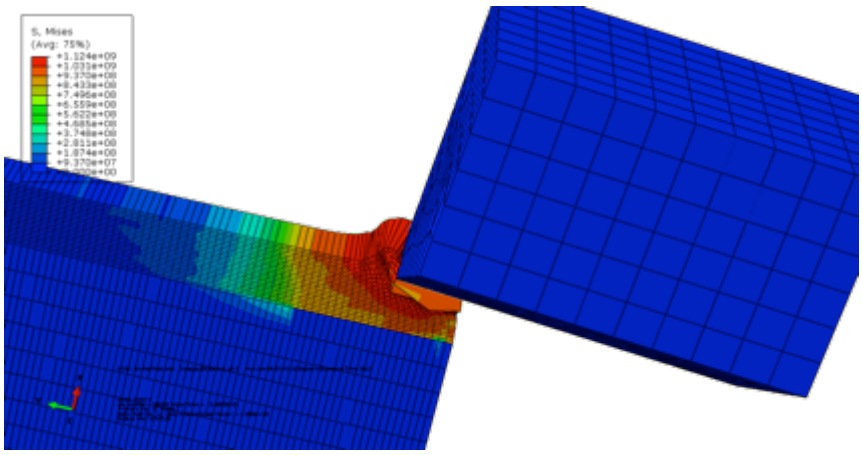

Figure 62: Initial boring contact

The boring process produces much higher local stress than the turning operation, despite being of a similar process. The stresses produced are both larger in magnitude and propagate deeper into the material. This is primarily due to the boring process being a method of scraping off material instead of shaving the material away. Based on the simulated boring results, it would be expected to see higher hardness values around the segments that undergo the boring process, as opposed to the other processes. Since the boring process is only used on the inside of the abutments, it stands to reason that there will be a higher hardness rating along the inside of the hollowed portion of the abutments. This was also observed in the experimental results of the prototype and market abutments. Maximum boring residual stresses were found to be up to 900 MPa and progressed up to 1000 micrometers into the work piece.

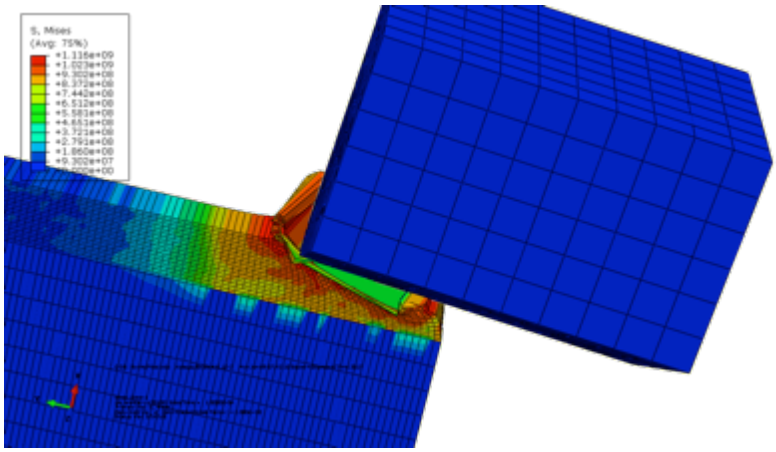

Figure 63: Boring tool progressing into workpiece

4.3 Comparison Between Experimental and Numerical Results

This segment aims to tie the two previous segments together, indicating correlations between the experimental and numerical testing.

Based on the drilling and broaching simulated processes, it would be understandable to find the highest levels of hardness around the head area of the screw. In the experimental data, the hardness values around the areas associated with the drilling and broaching were found to be generally higher than the rest of the locations on the screw, which is most evident when viewing the hardness profiles for the first set of components. For the rest of the screw, the hardness values around the threading of the screw tended to be relatively similar. Whether the values were taken at the crests of the threads or in troughs of the threads the hardness values were very similar in scale and tended to follow the same variation patterns. In accordance with the previous studies involving residual stress and cold work, it makes sense to expect lower and similar values, as the amount of residual stress will decrease with successive cuts, as shown from the numerical and previous study results. The centre of the screw tended to be largely undeformed, compared to the baseline of the tensile samples used. This coincides with both the literature and modeling, as they both indicated that the stress profiles would not extend very deep into the component.

Similar to the screws, the abutments showed good correlation between experimental and numerical results, as well as the inner portion of the abutments, where the boring was performed, gave higher hardness results for both the experimental and modeling studies. The upper ridges of the abutments also tended to give higher hardness values, indicating more cold work in the less shallow areas. This also coincides with the used multiple cutting processes and is reflected in the experimental data. Additionally, the head area of the abutments showed increasing levels of cold work as the points where the values were taken progressed closer to the end of the abutment. This is most likely due to the boring process having a more prevalent effect, as the component gets thinner, leaving the stresses produced during the boring process to eclipse those of the turning process on the outer portion of the abutment head.

Overall, the experimental and numerical results show good correlation, and are both indicative of the level of cold work that the components will, and do, undergo. All of these

aspects are also mirrored in the microstructure of the components, as the grains are not heavily distorted except at the very extremities of the components. Based on both the numerical and experimental results, it can be determined that the prototype components produced by the dental laboratory should have a significantly adequate level of comparability to the components that are currently on the market. Furthermore, with additional data and parameters, modeling of the machining processes could be used to help identify and reduce areas of higher residual stresses, which may aid in reducing failure of dental components due to surface cracking or wear, and for improving implant lifespan.

While there was no information available on the cutting parameters and tool bits used to make the imported market components, higher residual stress levels in the boring and broaching processes were in agreement with the higher hardness values discovered in the abutment interiors and screw heads, which correspond to the location where these processes were performed. Based on correlation between residual stresses, strain hardening, and material hardness values discussed earlier, it was expected that the numerical models would show higher residual stress values in these locations. Further images from the numerical modeling are available in Appendix A.

5 Conclusions

Dental implant abutments and screws are successfully tested through visual inspection, micro-hardness testing, and microstructure analysis. The manufacturing processes were successfully simulated for residual stress patterns. Prototypes showed good design around the edges and corners of the abutment valley segments, as those areas were rounded to reduce stress concentrations. Contrarily, the head areas were sharper, thereby leading to potential crack initiation and propagation.

Generally, hardness values of the components are relatively steady at levels significantly below the critical values as determined using failed tensile test samples. Screw hardness values taken around the head segment indicate higher levels of cold work due to the broaching process. This level of cold work is higher for the 50% feed rate samples. Abutment hardness values indicated a rising trend towards the interior hollow of the abutments, indicating an increased level of cold work due to the boring process.

Surface etching and microstructure analysis revealed no visible grain deformation or recrystallization in the samples, which is in good agreement with hardness values acquired during hardness testing, apart from at the extremities of the machined component.

Process modeling showed low levels of residual stresses past a relatively small depth under the sample surface. Multiple successive cutting steps did not appear to significantly impact the depth of residual stresses, although they did have a minor effect on the surface residual stress values that decreased with subsequent cuts. The inclusion of heating effects did not appear to significantly impact the residual stresses for a single cut model. Boring and broaching models indicated the highest produced levels of residual stresses. A good agreement is shown between simulated models and experimentally acquired data. Simulations were able to display stress distribution patterns during manufacturing and can be modified to optimize simulated testing.

Prototype abutment components had higher stress concentration areas towards the head, as opposed to the market components with the more critical areas in the body sections.
Prototype components showed similar levels of cold work and grain structure as market components, indicating similar characteristics.

The relationship between the residual stresses and the hardness of Ti6Al4V was examined and correlations were made between high hardness values and high residual stress

values. Boring and broaching procedures produced the highest hardness values in tested components, while the numerical models for broaching and boring also produced the highest residual stresses.

Experimental results indicate that both prototype and market abutments and screws exhibited similar properties, indicating that the used process parameters are in a good range and the production quality was appropriate.

Overall, the present work successfully demonstrated patterns of cold work, strain hardening, and residual stresses produced in machined dental implant abutments and screws, through both experimental testing and simulated modeling. This provides a basis for the optimization of dental implant fabrication using micromachining. It can also help the local industry partner to develop an in-house quality assurance methodology. As such, a basis is laid for potential future local production of dental implants, which can contribute in reducing waiting times and costs for patients while improving the profit margin for dental laboratories.

6 Outlook

The current work has focused on the investigation of dental abutments and screws using visual inspection, Vickers hardness, and microstructure analysis. Additionally, numerical models focused primarily on pattern recognition for residual stress distributions. The following suggests future work that can potentially further advance research and development of dental implants:

- For validation and accurate measurement of actual residual stresses in both dental implant and tensile sample components, the use of x-ray diffraction or other applicable testing mechanisms is suggested for determining actual residual stress values.
- While the present work uses the behavioral patterns of steel as a basis for analysis, further testing and research into the exact relationship between residual stresses, cold working, Vickers hardness, and service life for Ti6Al4V Titanium alloys would be beneficial for both similar work and general application of titanium alloys.
- This study was performed with a limited number of samples. Therefore, a larger batch would allow statistical averages and variations to be determined, as opposed to individual specimen testing.
- Inclusion of various cooling fluids and their interactions with generated heat on the workpiece and tool bit can allow for more accurate numerical modeling.
- The effect of heat due to workpiece - tool bit friction over long periods of fabrication and multiple component production would help to give a better idea of how many components can be manufactured in a single session without compromising component integrity.
- Importing more accurate models for tool bits from programs other than ABAQUS would enhance model accuracy.
- Simulating an entire machining cycle may reveal further information not available, due to processing speed and power, as opposed to individual process evaluation. This will give a better understanding of how the machining processes interact with each other.
- Determining set values for the broaching tool instead of using various custom broaches would enhance accuracy of residual stress analysis in screw heads.

References

[1] J. Sentlingar, “Dental Implants,” *Prosper Family Dentistry*, 2016. [Online]. Available: http://www.prosperfamilydentistry.com/dental-implants/. [Accessed: 14-Apr-2017].

[2] P. Moy, D. Medina, V. Shetty, and T. Aghaloo, “Dental Implant Failure and Associated Risk Factors,” *Int. J. Oral Maxillofac. Implants*, vol. 20, no. 4, pp. 569–577, Aug. 2005.

[3] American Academy of Implant Dentistrry, “Dental Implants Facts and Figures.” [Online]. Available: http://www.aaid.com/about/press_room/dental_implants_faq.html.

[4] J. Pinkney, “Engage Grant Meeting for Milident Testing,” Dec-2014.

[5] Dunedin Dental Attachments, “Nobel Active Compatible.” [Online]. Available: http://www.ddat.com.au/product-category/nobel-active-compatible/.

[6] C. Barbosa, J. Lopes do Nascimento, R. O. Centeno, I. Vieira Caminha, and I. de Cerquiera Abud, “Failure Analysis of Titanium-Based Dental Implants,” *J. Fail. Anal. Prev.*, vol. 10, pp. 138–142, 2010.

[7] S. Gupta, “Oral and Maxillofacial Devices,” in *Mechanics of Biomaterials*, Cambridge: Cambridge University Press, 2011, pp. 505–559.

[8] A. Bellona, “Different Types of Dental Implants to Choose From,” *Dentaledu*, 2017. [Online]. Available: http://www.dentaledu.tv/types-of-implants/. [Accessed: 14-Apr-2017].

[9] K. Min Gun, “Fatigue Properties on the Failure Mode of a Dental Implant in a Simulated Body Environment,” *Met. Mater. Int.*, vol. 17, no. 5, pp. 705–711, Oct. 2011.

[10] R. Sadid-Zadeh, A. Kutkut, and H. Kim, “Prosthetic Failure in Implant Dentistry,” *Dent. Clin. North Am.*, vol. 59, pp. 195–214, 2015.

[11] H. J. S. Meijer, J. H. Kuiper, F. J. M. Starmans, and F. Bosman, “Stress Distribution around Dental Implants: Influence of Superstructure, Length of Implants and Height of Mandible,” *J. Prosthet. Dent.*, vol. 68, no. 1, pp. 96–102, Jul. 1992.

[12] A. Freitas-Júnior, E. Almeida, E. Bonfante, N. Silva, and P. Coelho, “Reliability and Failure Modes of Internal Conical Dental Implant Connections,” *Clin. Oral Implants Res.*, vol. 24, pp. 197–202, 2013.

[13] K. Shemtov-Yona and D. Rittel, “Identification of Failure Mechanisms in Retrieved Fractured Dental Implants,” *Eng. Fail. Anal.*, vol. 38, pp. 58–65, Jan. 2014.

[14] K. ’ichi Yokoyama, T. Ichikawa, H. Murakami, Y. Miyamoto, and K. Asaoka, “Fracture mechanisms of retrieved titanium screw thread in dental implant,” *Biomaterials*, vol. 23, no. 12, pp. 2459–2465, Jun. 2002.

[15] H.-C. Choe, J.-K. Lee, and C.-H. Chung, “Analyses of fractured implant fixture after prolonged implantation,” *Met. Mater. Int.*, vol. 10, no. 4, pp. 327–335, Jul. 2004.

[16] M. G. Manda, P. P. Psyllaki, D. N. Tsipas, and P. T. Koidis, “Observations on an in vivo Failure of a Titanium Dental Implant/Abutment Screw System: A Case Report,” *J. Biomaedical Mater. Res.*, vol. 89B, no. 1, pp. 264–273, Oct. 2008.

[17] L. Sbordone, T. Traini, A. Scarano, C. Bortolaia, and A. Piattelli, “Scanning electron microscopy fractography analysis of fractured hollow implants,” *J. Oral Implantol.*, vol. 36, no. 2, pp. 105–111, 2010.

[18] B. Boardman, “Fatigue Resistance of Steels,” in *ASM Handbook, Volume 1: Properties and Selection: Irons, Steels, and High-Performance Alloys*, vol. 1, ASM International, pp. 673–688.

[19] A. Bajaj, “Implants: Larger Interfacial Surface Area,” *Br. Dent. J.*, vol. 197, no. 9, pp. 587–589, Nov. 2004.
[20] S. Dittmer, M. Dittmer, P. Kohorst, M. Jendras, L. Borchers, and M. Stiesch, “Effect of Implant-Abutment Connection Design on Load Bearing Capacity and Failure Mode of Implants,” *J. Prosthordontics*, vol. 20, pp. 510–516, Jan. 2011.
[21] F. Gil, M. Herrero-Climent, P. Lazaro, and J. Rios, “Implant-Abutment Connections: Influence of the Design on the Microgap and their Fatigue and Fracture Behaviour of Dental Implants,” *J. Mater. Sci.*, vol. 25, pp. 1825–1830, 2014.
[22] J.-H. Lee, V. Frias, K.-W. Lee, and R. Wright, “Effect of Implant Size and Shape on Implant Success Rates: A Literature Review,” *J. Od Prosthet. Dent.*, vol. 94, pp. 377–381, Oct. 2005.
[23] C. Wyatt and G. Zarb, “Treatment Outcomes of Patients with Implant-Supported Fixed Partial Prostheses,” *Int. J. Maxillofac. Implants*, vol. 13, pp. 194–201, 1998.
[24] J. Brunski, “Biomechanical Factors Affecting the Bone-Dental Implant Interface,” *Clin. Mater.*, vol. 10, pp. 153–201, Mar. 1991.
[25] J. Mahon, B. Norling, and R. Phoenix, “Effect of Varying Fixture Width on Stress and Strain Distribution Associated an Implant Stack System,” *Implant Dent.*, vol. 9, pp. 310–320, 2009.
[26] S. Olate, M. Lyrio, M. de Moraes, R. Mazzonetto, and R. Moreira, “Influence of Diameter and Length of Implant on Early Dental Implant Failure,” *J. Oral Maxillofac. Surg.*, vol. 68, no. 2, pp. 414–419, Feb. 2010.
[27] E. Holmgren, R. Seckinger, R. Kilgren, and F. Mante, “Evaluating Parameters of Osseointegrated Dental Implants Using Finite Element Analysis-A Two Dimensional Comparative Study Examining the Effects of Implant Diameter, Implant Shape, and Load Direction,” *J. Oral Implantol.*, vol. 24, pp. 80–88, 1998.
[28] C. Schmitt *et al.*, “Performance of conical abutment (Morse Taper) connection implants: A systematic review,” *J. Biomaedical Mater. Res.*, vol. 102, no. 2, pp. 552–574, 2014.
[29] M. McCracken, “Dental Implant Materials: Commercially Pure Titanium and Titanium Alloys,” *J. Prosthordontics*, vol. 8, no. 1, pp. 40–43, Mar. 1999.
[30] American Society for Testing Materials, “ASTM F 1472-93: Standard specification for wrought Ti- 6A1-4V alloy for surgical implant applications,” in *Annual Book of ASTM Standards*, Philadelphia, PA: American Society for Testing and Materials, 1993.
[31] Z. Özkurt and E. Kazazoglu, “Zirconia Dental Implants: A Literature Review,” *J. Oral Implantol.*, vol. 37, no. 3, pp. 367–376, 2011.
[32] R. Osman and M. Swain, “A Critical Review of Dental Implant Materials with an Emphasis on Titanium versus Zirconia,” *Materials*, vol. 8, pp. 932–958, Mar. 2015.
[33] C. Abraham, “A Brief Historical Perspective on Dental Implants, Their Surface Coatings and Treatments,” *Open Dent. J.*, vol. 8, pp. 50–55, 2014.
[34] O. Takakuwa, Y. Kawaragi, and H. Soyama, “Estimation of the Yield Stress of Stainless Steel from the Vickers Hardness Taking Account of the Residual Stress,” *J. Surf. Eng. Mater. Adv. Technol.*, vol. 3, pp. 262–268, Oct. 2013.
[35] D. Tabor, “The Physical Meaning of Indentation and Scratch Hardness,” *Br. J. Appl. Phys.*, vol. 7, no. 5, pp. 159–166, 1956.
[36] J. Kumar, “Investigations into the Surface Quality and Micro-Hardness in the Ultrasonic Machining of Titanium (ASTM GRADE-1),” *J. Braz. Mech. Sci. Eng.*, vol. 36, pp. 807–823, 2014.

[37] D. Luo, “Strong strain hardening ability in an as-cast Mg-3Sn-1Zn alloy,” *Mater. Lett.*, vol. 94, pp. 51–54, 2013.
[38] van der Merwe, P; Coetsee, J.S.; and van den Berg, J.G., “The Effect of Workhardening and Residual Stresses Due to Cold Work of Forming on the Strength of Cold-Formed Stainless Steel Lipped Channel Sections,” (1990). *International Specialty Conference on Cold-formed Steel Structures.* 2.
[39] Y. Nan, Y. Ning, H. Liang, H. Guo, Z. Yao, and M. Fu, “Work-hardening effect and strain-rate sensitivity behavior during hot deformation of Ti–5Al–5Mo–5V–1Cr–1Fe alloy,” *Mater. Des.*, vol. 82, pp. 84–90, Oct. 2015.
[40] M. Fernández, L. Delgado, M. Molmeneu, D. García, and D. Rodríguez, “Analysis of the Misfit of Dental Implant-Supported Prostheses Made with Three Manufacturing Processes,” vol. 3, no. 2, pp. 116–123, Feb. 2014.
[41] R. Walsh, *Handbook of Machining and Metalworking Calculations*. New York: McGraw-Hill, 2001.
[42] K. Sharma, D. Mahto, and S. Sen, “In metal turning, effect of various parameters on cutting tool: a review,” *Int. J. Appl. Innov. Eng. Manag.*, vol. 2, no. 8, pp. 32–38, Aug. 2013.
[43] T. Özel, T.-K. Hsu, and E. Zeren, “Effects of cutting edge geometry, workpiece hardness, feed rate and cutting speed on surface roughness and forces in finish turning of hardened AISI H13 steel,” *Int. J. Adv. Manuf. Technol.*, vol. 25, pp. 262–269, Aug. 2004.
[44] T. Gietzelt and L. Eichhorn (2012). Mechanical Micromachining by Drilling, Milling and Slotting, Micromachining Techniques for Fabrication of Micro and Nano Structures, Dr. Mojtaba Kahrizi (Ed.), ISBN: 978-953-307-906-6, InTech, Available from: http://www.intechopen.com/books/micromachining-techniques-for-fabrication-of-micro-and-nano-structures/mechanical-micromachining-by-drilling-milling-and-slotting
[45] F. Akbar, P. Mativenga, and M. Sheikh, “An Experimental and Coupled Thermo-Mechanical Finite Element Study of Heat Partition Effects in Machining,” *Int. J. Adv. Manuf. Technol.*, vol. 46, pp. 491–507, 2010.
[46] J.-C. Su, K. Young, S. Srivatsa, J. Morehouse, and S. Liang, “Predictive Modeling of Machining Residual Stresses Considering Tool Edge Effects,” *Prod. Eng. Res. Dev.*, vol. 7, pp. 391–400, 2013.
[47] J. Almen and Black P, *Residual Stresses and Fatigue in Metals*. New York: McGraw-Hill, 1963.
[48] C. Liu and M. Barash, “Variables governing patterns of mechanical residual stress in a machined surface,” *J. Eng. Ind.-Trans. ASME*, vol. 104, no. 3, pp. 257–264, 1982.
[49] C. Lin, Y. Lin, and C. Liu, “Effect of Thermal Load and Mechanical Load on the Residual Stress of a Machined Workpiece,” *Int. J. Mech. Sci.*, vol. 33, no. 4, pp. 263–278, 1991.
[50] N. Canter, “The Possibilities and Limitations of Dry Machining,” *Tribol. Lubr. Technol.*, pp. 40–44, Mar. 2009.
[51] T. Ginta and N. Amin, “Surface Integrity in End Milling Titanium Alloy Ti-6Al-4V Under Heat Assisted Machining,” *Asian J. Sci. Res.*, vol. 6, no. 3, pp. 609–614, 2013.
[52] A. Wilby and D. Neale, “Defects Introduced into Metals During Fabrication and Service,” *Mater. Sci. Eng.*, vol. 3, 2012.
[53] T. Furusawa, H. Hino, S. Tsuji, S. Koroyasu, and A. Ichikawa, “Generation of Defects Due to Machining of TiAl Intermetallic Compound and Their Effects on Mechanical Strength,” *Trans. ASME*, vol. 126, pp. 506–514, Aug. 2004.

[54] S. Rizzuti and D. Umbrello, “Finite Element Simulation of Machining of Ti6Al4V Alloy,” AIP Conference Proceedings 1353, 633 (2011); doi: 10.1063/1.3589586
[55] J. Mackerle, “Finite-element analysis and simulation of machining: a bibliography (1976–1996),” *J. Mater. Process. Technol.*, vol. 86, pp. 17–44, Jun. 1997.
[56] W. Song, “Development of predictive force models for classical orthogonal cutting and turning operations incorporating tool flank wear effects,” PhD Thesis, Queensland University of Technology, Brisbane, Australia, 2006.
[57] Z. Zhang and Q. Chen, “Comparison of the Eulerian and Lagrangian methods for predicting particle transport in enclosed spaces,” *Atmos. Environ.*, vol. 41, no. 25, pp. 5236–5248, 2007.
[58] J. Donea, A. Huerta, J.-P. Ponthot, and A. Rodriguez-Ferran, “Arbitrary Lagrangian-Eulerian Methods,” in *Encyclopedia of Computational Mechanics*, vol. 1, John Wiley & Sons, Ltd., 2004.
[59] D. Umbrello, “Finite element simulation of conventional and high speed machining of Ti6Al4V alloy,” *J. Mater. Process. Technol.*, vol. 196, pp. 79–87, Nov. 2006.
[60] R. Muhammad, A. Roy, and V. Silberschmidt, “Finite Element Modelling of Conventional and Hybrid Oblique Turning Processes of Titanium Alloy,” in *CIRP 8*, 2013, pp. 509–514.
[61] G. Styger, R. Laubscher, and G. Oosthuizen, “Effect of constitutive modeling during finite element analysis of machining-induced residual stresses in Ti6Al4V,” 2nd CIRP Conference on Surface Integrity, 2014. pp.293-301
[62] P. Nieslony, W. Grzesik, P. Laskowski, and J. Sienawski, “Numerical and experimental analysis of residual stresses generated in the machining of Ti6Al4V,” presented at the 2nd CIRP Conference on Surface Integrity.
[63] J. Strenkowski, A. Shih, and J.-C. Lin, “An analytical finite element model for predicting three-dimensional tool forces and chip flow,” *Anal. Finite Elem. Model Predict. Three-Dimens. Tool Forces Chip Flow*, vol. 42, pp. 723–731, Feb. 2001.
[64] A. Markopoulos, “Questions and answers on machining modeling,” in *Finite Element Method in Machining Processes*, 1st ed., Athens, Greece: Springer-Verlag London, 2013, p. 18.
[65] Rajam, Sham. "Design and finite element analysis of the broaching tools." Electronic Thesis or Dissertation. Ohio University, 1997. *OhioLINK Electronic Theses and Dissertations Center*. 16 Apr 2017.
[66] V. Schulze, J. Osterried, and T. Straub, “FE analysis on the influence of sequential cuts on component conditions for different machining strategies,” presented at the 1st CIRP Conference on Surface Integrity (CSI), 2011, vol. 19, pp. 318–323.
[67] L. Vijayaraghavan, “Evaluation of Stress and Displacement of Tool and Workpiece on Broaching,” *Int J Mach Tool Res*, vol. 21, no. 3–4, pp. 263–270, Apr. 1981.
[68] F. Zanger, N. Boev, and V. Schulze, “Surface quality after broaching with variable cutting thickness,” presented at the 2nd CIRP 2nd CIRP Conference on Surface Integrity (CSI), 2014, vol. 13, pp. 114–119.
[69] H. Wern, “Finite-element solutions for mechanical drilling methods: A new integral formalism,” *J. Comput. Appl. Math.*, vol. 63, pp. 365–372, 1995.
[70] O. Isbilir and E. Ghassemieh, “Finite Element Analysis of Drilling of Titanium Alloy,” *Procedia Eng.*, vol. 10, pp. 1877–1882, 2011.
[71] N. Kakade and J. Chow, “Finite element analysis of engine bore distortions during boring operation,” *J. Eng. Ind.*, vol. 115, pp. 379–384, Nov. 1993.

[72] L.-M. Wang and Y.-F. Wu, “Effect of corner radius on the performance of CFRP-confined square concrete columns: Test,” *Eng. Struct.*, vol. 30, no. 2, pp. 493–505, May 2007.
[73] F. Shah, M. Trobos, P. Thomsen, and A. Palmquist, “Commercially pure titanium (cp-Ti) versus titanium alloy (Ti6Al4V) materials as bone anchored implants — Is one truly better than the other?,” *Mater. Sci. Eng.*, vol. 62, pp. 960–966, May 2016.
[74] D. Hornbach and P. Prevéy, “The Effect of Prior Cold Work on Tensile Residual Stress Development in Nuclear Weldments,” *J. Press. Vessel Technol.*, vol. 124, no. 3, pp. 359–365, Aug. 2002.
[75] R.K. Nalla et. al., “On the influence of mechanical surface treatments—deep rolling and laser shock peening—on the fatigue behavior of Ti–6Al–4V at ambient and elevated temperatures,” *Mater. Sci. Eng.*, vol. A355, pp. 216–230, Jan. 2003.
[76] C. Liu and Y. Guo, “Finite element analysis of the effect of sequential cuts and tool chip friction on residual stresses in a machined layer,” *Int. J. Mech. Sci.*, vol. 42, pp. 1069–1086, Apr. 1999.
[77] L. Gammon, R. Briggs, J. Packard, K. Batson, R. Boyer, and C. Domby, “Metallography and Microstructures of Titanium and Its Alloys,” in *ASM Handbook, Volume 9: Metallography and Microstructures*, vol. 9, ASM International, 2004, pp. 899–917.

Appendix A – Supplementary FEA Images

Supplementary Boring Images

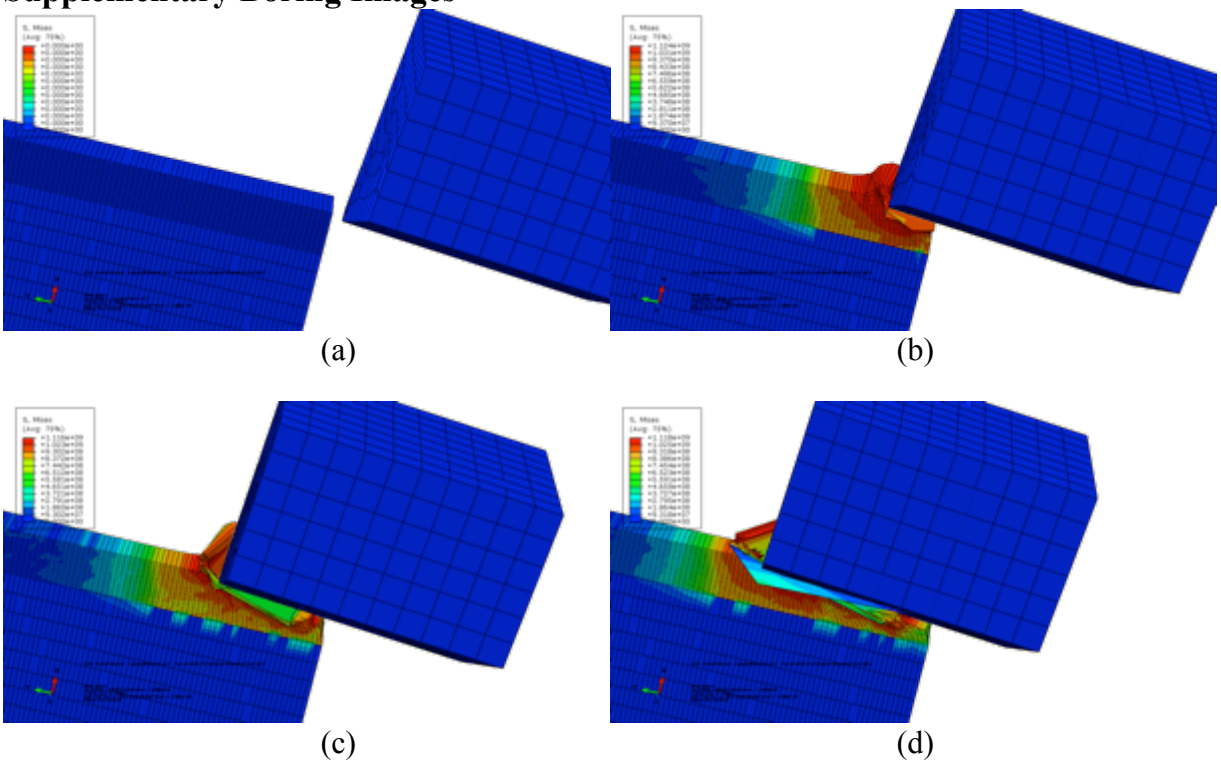

(a) (b)

(c) (d)

Figure A-1: Images (a), (b), (c), and (d) display stress values at progressive time periods during the boring process

Supplementary Broaching Images

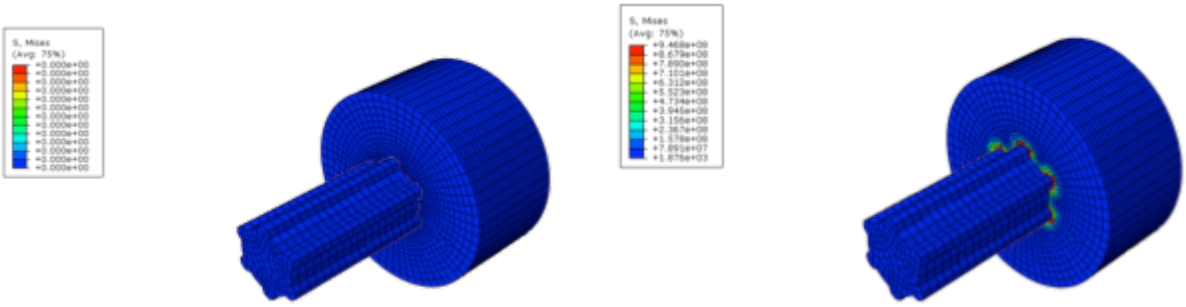

(a) (b)

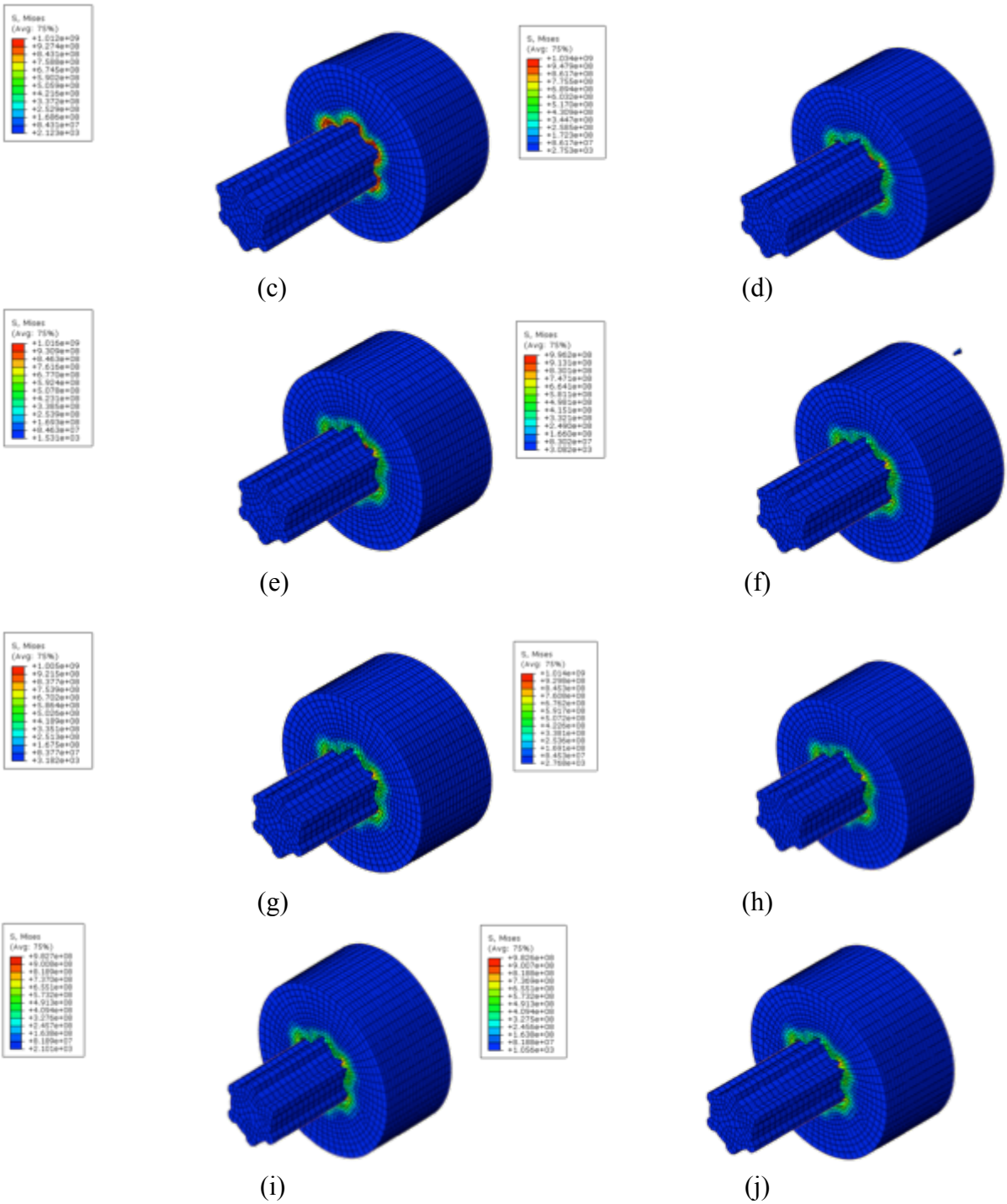

Figure A-2: Stress values at progressive time periods during the broaching process, with (a) through (g) the insertion of the tool bit and (h), (i), and (j) the removal step

Supplementary Drilling Images

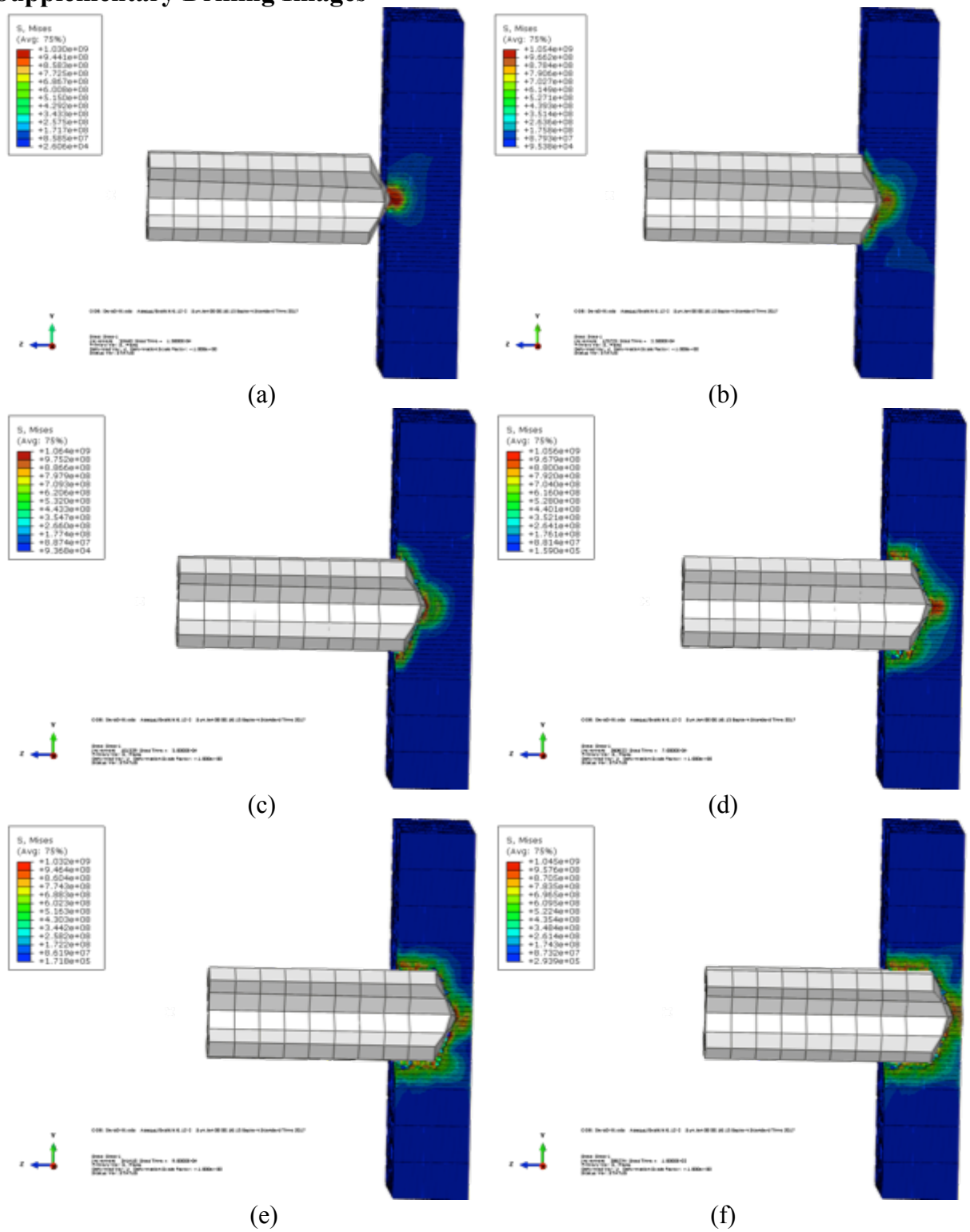

Figure A-3: Images (a) through (f) indicate stress values and progressive time periods during the drilling process

Supplementary Turning Images

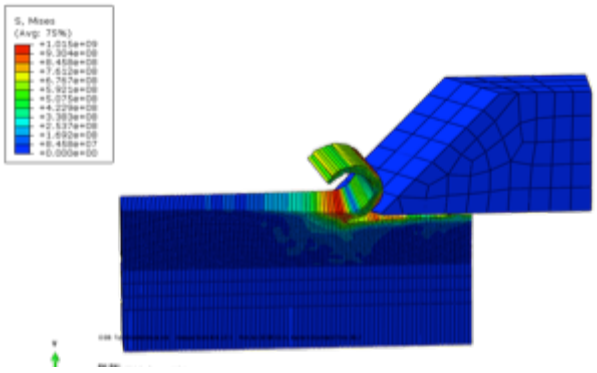

(a)

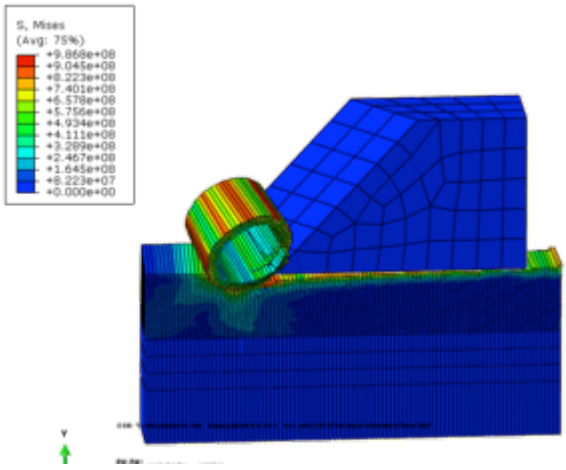

(b)

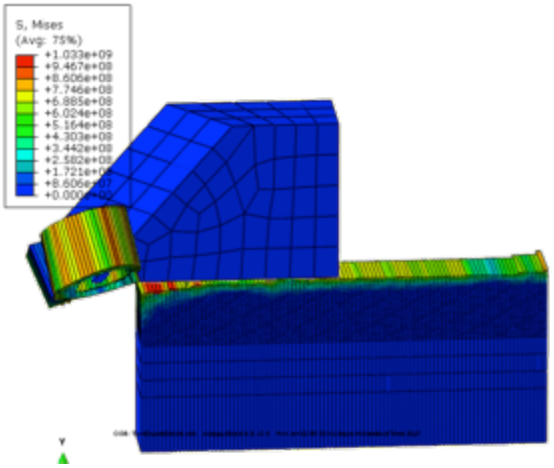

(c)

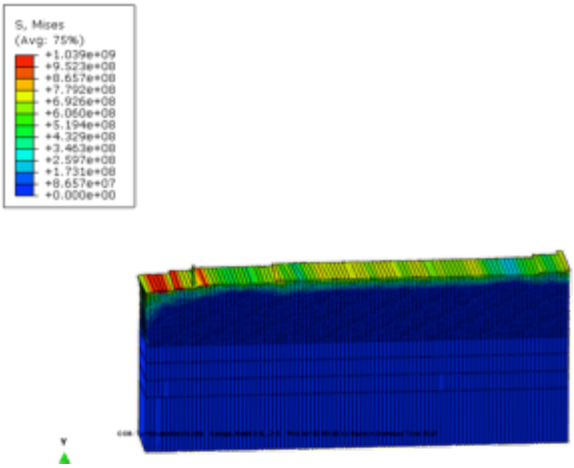

(d)

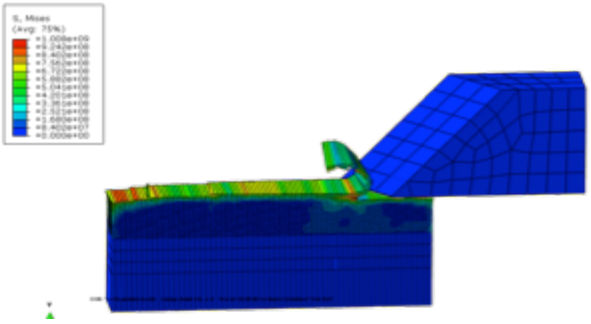

(e)

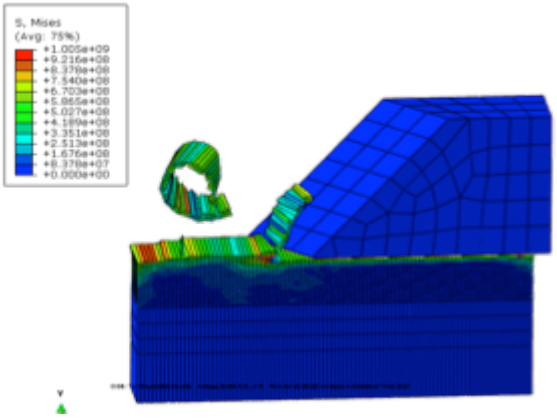

(f)

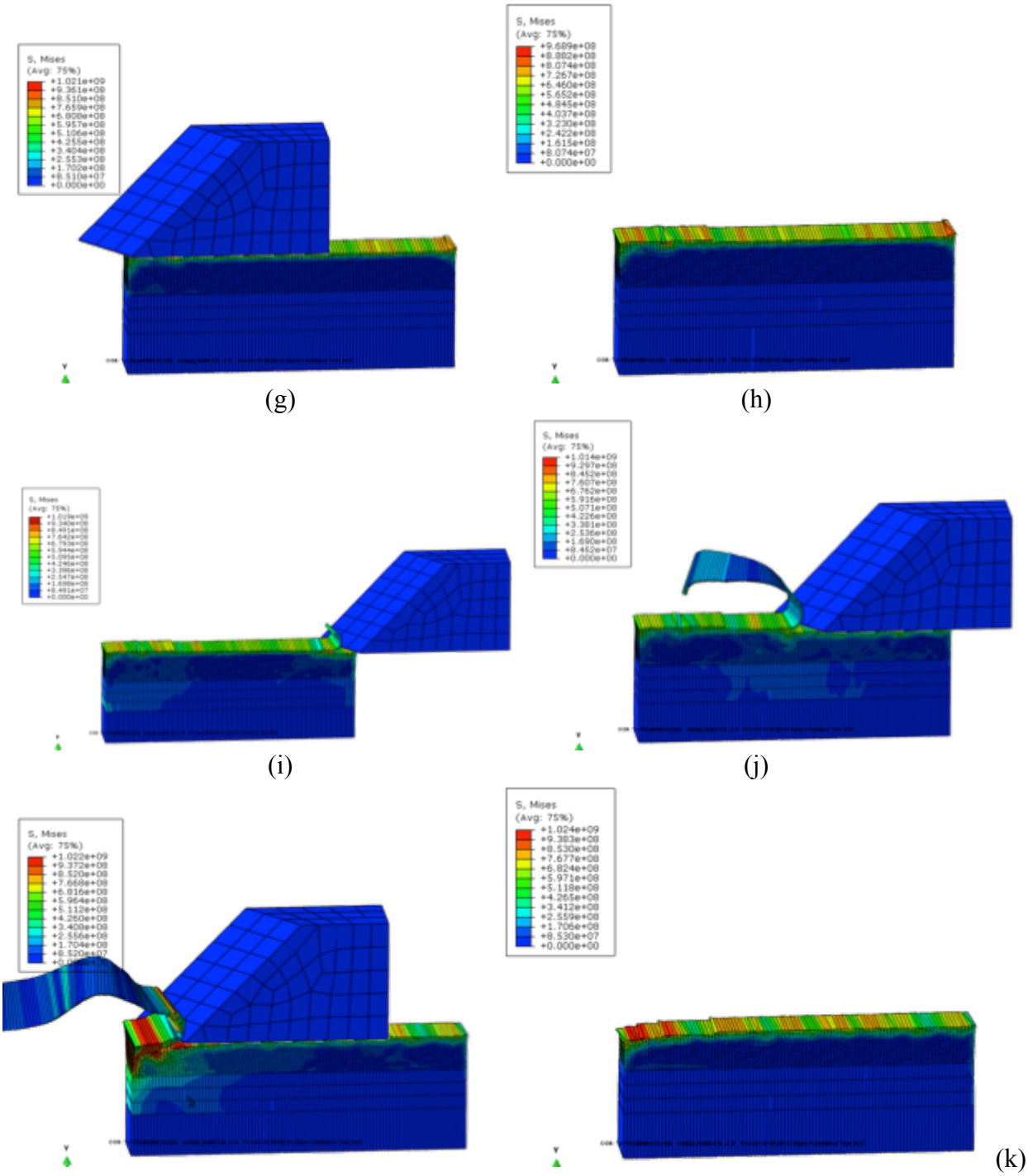

Figure A-4: Stress values during progressive time periods during the turning process with images (a) through (d) during the first cut, (e) through (h) the second cut, and (i) through (l) the third cut

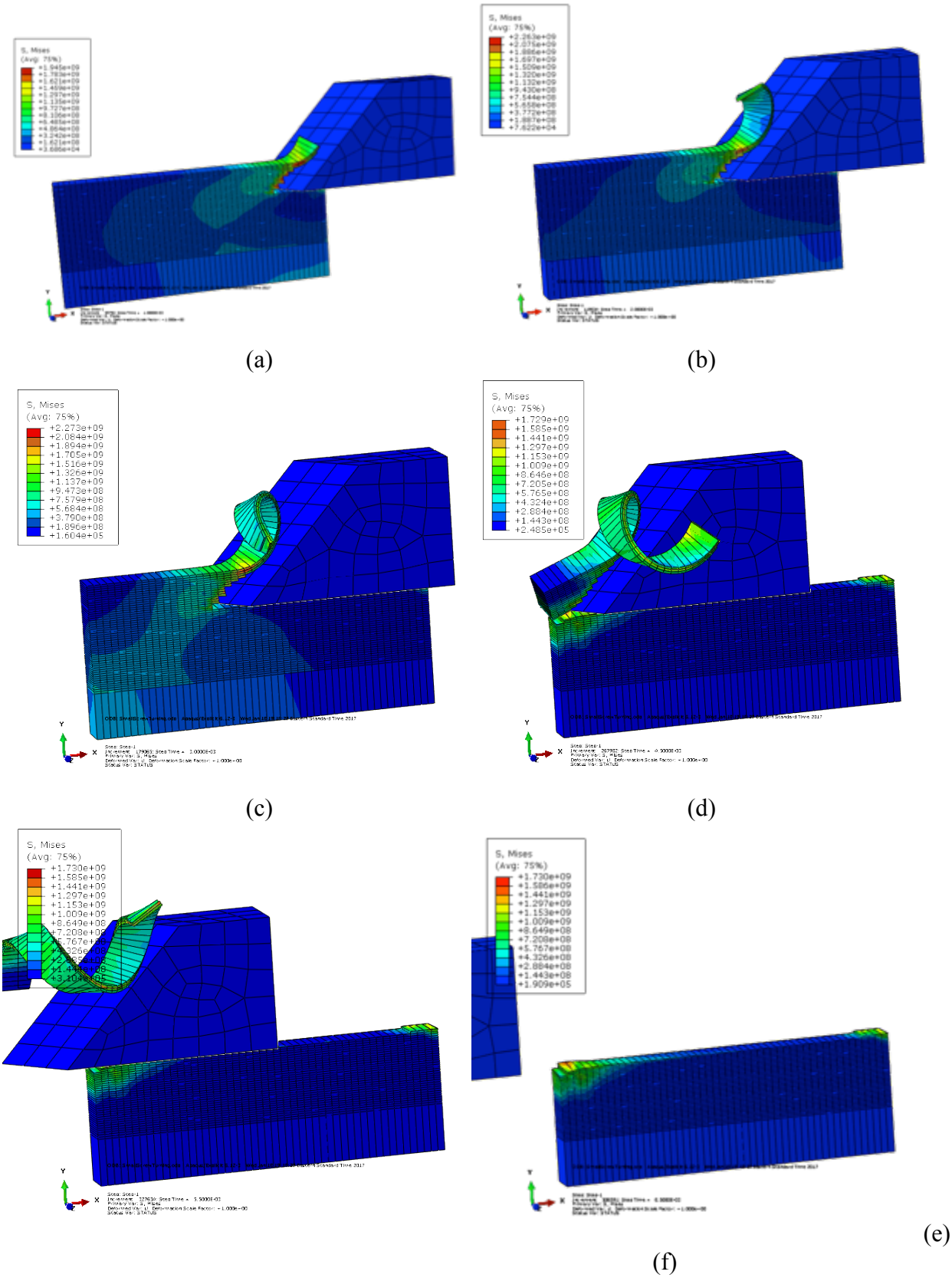

Figure A-5: Stress values during progressive time steps of thermal and mechanical turning

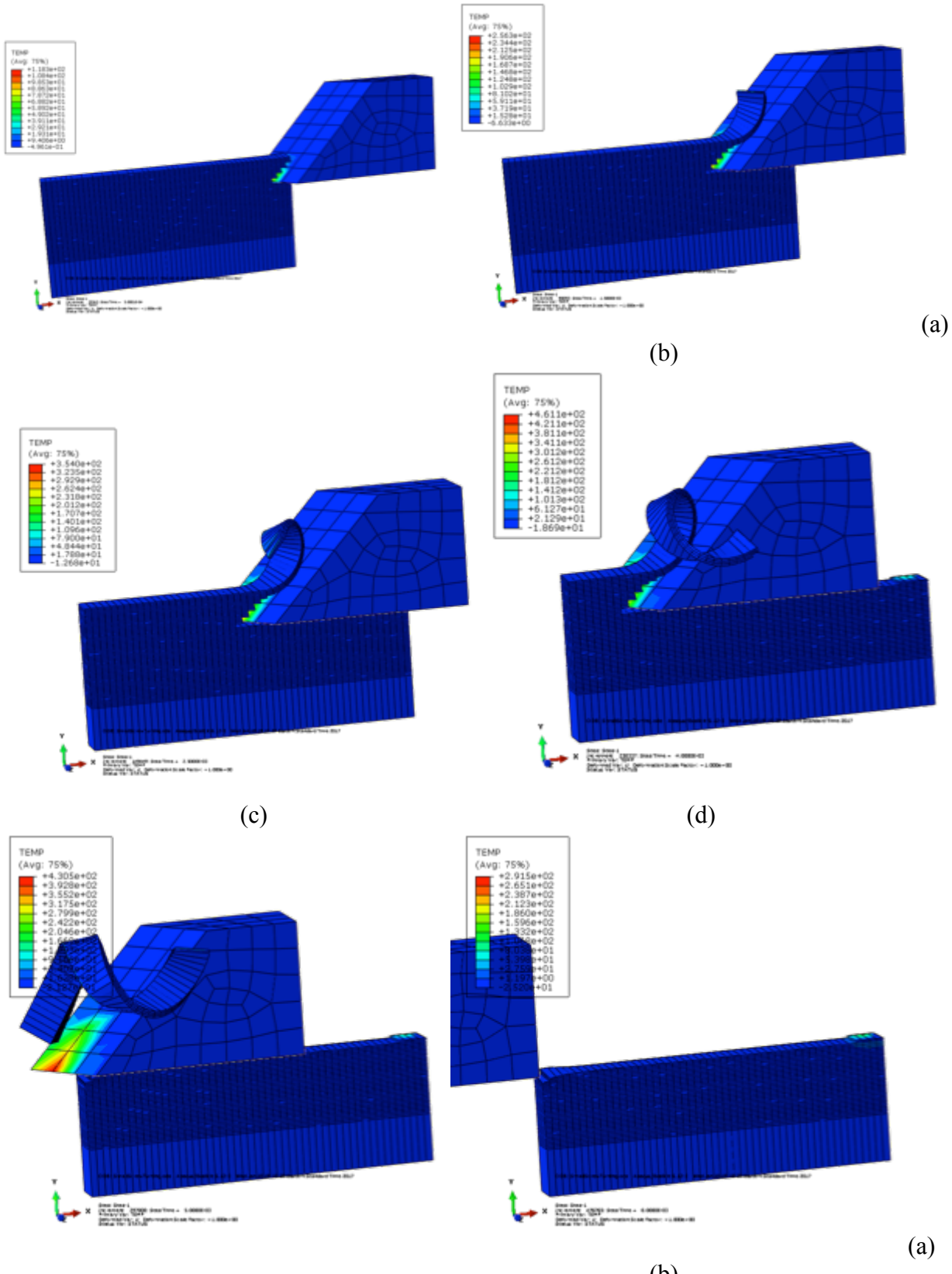

Figure A-6: Temperature values at progressive time steps of thermal and mechanical turning